https://doi.org/10.5194/cp-2022-59
Preprint. Discussion started: 31 August 2022

Climate of the Past Discussions

The climate and vegetation of Europe, North Africa and the Middle East during the Last Glacial Maximum (21,000 years BP) based on pollen data

Basil A.S. Davis[1], Marc Fasel[2], Jed O. Kaplan[3], Emmanuele Russo[4], Ariane Burke[5]

[1]Institute of Earth Surface Dynamics, University of Lausanne, Lausanne, 1015, Switzerland
[2]enviroSPACE lab, Institute for Environmental Sciences, University of Geneva, Geneva, 1211, Switzerland
[3]Department of Earth Sciences, The University of Hong Kong, Hong Kong, Peoples Republic of China
[4]Department of Environmental Systems Science, ETH Zurich, Zurich, 8092, Switzerland
[5]Laboratoire d'Ecomorphologie et de Paleoanthropologie, Departement d'Anthropologie, Universite de Montreal, Montreal, Quebec, H3C 3J7, Canada

Correspondence to: Basil A. S. Davis (basil.davis@unil.ch)

Abstract. Pollen data represents one of the most widely available and spatially-resolved sources of information about the past land cover and climate of the Last Glacial Maximum (21,000 years BP). Previous pollen data compilations for Europe, the Mediterranean and the Middle East however have been limited by small numbers of sites and poor dating control. Here we present a new compilation of pollen data from the region that improves on both the number of sites (63) and the quality of the chronological control. Data has been sourced from both public data archives and published (digitized) diagrams. Analysis is presented based on a standardized pollen taxonomy and sum, with maps shown for the major pollen taxa, biomes and total arboreal pollen, as well as quantitative reconstructions of forest cover and winter, summer and annual temperatures and precipitation. The reconstructions are based on the modern analogue technique (MAT) with a modern calibration dataset taken from the latest Eurasian Modern Pollen Database (~8000 samples). A site-by-site comparison of MAT and Inverse Modelling methods shows little or no significant difference between the methods for the LGM, indicating that no-modern-analogue and low CO2 conditions during the LGM do not appear to have had a major effect on MAT transfer function performance. Previous pollen-based climate reconstructions based on MAT show a much colder and drier climate for the LGM than both Inverse Modelling and climate model simulations, but our new results suggest much greater agreement. Differences between our latest MAT reconstruction and those in earlier studies can be largely attributed to bias in the small modern calibration dataset previously used. We also find that quantitative forest cover reconstructions show more forest than that previously suggested by biome reconstructions, but less forest than that suggested by simple percentage arboreal pollen, although uncertainties remain large. Overall, we find that LGM climatic cooling/drying was significantly greater in winter than in summer, but with large site to site variance that emphasizes the importance of topography and other local factors in controlling the climate and vegetation of the LGM.

https://doi.org/10.5194/cp-2022-59
Preprint. Discussion started: 31 August 2022

Climate of the Past Discussions
Open Access
EGU

1 Introduction

During the Last Glacial Maximum (LGM) ~21,000 years BP (Mix et al., 2001), the climate, vegetation and landscape of Europe and its surrounding regions were very different than today. Scandinavia and a large part of the British Isles were covered by a single ice sheet, with separate ice sheets covering the Alps and Pyrenees, while many smaller and lower mountainous areas were also glaciated. As a result of this global build-up of ice on land, sea levels were around 120 meters lower than today, resulting in the retreat of Atlantic and Mediterranean coastlines and the emergence on land of the English Channel and North Sea basin. Falling sea levels also led to the disconnection of the Black Sea from the Mediterranean, and a subsequent drop in Black Sea water levels as evaporation exceeded inflow. On land, permafrost and periglacial processes occurred immediately to the south of the Scandinavian ice sheet, while the massive discharge of glacial clays and sands provided material to be redeposited by the wind as belts of loess across northern France, Benelux, Germany and central Europe. Under these cooler and drier climatic conditions, forests are thought to have retreated to the relative shelter of Southern Europe and the Mediterranean, while relatively unproductive steppe and boreal scrub dominated the region north of the Alps.

This traditional view of the LGM has been established for many years, but many details concerning the climate and vegetation of the LGM remain debated. Much of this debate concerns information derived from the pollen record, which represents one of the most widely available and spatially-resolved sources of information concerning LGM vegetation and climate, and the primary terrestrial proxy used to evaluate climate models in the Palaeo-model Inter-comparison Project (PMIP) (Bartlein et al., 2011; Harrison et al., 2014).

For example, climate model simulations continue to indicate a climate that is less cold and more humid than pollen-based reconstructions (Jost et al., 2005). These pollen climate reconstructions are similar to those based on glaciological modelling (Allen et al., 2008a). On the other hand, the pollen-based reconstructions that show the greatest disagreement with climate models have themselves been criticized for not considering the possible effect of low atmospheric CO2 on the physiological relationship between plants and climate (Ramstein et al., 2007). Pollen-climate reconstructions based on inverse modelling that account for these low CO2 effects show less cooling and drying and consequently greater agreement with climate models (Ramstein et al., 2007; Wu et al., 2007).

Further data-model discrepancies have also been highlighted concerning LGM vegetation cover. Earlier pollen synthesis studies, especially those that applied the biomisation method (Elenga et al., 2000) give the impression that non-glaciated areas of LGM Europe were dominated by treeless steppe, while vegetation models driven by climate model simulations indicate large areas of forest and woodlands (Binney et al., 2017; Kaplan et al., 2016; Velasquez et al., 2021). The apparent data-model discrepancy associated with steppe has led to the suggestion that early humans, which are not included in vegetation models, could have reduced the forest cover with only a relatively moderate use of fire because of the cold climate and slow speed of vegetation recovery (Kaplan et al., 2016). This debate is important because of studies that have shown the sensitivity of the climate system to vegetation boundary conditions during the LGM (Ludwig et al., 2017; Velasquez et al., 2021). This suggests that

https://doi.org/10.5194/cp-2022-59
Preprint. Discussion started: 31 August 2022

Climate of the Past Discussions
Open Access
EGU

accurate knowledge of the vegetation cover during the LGM is a necessary prerequisite to understanding the role of other influences on the climate system at this time.

More recent pollen and macrofossil studies from eastern Central Europe have shown that at least in this region there existed areas of open boreal forest and woodland with some temperate broadleaf species (Kuneš et al., 2008; Willis and Van Andel, 2004). The evidence of forest, and particularly elements of temperate broadleaf forest, north of the Alps has come to represent a challenge to the traditional view that forest species only survived the LGM in sheltered refugia far to the south of the Fenoscandian ice sheet and close to the moderating influence of the Mediterranean Sea. The presence of micro-refugia north of the Alps is important because it would represent a very different baseline for understanding the later rate and route of plant migrations under the rapid warming that occurred during the Late Glacial to Holocene transition (Douda et al., 2014; Giesecke, 2016; Krebs et al., 2019; Nolan et al., 2018), as well as understanding patterns of present-day genetic diversity (Normand et al., 2011; Svenning et al., 2008).

Much of this debate has been informed by an increasing number of LGM pollen studies from an ever-broader geographical area, and especially from an increasing number of studies from north of the Alps. Nevertheless, the synthesis of these studies into a single narrative is made difficult by several factors, for instance: different taxonomic definitions, pollen percentages calculated from non-standardized pollen sums, and quantitative analyses such as climate reconstructions that are based on different training sets and methodologies. This has led to some modelling studies ignoring the pollen record completely, on the basis that data from the LGM is too scarce (Janská et al., 2017). Where standardized methods have been applied to multiple LGM pollen records, poor dating control has resulted in the inclusion of many records that may not actually be from the selected LGM time window. This is particularly important because the 21 ± 2.0 ka time slice commonly used to represent the LGM period in PMIP data-model comparisons and other synthesis studies (MARGO members, 2009; Bartlein et al., 2011) occurs immediately after the glacial maxima in the Alps, which occurs around 26-23 ka (Heiri et al., 2014; Spötl et al., 2021), and is therefore likely to be represented by a different vegetation and climate.

For example, of the 18 European pollen records used in the PMIP benchmarking dataset (Bartlein et al., 2011), 10 fall into the worst class (‘poor’) in the COHMAP chronological quality classification scheme if relative dating such as pollen correlation is excluded. More recent synthesis studies have also relied heavily on records from the European Pollen Database (EPD) which currently has 116 records with samples of LGM age (as of June 2022). Many of these records however are based on chronologies that are considered reliable for the Holocene (Giesecke et al., 2014), but have large uncertainties for the LGM as a result of 1) excessive extrapolation back in time from Holocene age dates, 2) the use of pollen correlation or other relative dating despite poorly defined regional biostratigraphy, or 3) the inappropriate use of radiocarbon dates contaminated with old carbon. We found that 104 of these 116 EPD records (Neotoma, 2021) fall into the worst class (‘poor’) in the COHMAP chronological quality classification.

Here we address these problems using a new synthesis of LGM pollen records from throughout Europe, the Mediterranean and the Middle East (EurMedMidEst) based on rigorous quality control criteria. Records were

https://doi.org/10.5194/cp-2022-59
Preprint. Discussion started: 31 August 2022

Climate of the Past Discussions

compiled from an extensive review of public databases and archives, and the scientific literature. Pollen records were selected according to the robustness of their chronological control around the PMIP LGM time-window (21 ± 2 ka), and combined into a single dataset based on a harmonized taxonomy and standardized pollen sum. The dataset was then analysed so that standardised maps could be produced to show the distribution of the major pollen taxa, biomes and total arboreal pollen at the LGM. In addition, quantitative reconstructions of forest cover as well as winter, summer and annual temperatures and precipitation were undertaken using the Modern Analogue Technique (MAT), utilizing the latest Eurasian Modern Pollen Database II calibration dataset. These climate reconstructions are compared and evaluated against previous LGM pollen-climate reconstructions, as well as reconstructions based on other proxies. The dataset and results are fully documented and the complete data files are provided in the supplementary information.

2 Methods

2.1 Pollen Data

LGM fossil pollen data from Europe and bordering regions including North Africa and the Middle East were selected and collated into a single standardized project database. This data was sourced from the EPD/Neotoma database (Williams et al., 2021), the Pangaea data archive, publications in scientific journals, and from the original authors. We selected LGM pollen sites/data according to strict quality control criteria. Where possible, primary raw pollen counts were used where this was available. Where the original electronic data was not available, the data was digitized from the published diagram. Overall, 35 out of 63 records were digitized, while the rest of the data consisted of raw pollen counts (Table 1).

The distribution of sites included in our study reflects the distribution of suitable archives, with fewer records available from climatically or environmentally challenging regions (Fig. 1). High rates of erosion and a drier and colder climate during the LGM reduced the number of suitable anoxic sediment sinks for pollen preservation, especially in Central Europe between the Scandinavian and Alpine ice sheets. Lakes sites are the most numerous archive and tend to be located in the more sheltered and topographically favourable regions of Southern Europe and the Mediterranean. Peat is the next most important archive, followed by alluvial and colluvial sediments, as well as cave sites, the later also often being known for their archaeological significance. Sites located at the ice margins that appear to be under the ice reflect uncertainties in the location of the ice margin both in time and space during the LGM, as well as the fact that the selected time window for this study (21 ± 2 ka) is later than the maximum ice advance in some regions (Hughes and Gibbard, 2015). For completeness, we also include marine records which have the advantage of more continuous deposition and often better dating over the LGM period, but which are prone to taphonomic biases compared to terrestrial records. These biases are discussed later in this section.

LGM pollen records were selected according to a number of quality control criteria, but primary amongst these was the existence of sufficient independent chronological control points to accurately identify samples that would fall within the 21 ± 2 ka BP time-slice of interest. We have used all of the samples within this time frame where

https://doi.org/10.5194/cp-2022-59
Preprint. Discussion started: 31 August 2022


Climate of the Past Discussions

158 the samples have been available in electronic form, else we have used the sample closest to the target time (21 ka
159 BP). For records taken from the EPD we have used the latest Bayesian age-depth models where these were
160 available (Giesecke et al., 2014), otherwise we have used the dates and chronology proposed by the original
161 authors. We classified chronologies according to the COHMAP chronological quality scheme for the LGM period
162 (Anderson et al., 1988; Yu and Harrison, 1995), which classifies record quality from 1-6 depending on whether a
163 date falls within 2000 14C years (or less) of the time being assessed, or whether bracketing dates fall within 6000
164 and 8000 14C years (or less) about the time being assessed (Table. 2). Chronologies based on dates that fall outside
165 of these limits fall into COHMAP class 7, and are regarded as 'poorly dated' with respect to the LGM. Importantly,
166 we have only included radiometric and other absolute dates (such as varves) in this assessment, and have excluded
167 dates based on correlation with regional pollen records. These pollen-based stratigraphic dates have been widely
168 used in previous LGM studies, but do not include estimates of uncertainty and are generally regarded as unreliable
169 at this time given the sparsity of well dated pollen sites and samples on which to base any correlation (Giesecke
170 et al., 2014).
171
172 All records that were classified as poorly dated (COHMAP class 7) were subsequently excluded from our analysis.
173 This has meant that many of the pollen records used in previous studies were excluded, including 10 of the 18
174 LGM records used by PMIP and associated studies in Europe (Bartlein et al., 2011; Elenga et al., 2000; Jost et al.,
175 2005; Peyron et al., 1998; Wu et al., 2007; Cleator et al., 2020). We also excluded 104 of the 116 records in the
176 EPD with samples that fall within our LGM time window. Many of these EPD pollen records have been used in
177 more recent studies, although the exact record (EPD site #Entity) is often not stated. We estimate that we have
178 excluded 16 of the 17 European sites used by Binney et al. (2017) (this study only included sites above latitude
179 40N), 5 of the 6 European sites used by Allen et al. (2010), 28 of the 33 sites used by Cao et al. (2019) and 27 of
180 the 71 sites used by Kaplan et al. (2016).
181
182 Other quality control criteria were also used in the selection of LGM pollen records. Published pollen diagrams
183 that only included a small part of the terrestrial pollen assemblage, or only presented summary taxa, were
184 excluded. Records were also excluded where the dating information was incomplete, for instance where
185 radiocarbon dating uncertainties were not published or where it was not possible to determine if the date shown
186 was in calibrated or uncalibrated radiocarbon years.
187
188 The modern pollen data for the climate and tree cover reconstructions were sourced from the latest version 2 of
189 the Eurasian Modern Pollen Database (Davis et al., 2020), which is managed as part of the EPD. The EMPD2
190 includes 8133 modern pollen samples from across the Palearctic biogeographic region from Europe to the far East
191 of Asia. The taxa from both the fossil and modern pollen data were consolidated into 120 of the most commonly-
192 occurring terrestrial taxa types. This taxa list was designed to be compatible with the biomisation scheme used in
193 our study (Peyron et al., 1998; Tarasov et al., 2000) and that used in the Holocene mapping study of Brewer et al.
194 (2017). The count of Larix was amplified by a factor of 10 due to its low pollen representation (Binney et al.,
195 2017).
196
197 **2.2 Biomisation**

https://doi.org/10.5194/cp-2022-59
Preprint. Discussion started: 31 August 2022

Climate of the Past Discussions

We converted pollen assemblages to biomes based on the European biomisation scheme of Peyron et al (1998), which in turn is based on Prentice et al. (1996). The method is described in detail in Collins et al. (2012). We expanded the number of taxa included in the biomisation procedure proposed by Peyron et al (1998) to include taxa from the Northern Eurasian biomisation procedure of Tarasov et al. (1998). The inclusion of additional Northern Eurasian taxa reflects recent evidence that modern analogues of LGM vegetation occur in parts of Siberia (Magyari et al., 2014a). The biomisation procedure (Prentice et al. 1996) assigns each taxa to a plant functional type (PFT) and calculates a score for each of these PFT's based on the sum of the square root of the percentage of each of the taxa included in that PFT. To reduce the influence of long-distance transport, taxa below 0.5% are removed at the start of the procedure. Each biome is then assigned one or more PFT's and a score for each biome is calculated as the sum of the associated PFT scores. The biome with the highest score is then viewed as the dominant biome. Where the highest score is the same for more than one biome, the dominant biome is decided based on a hierarchy of unique PFT's. Peyron et al. (1998) also included a procedure for distinguishing warm and cold steppe biomes based on re-assigning certain steppe PFT's according to the presence or otherwise of PFT's indicative of cold or warm conditions. Following the Biome6000 project ((Elenga et al., 2000) and Allen et al. (2010), we did not apply this additional procedure and present only the merged steppe biome. In summary, the biomisation procedure categorised 39 arboreal pollen taxa and 39 non-arboreal taxa into 22 plant functional types (PFT's), which were then combined into 12 biomes.

2.3 Quantitative climate reconstruction

We reconstructed climate from pollen data based on a standard Modern Analogue Technique (MAT) that used PFT scores to match fossil samples with modern calibration pollen samples (as used by Davis et al., 2003). This is a similar approach to that used by Peyron et al. (1998) and Jost et al. (2005) who also applied pollen PFT scores to reconstruct LGM climate from pollen data, but who used a neural network technique which is a variant of the standard MAT (Chevalier et al., 2020). PFT scores have been used in previous large-scale European pollen-based climate reconstructions for the Holocene (Davis et al., 2003; Mauri et al., 2014, 2015), where performance was found to be better than the conventional approach based on individual taxa (eg Marsicek et al., 2018). A particular advantage of the PFT approach for the LGM is that it can help overcome problems associated with vegetation (pollen) assemblages that may have no modern analogue (Davis et al. 2003). This can be a problem during the LGM when the climate and environment could be expected to be very different from today, and when many taxa formed unusual vegetation assemblages as a result of their forced retreat to sheltered refugia locations. The problem of modern analogues is also addressed in our reconstruction by using the latest EMPD2 modern pollen dataset for calibration purposes. The EMPD2 provides a large number of potential modern analogues for many different LGM vegetation types and climates found today across the Palearctic region. PFT scores were calculated according to the methods outlined already in the Biomisation section, then normalized so that each sample was proportional to every other sample (Juggins and Birks, 2012).

The MAT method was applied using the Rioja program for R (Juggins, 2020). The modern calibration data was taken from the latest version 2 of the EMPD (as detailed earlier). The EMPD2 includes 8133 samples, which is

https://doi.org/10.5194/cp-2022-59
Preprint. Discussion started: 31 August 2022


Climate of the Past Discussions
Open Access
EGU

considerably larger than the modern datasets used in previous LGM pollen-based reconstructions. For instance, Peyron et al. (1998) used a calibration dataset of 683 samples, which was updated by Jost et al (2005) to include an additional 185 samples. These datasets were also mainly taken from the steppes of Kazakstan and Mongolia, while the EMPD2 covers a much wider area, spanning most of the Eurasian Palearctic region (Davis et al., 2020). The size and distribution of the modern training set in climate and vegetation space is important because in order for the method to work effectively, it is necessary to have samples representative of the likely vegetation and climate space that could be occupied by the fossil assemblage (Chevalier et al., 2020; Juggins, 2013).

A known problem with MAT is the role of spatial auto-correlation in providing unrealistically low estimates of uncertainty (Chevalier et al., 2020; Telford and Birks, 2009). This results from the fact that closely analogous modern pollen samples can also be located closely in physical space, and therefore in climate space. To reduce this problem it is possible to systematically exclude closely located modern samples from the analogue matching process, for instance, by excluding samples that fall within a certain spatial range (h-block filter) (Telford and Birks, 2009). While this approach can help, there are also three main problems associated with it. The first is error substitution, since removing samples also reduces the number of potential analogues, creating a different source of error that is not easy to categorise. Secondly, multiple samples taken from the same location are actually a strength of pollen training sets, since they are more likely to capture the full range of the assemblage diversity associated with a given climate. Thirdly, current methods that limit spatial range such as the h-block filter only do so on the horizontal axis, and do not consider the fact that samples can also be found at different elevations. In hilly or mountainous regions samples can therefore be excluded because they are closely located in horizontal space, but in fact they actually occupy very different climates and vegetation associations, contradicting the logical premise of the h-block filter. It was therefore decided not to apply this filter.

Climate reconstructions are presented as anomalies. These have been calculated with respect to modern climate at each core site location using WorldClim 2 (Fick and Hijmans, 2017), which was also used to assign the modern climate for the modern pollen samples in the transfer function (Davis et al., 2020).

2.4 Quantitative tree cover reconstruction

It has long been recognized that the proportional representation of individual pollen taxa in a pollen assemblage does not necessarily reflect the proportion of land area covered by that taxa in the pollen source area surrounding the sample site. These differences can be caused by varations in pollen productivity, differential transport, deposition and preservation of pollen grains, and even the ease or otherwise of the identification of pollen grains themselves. This can make the interpretation of pollen taxa percentages difficult, even for relatively simple questions such as the proportion of forest to non-forest in the landscape.

There have been two main methods developed to account for this quantification problem, one using a physical modelling technique (PMT) based on estimates of pollen production for individual taxa (Gaillard et al., 2010), and the other using a MAT very similar to that used in pollen-climate reconstructions (Williams and Jackson, 2003). Both approaches have been widely applied during the Holocene in Europe (Zanon et al., 2018), but we

https://doi.org/10.5194/cp-2022-59
Preprint. Discussion started: 31 August 2022


Climate of the Past Discussions

know of no previous study that has applied either of these approaches to the LGM. The LGM presents a number of challenges, not least the problem of potential missing vegetation analogues, as well as low atmospheric CO2, which has been shown to influence pollen productivity (Leroy and Arpe, 2007).

Here we use the MAT to provide quantitative estimates of forest cover, following the approach of Zanon et al. (2018) who applied this method to the Holocene pollen record of Europe. We apply MAT in exactly the same way as for the climate reconstructions described earlier, including the use of PFT scores to match fossil and modern pollen samples. Instead of modern climate values, we assigned an estimate of modern forest cover to each of our modern pollen sites. To do this we use a high resolution (~100m) remote sensing dataset derived from satellite observations (Hansen et al., 2013). Zanon et al. (2018) have shown that the MAT calibrated in this way gives comparable results to the PMT approach in Europe, at least for the Holocene. One of the main differences however is that the PMT is designed to provide estimates of the proportions of different taxa, whereas the MAT (as applied here) is designed to provide estimates of the proportion of forest cover. Where the PMT can only reconstruct the proportion of forest forming trees, irrespective of their size, the MAT (following Zanon et al. 2018) is calibrated specifically to reconstruct forest composed of trees over 5m tall. This follows the FAO definition of forest as "land spanning more than 0.5 hectares with trees higher than 5 meters and a canopy cover of more than 10 percent, or trees able to reach these thresholds in situ" (FAO Terms and definitions 2020 http://www.fao.org/3/I8661EN/i8661en.pdf).

2.5 Maps

We present our results in the form of maps that include the main physiographic features of the LGM in the study area. The maps are based on the WGS84 projection. Coastlines reflect LGM sea level at 120m below present, while ice sheets are based on Ehlers et al. (2011). Modern national country boundaries are also included for reference.

2.6 Marine pollen records

We have included marine pollen records in our analysis for reasons explained below, but it is important that these records should be viewed with caution, particularly when used for biome and quantitative MAT reconstructions, and when compared with terrestrial records from different archives. Biomisation methods have been applied to individual marine pollen records (Combourieu Nebout et al., 2009), as well as multi-site synthesis studies such as the ACER project (ACER project members et al., 2017). However, marine records were specifically excluded from the Biome6000 project (Elenga et al., 2000). Similarly, quantitative climate methods have been applied to individual marine pollen records (Combourieu Nebout et al., 2009; Fletcher et al., 2010), as well as multi-site synthesis studies (Brewer et al., 2008). However, marine records have also been specifically excluded from other major pollen-climate studies (Cheddadi et al., 1996; Davis et al., 2003; Marsicek et al., 2018), as well as quantitative forest cover reconstructions (Zanon et al. 2018).

https://doi.org/10.5194/cp-2022-59
Preprint. Discussion started: 31 August 2022

Climate of the Past Discussions

Discussion on the advantages and problems associated with marine records can be found elsewhere (Chevalier et al., 2020; Daniau et al., 2019), but are reviewed briefly here where relevant to the methodologies applied in this study. Marine sedimentary records provide continuous and well dated pollen records for the LGM that are often lacking from many terrestrial regions, especially in arid areas with few alternative anaeorobic sediment sinks. Conversely however, pollen source areas for marine sites may be many hundreds of kilometers from the coring site and may be liable to change through time in response to changes in distance to the coastline, rates of river discharge and ocean and atmospheric dynamics. This can theoretically give rise to changes in the vegetation shown in the pollen assemblage recorded at the marine site without any actual change in climate or other environmental pressure. The large and indeterminable source area of marine records also mean that it is difficult to apply quantitative MAT reconstruction methods, not least because the mean climate or forest cover of the source area is almost impossible to determine. In addition, the pollen record and the calibration dataset to which it is being compared are composed largely of terrestrial lakes and bog sites with much smaller and more homogeneous source areas. This creates a series of problems, the more obvious of which is the calculation of anomalies, since we cannot assume that the modern climate at the (marine) coring site location is representative of the (terrestrial) source area. In this study we have taken the closest point on land as the modern climate for the calculation of anomalies. The next problem is that the large source area may capture a combination of different vegetation types that is not going to be represented in a calibration dataset based on samples from terrestrial sites with much smaller source areas, for instance a mixture of coastal and mountain vegetation, or even vegetation from different continents (Magri and Parra, 2002). However, in our analysis we did not find any sample from a marine record that did not have a reasonable modern analogue in our training set (chord distance <0.3)(Huntley, 1990), even though we did not adjust the pollen assemblage for the over-representation of Pinus in the marine pollen samples.

Typically, the Pine component is excluded from the terrestrial pollen sum when calculating percentages for marine pollen samples, and in some cases Pine has been excluded entirely from the samples used in marine pollen-climate reconstructions (Combourieu Nebout et al., 2009). The problem with excluding Pinus is two-fold, the first is that Pinus often represents the main forest forming tree in the Koeppen Csb climate zone on the Atlantic coast where many marine sites are located (García-Amorena et al., 2007), as well as representing the most abundant tree taxa in Europe during the LGM (Figure A1c). The second problem is that the remaining terrestrial taxa often constitute a very small number of pollen grains in a typical marine pollen sample (<100 grains), which can result in pollen assemblages that are not based on a statistically stable count of the pollen sample (Chevalier et al., 2020).

3. Results

3.1 Vegetation & Biomes

Results of the biomisation analysis shows that steppe (STEP) was the most common biome at the LGM across the study area, occurring at 36 out of 63 sites, indicating that the landscape was largely dominated by cool temperate grasslands across much of western Central Europe, central and eastern Mediterranean, as well as North Africa and the Middle East (Fig. 2). However, at the same time we also find that there were a significant number of sites

https://doi.org/10.5194/cp-2022-59
Preprint. Discussion started: 31 August 2022

Climate of the Past Discussions

where we find woody and forest biomes occur, more particularly in southern and eastern Iberia, northern Italy and central eastern Europe. The most dominant of these forest and woody biomes are taiga (TAIG) in the north, and cool-mixed forest (COMX) and xerophytic woodlands (XERO) in the south.

As would be expected, the dominance of STEP biomes is generally reflected in low arboreal pollen percentages across the same areas/sites (Fig. 3 & 4). Exceptions to this rule can be found at marine sites such as [site #3] and [site #58] where STEP is reconstructed despite arboreal pollen percentages of 71 and 80 percent respectively. This apparent contradiction illustrates some of the idiosyncrasies of the biomisation method, especially when applying the method to marine pollen samples. In this case it is important to remember that the AP% is calculated from the sum of the percentages of each relevant taxa, but the score for each biome is the sum of the square root of the percentages of each of its constituent taxa. This results in biomes with taxa with large percentage values scoring proportionally smaller, and biomes with taxa with small percentage values scoring proportionally larger. For example, a single taxa at 50% has a square root of 7.07, but the sum of the square roots of 10 taxa each at 5% is 22.36 even though the sum of the percentages is the same 50%. This effect can be particularly pronounced in marine pollen samples because they are usually dominated by a single taxa (Pinus) that forms a high percentage of the total assemblage. Since there are often more non-arboreal taxa than arboreal taxa in a pollen assemblage, the non-arboreal taxa can dominate in the biomisation process even if collectively their percentage of the assemblage is a lot less than the arboreal taxa, resulting in a non-arboreal biome such as STEP having the highest biome score.

The main arboreal biomes found at the LGM include Taiga (TAIG), Cool Mixed Forest (COMX), Cool Conifer Forest (COCO) and Xerophytic Scrub (XERO), with just a single occurrence of Cold Mixed Forest (COMX) and Warm Mixed Forest (WAMX). We do not record any Temperate Deciduous Forest (TEDE), Tundra (TUND) or Desert (DESE) biomes at any site at the LGM.

An alternative picture of LGM tree-cover is provided by the MAT reconstructions (Fig. 5). MAT performance statistics for tree cover are shown in table 3, based on an evaluation using the modern training set. This shows a relatively large root mean square error (RMSE) of 21.03. and an R2 of 0.52 that is not as good as for the MAT climate analysis, but overall the results are comparable with previous MAT tree cover studies (Zanon et al., 2018). In general, the MAT values (site average 34%) show forest-cover around 16% less than that suggested from AP% (site average 50%) (Fig. 3), although sites with very low AP% also show higher values based on MAT. These differences are consistent with comparisons between MAT and AP% in Zanon et al (2018), although it should be noted that uncertainties related to the MAT reconstructions are large (± 23%). Zanon et al (2018) found that the differences between MAT and AP% were greatest over Northern Europe and in Arctic and sub-Arctic climate regions that are likely to be comparable to many areas of Europe during the LGM. These regions today are associated with tree-forming taxa such as Birch that fail to grow to a height of 5m or more, developing only as shrubs or krummholz forms.

Pollen taxa percentages are shown in figure 6, and distribution maps of the 33 most common taxa are shown in the supplementary figures A1a-f. Of the 21 arboreal taxa, Pinus generally has the highest values and is the most

https://doi.org/10.5194/cp-2022-59
Preprint. Discussion started: 31 August 2022


Climate of the Past Discussions

widespread, being present at all 63 sites. Other acicular arboreal taxa include Juniperus, which also has a wide distribution across EurMedMidEst although at lower values. The rest of the acicular arboreal taxa have more regional distributions. Picea is found mainly to the north of the study region, away from the Mediterranean, whilst Abies is generally found more to the south. Larix occurs only in the central European area including the northern edge of the Po plain just south of the Alps, whilst Cedrus is found mainly across south and west Europe in locations much further north than its Holocene and modern distribution which is confined mainly to Morocco and Lebanon (Collins et al., 2012). Temperate broadleaf arboreal taxa which also include cold-tolerant species such as Betula and Salix are relatively widely spread across the EurMedMidEst during the LGM, while less dought tolerant taxa such as Alnus, Carpinus and Corylus are found more to the south-west through to the north-east. Other temperate broadleaf arboreal taxa such as Quercus (deciduous) and Ulmus have a much more southern distribution, with Fraxinus, Olea, and Quercus (evergreen) being more prevalent in the south-west. In contrast, Fagus occurs more to centre and the east, while Tilia is found even in more northern locations of central Europe. The remaining arboreal taxa are more shrubby and drought adapted, with Ephedra and particularly Ephedra fragilis having a southern distribution, whilst the more cold adapted Hippophae being found even in the north of central Europe (similar to Tilia).

The main non-arboreal taxa generally indicate cool, dry and environmentally disturbed conditions across much of the EurMedMidEst. The most widely distributed taxon is Poaceae, which like Pinus, is found in all records. Other non-arboreal taxa with a widespread distribution include Rubiaceae, Apiaceae and Asteraceae (Asteroideae), while Plantago, Cayophyllaceae, Brassicaceae and Asteraceae (Cichorioideae) have a more southern and western distribution. Thalictrum can be found mostly at sites in the centre of the EurMedMidEst, along with Helianthemum which also extends to sites in the south-west. Other taxa such as Chenopodiaceae and Artemisia have a more southern distribution, reflecting their preference for drier and less cold climates.

3.2 Climate reconstruction evaluation

Evaluation of transfer function performance based on the modern training set is presented in table 3. This shows that root mean square error predicted (RMSEP) values were smallest for summer temperatures (2.21C), and largest for winter temperature (3.35C), with mean annual temperatures in between (2.28C). The weaker performance for winter temperatures largely reflects the much greater range of winter temperatures in the training set. In turn, this contributes to a better R2 performance for winter temperatures (0.91) than annual temperatures (0.9) and summer temperatures (0.81). Overall R2 performance for precipitation is weaker than for temperature, which is typical because of the higher spatial variability of precipitation compared to temperature. Summer precipitation has the strongest R2 performance (0.75) compared to winter and annual precipitation (both 0.69), as well as smaller RMSE values (52mm) than winter (78mm).

These results indicate good transfer function performance especially for temperature, and are comparable with those found in other continental scale pollen-climate studies (Bartlein et al., 2011). It is important to remember though that comparisons between studies can only be made with caution because results are often heavily

https://doi.org/10.5194/cp-2022-59
Preprint. Discussion started: 31 August 2022


Climate of the Past Discussions
Open Access
EGU

dependent on the nature of the modern pollen dataset used as the training set, which is not the same in all studies (Juggins, 2013).

The evaluation of pollen-climate transfer function performance using the modern training set necessarily only indicates performance for the present-day climate and vegetation. We therefore undertook two additional tests of our MAT methodology to assess performance during the LGM. The first test was to compare our MAT results with previous pollen-climate reconstructions based on the same LGM sites but using different methods. These previous reconstructions include the neural-network methodology of Peyron et al. (1998) and Jost et al. (2005) which we call MAT-NN, as well as the Inverse Modelling approach by Wu et al. (2007) which we call INV.

We found 10 sites/records in our dataset which were also included in these earlier analysis (Fig. 7). All of the other sites used in these earlier studies were excluded from our study because of poor dating control. While these previous studies almost certainly shared the same pollen dataset, this dataset has never been placed in the public domain and no metadata provided other than the name of the site and the publication. In other words, it is not known if 1) the data represented a single sample or the mean of multiple samples within a time-window, 2) what the actual depth/age of those samples were or the actual sediment core in the case of multiple cores, 3) if the data was digitized or had a restricted taxa list (as was the case with the data from Huntley & Birks (1983), which is a likely source). While these aspects are unknown, it seems likely that the pollen data we used in our analysis was very similar if not identical in most cases, and in fact we found that the biomes reconstructed from our pollen dataset for these 10 sites are identical to the biomes reconstructed using the earlier pollen dataset (Elenga et al., 2000).

We compare our MAT with the MAT-NN and INV reconstructions in figure 7. On average across all 10 records, the MAT and INV methods give almost identical results for both anomalies of mean annual temperature (MAT -6.6C, INV -7.2C) and precipitation (MAT 158mm, INV 165mm). Uncertainties are also similar for both methods. In contrast, the MAT-NN method gives much cooler mean annual temperature anomalies (MAT-NN -13.9C) and drier precipitation anomalies (MAT-NN -474mm). On a site by site basis the MAT and INV methods show closer agreement for temperatures than precipitation, although precipitation has proportionally larger uncertainties. The reconstructions based on these two methods are close enough that the uncertainties overlap at all sites for both temperature and precipitation, except the precipitation reconstruction at Lac de Bouchet (site 25). The reason for this is not clear, but there could easily be differences with the pollen data analysed by Wu et al. (2007) in their INV reconstruction since the pollen record at Lac de Bouchet (Reille and de Beaulieu, 1988) includes multiple cores each with many different samples covering the LGM period.

The second evaluation of the MAT reconstruction method is based on comparison with a chironomid summer temperature record from Lago della Costa (site #34) in Northern Italy, analyzed by Samartin et al. (2016). We compare the chironomid record with our MAT reconstruction using pollen data that Samaratin et al (2016) also analysed from the same core. The results are presented in Fig. 8 and are shown as anomalies compared to the present day over our LGM time-window (19-23k BP). Our pollen-climate reconstruction is for JJA mean temperate, while the chironomid reconstruction is for July mean temperature, with the anomalies based on the

https://doi.org/10.5194/cp-2022-59
Preprint. Discussion started: 31 August 2022

modern equivalent JJA and July mean temperatures respectively. The average anomaly values for all 8 samples reconstructed by the pollen-climate MAT are -10.2 ± 3.5C, and for the chironomids -9.5 ± 3.0C. This indicates that pollen and chironomid average summer temperature reconstructions are almost identical taking into account the overlapping uncertainties, while also showing a strong similarity on a sample-by-sample basis throughout the time-series.

3.3 Climate reconstruction

Reconstructed LGM temperatures indicate an overall mean annual cooling of -7.2 ± 3.3C, with a greater cooling of around -9.3 ± 4.5C in winter and -5.0 ± 3.2C in summer (Fig. 9). All sites apart from Lake Van [62] in eastern Turkey show cooler temperatures at the LGM compared to modern (Fig. 10), and even at this site cooler conditions fall within the uncertainties. With greater cooling in winter compared to summer, the difference in temperature between winter and summer also increased (shown by positive anomalies) at most (but not all) sites (Fig. 10). This increase in continentality was around +4.2C on average across all sites (Fig. 9).

We reconstruct an overall decline in mean annual precipitation of around -91 ± 270mm (-13%) at the LGM. Most of this decline is in winter (-38 ± 90mm) (-21%), while in summer a small increase is shown (10 ± 57mm) (6%), although uncertainties are large (Fig. 11). Compared to temperature there is significant seasonal and spatial variability in positive and negative precipitation anomalies (Fig. 12). Positive anomalies appear more predominant in eastern and southern Spain and in central eastern Europe in both summer and winter, while positive anomalies are found more generally in summer across sites in Southern Europe and the Mediterranean. These more positive summer anomalies also reflect a relative shift from winter to summer in the seasonality of precipitation in this region.

4.0 Discussion

Before we consider the results of our analysis it is important to provide some context in terms of European LGM geography and environment, which was very different from today (Fig. 1). Major ice sheets covered Scandinavia and much of the UK, the Alps, and the Pyrenees. Sea level was 120m lower, resulting in much of the North Sea and English Channel becoming dry land, and the European coastline extending over 100 km out into the Atlantic and Mediterranean, especially around the Bay of Biscay and Adriatic. The Black Sea was no longer connected to the Mediterranean, and was smaller with a water level around 100m lower than today (Genov, 2016). These changes in sea or water level had two main consequences, the first being that the marine sites were closer to land, and therefore closer to (low lying) terrestrial vegetation and (pollen carrying) river discharge points than they are today. The second consequence of lower seas levels is that terrestrial pollen sites were located further from the moderating effect of the ocean than they are today, resulting in a localised modification of the climate experienced by the site irrespective of regional or global changes.

The maps used in our analysis shows the maximum ice sheet at 21k ± 2k (Ehlers et al., 2011). The precise geographical location of the ice sheet is difficult to resolve at a fine spatial scale, however, which explains why

https://doi.org/10.5194/cp-2022-59
Preprint. Discussion started: 31 August 2022


Climate of the Past Discussions

some sites close to the ice margin appear to be actually located under the ice (for example sites site #46 & site #54). The resolution of the map also shows the occurrence of permanent ice not only to the north and over the Alps, but also on many subsidiary areas of high ground across central and southern Europe, including areas such as the Pyrenees, Massif Central, Vosges and Carpathian Mountains. While global ice volume may have peaked ~21 ka individual ice sheets in Europe and other areas are known to have reached their maximum extent at different times (Hughes et al., 2016). The larger ice sheets are likely to have had a significant influence on regional climate and environmental conditions across Europe, but the smaller ice sheets had similar if more localized impacts as well. Surrounding each ice sheet would have been an unglaciated area of active peri-glacial processes and newly created and unstable ground. This would include outwash plains, impounded lakes and recently drained lake beds, seasonally and sporadically flooded areas, moraines, kettle holes and other glaciological and peri-glacial features. Soils in these areas would be non-existent or skeletal, and vegetation would find it difficult to obtain nutrients and water for survival, irrespective of the prevailing climatic conditions. Outside of these areas, permafrost is also likely to have been present, particularly north of the Alps (Vandenberghe et al., 2014), which would also act as an impediment to vegetation growth.

In terms of regional climate, the major ice sheets would have provided significant barriers to westerly atmospheric circulation, or even north-south circulation in the case of the Alps and Pyrenees. As well as representing a physical obstruction, the thermodynamic response of the atmosphere to these high, cold obstructions would have been to encourage the formation of areas of semi-permanent high pressure, similar to those found today for instance over the Greenland ice sheet. In addition, the Laurentide ice sheet located over North America would have generated downstream effects over Europe. These physical and thermodynamic effects would have affected the direction of storm tracks, as well as more local climatic effects commonly associated with ice sheets such as strong katabatic winds.

4.1 Vegetation Cover

The nature and extent of forest cover during the LGM remains a matter of considerable debate. Vegetation models driven by LGM climate model simulations generally indicate extensive areas of boreal forest north of the Alps, and a mix of temperate and warm-temperate woodland to the south across southern Europe and much of the Mediterranean. Treeless areas such as steppe are mainly confined to those areas where it is also found today, namely inland Iberia, Ukraine, southern Russia and Turkey, while Tundra is found to the north close to the Scandinavian Ice Sheet (Allen et al., 2010; Cao et al., 2019; Prentice et al., 2011; Velasquez et al., 2021).

Evaluation of these vegetation-model simulations against data has been largely based on comparison with compilations of pollen-biome reconstructions (Prentice et al., 2011; Allen et al., 2010; Cao et al., 2019; Velasquez et al., 2021). Early studies were based on only a limited number of sites from southern Europe, and showed steppe at all sites in contradiction with model simulations (Elenga et al. 2000). More recent pollen compilations have included more sites especially to the north that have revealed a more mixed picture of vegetation cover, with forest biomes at some sites both south and north of the Alps that appear more consistent with model simulations (Binney et al., 2017; Cao et al., 2019). However, many of these pollen sites used in these studies were assigned an LGM

https://doi.org/10.5194/cp-2022-59
Preprint. Discussion started: 31 August 2022


Climate of the Past Discussions
Open Access
EGU

556 age based on poor or incorrect dating control, and likely date to MIS3, the Late-Glacial or even the Holocene.
557 Nevertheless, based on our compilation of more securely dated LGM pollen sites, we also show a wider
558 distribution of forest biomes particularly in Iberia, northern Italy and Central Europe, although with greater areas
559 of steppe than suggested by the models over the remaining regions.
560
561 However, the interpretation of biome reconstructions requires care since the forest cover and vegetation
562 composition may not be as clear as the dominant biome suggests. For instance, we find that steppe is still
563 reconstructed as the dominant biome at some sites despite arboreal pollen forming 70-80% of the pollen
564 assemblage. In addition, it is important to remember that pollen-biomes are based only on the proportion of taxa
565 that can form forest and woodland, while these taxa may in fact exist only as shrubs or stunted krummholz forms
566 in the challenging climate and environment of the LGM. Alternatively, similar conditions may favour low-lying
567 non-arboreal taxa forms with poor pollen dispersion or even insect pollinated taxa forms that may be poorly
568 represented in the pollen assemblage, giving greater prominence to arboreal taxa whose pollen may be the result
569 of long-distance transport.
570
571 Quantitative MAT based reconstructions of forest cover can overcome some of these problems where they can be
572 detected based on the composition of the pollen assemblage when compared with the modern land-cover. Chord-
573 distance measurements of the match between fossil and modern pollen assemblages indicate good LGM analogues
574 exist in our large Eurasian modern pollen dataset. The results of the MAT forest cover reconstruction indicates
575 that forest cover was low but not entirely devoid of woodland in most areas, similar to the modern boreal forests
576 of Siberia and consistent with a steppe-tundra-woodland mosaic proposed by many authors (e.g. Birks and Willis,
577 2008; Willis and Van Andel, 2004). Uncertainties are large, but for comparison the MAT site-average of 33% is
578 slightly less than the average today over the Boreal region of Europe (43%) and slightly more than the average
579 today over Mediterranean region (27%) (Zanon et al. 2018).
580
581 By calculating the percentage of each of the taxa in each LGM pollen sample using a standardized pollen sum,
582 we are able to make direct comparisons between different LGM pollen records and their taxa percentages (Figure
583 6, A1). The results show a preponderance of boreal forest taxa to the north of the Alps, consistent with biome
584 results mentioned earlier. Pinus is the most common forest forming taxa in this boreal zone, together with Picea,
585 and including Larix to the east and Abies to the west. The occurrence of Betula and Juniperus also suggests
586 shrubby elements consistent with arctic shrub-tundra, although high Poaceae and other herbaceous taxa such as
587 Artemisia and Chenopodiaceae indicate more steppe than tundra. Other deciduous taxa found north of the Alps
588 include cold tolerant generalists such as Corylus and Alnus, as well as low percentages of relatively thermophilous
589 taxa in the east, such as Carpinus and Tilia.
590
591 These results are consistent with charcoal (Magyari et al., 2014a; Willis and Van Andel, 2004), malacological
592 (Juřičková et al., 2014), biomarkers (Zech et al., 2010) and genetic evidence (Stivrins et al., 2016; Willis and Van
593 Andel, 2004) that the main forest region north of the Alps was in the eastern region of Central Europe around the
594 Carpathian basin. This was also an area where cold and moisture sensitive deciduous taxa were also able to survive
595 (Magyari et al., 2014), although evidence of temperate taxa found in the pollen record has yet to be supported by

https://doi.org/10.5194/cp-2022-59
Preprint. Discussion started: 31 August 2022


Climate of the Past Discussions

charcoal and macrofossil records (Feurdean et al., 2014). Our pollen evidence indicates an open taiga or cool mixed forest that extended in central and eastern Europe to areas close to the Scandinavian and Alpine ice caps, as proposed by Willis and Van Andel (2004) and Huntley and Allen (2003), although whether this represents isolated pockets of forest or an extended open steppe-forest is difficult to determine (Kuneš et al., 2008). Even steppe or tundra areas in western Europe show a low but significant presence of the pollen of tree taxa at sites close to the ice sheets that are unlikely to be solely the result of long distance transport or reworking (Kelly et al., 2010). The presence of woodland in these areas is also supported by mammalian remains, for instance at Kents Cavern in SW England (Stewart and Lister, 2001).

Overall however, our results clearly show a much greater predominance of thermophilious and moisture sensitive deciduous taxa south of the Alps, particularly in Iberia and Northern Italy, where temperate broadleaf forests survived in sheltered refugia (Kaltenrieder et al., 2009). Most of these appear to be in hilly areas with the ability to generate orographic rainfall (Monegato et al., 2015), on south facing slopes to make the most of the sun's radiant energy and located above the valley floor to escape frost and flooding. We might also expect these areas to be sheltered from cold northerly winds, and benefit from relatively mild and moisture laden winds coming from the Mediterranean Sea. For instance, the presence of woodland and low glacier altitudes along the southern slopes of the Alps around the Po Valley and Trentino region is consistent with strong orographic rains generated by southerly and easterly winds that today can be generated by low pressure located south of the Alps in the Gulf of Genoa, and consistent with a southerly storm track around the Alps (Kehrwald et al., 2010; Luetscher et al., 2015). Generally, as might be expected, areas of forest reconstruct similar or increased precipitation compared to today, and areas of steppe indicate deceased precipitation (see next section).

Independent evidence of LGM vegetation is provided by archaezoological data. This data supports the palynological evidence for the existence of forest and woodland refugia across the ice-free areas of Europe at latitudes north of the Alps. For instance, large vertebrates in these areas show patterns of extirpation and extinction in response to shifts in climate and vegetation cover that is different for different species, indicating a variety of environments and niches (Lister and Stuart, 2008; Stewart and Lister, 2001). As with the pollen record, the presence of temperate adapted large vertebrate taxa within the glacial landscape of Western Europe also suggests the existence of temperate "micro-refugia" (Stewart and Lister, 2001) , consistent with suggestions that temperate arboreal taxa were not entirely extirpated from the region during the LGM (Magri, 2010). Further east, mammal assemblages indicate generalized loss of forest components in the East European Plain (Puzachenko et al., 2021) which is consistent with our data indicating low forest cover in this region. In other areas, evidence of the prevailing land cover at the LGM comes from studies of small vertebrate communities, which have a closer affinity to the prevailing environment than large vertebrates (López-García and Blain, 2020) that have the propensity to migrate large distances, often on a seasonal basis. These studies of small vertebrate assemblages also support the existence of temperate "micro-refugia" in France (Royer et al., 2016) and the existence of woodland components in many regions across Southern Europe including parts of Iberia (Bañuls-Cardona et al., 2014) Italy (Berto et al., 2019) and the Balkan Peninsula (Mauch Lenardić et al., 2018).

https://doi.org/10.5194/cp-2022-59
Preprint. Discussion started: 31 August 2022


Climate of the Past Discussions

Other paleobotanical evidence also supports our land cover reconstruction. Schafer et al. (2016) suggest leaf wax patterns from palaeosols in Spain may indicate the presence of drought intolerant deciduous trees and more humid conditions during the LGM. Significantly, none of the pollen sites indicate that temperate broadleaf forests were dominant, and broadleaf temperate taxa always appear part of a mixed woodland together with cold or aridity adapted evergreen and needleaf taxa, including typical Mediterranean taxa. This type of mixed vegetation probably extended to the Balkans where the hilly terrain and proximity to the Mediterranean would appear to have provided favourable climatic conditions, although we still lack LGM sites from this region. At sites in central and southern Italy and east through Greece and Turkey to the Middle East (and including North Africa), the vegetation appears drier with a greater prevalence of steppe. Only a site in Georgia in the Caucasian mountains indicates the presence of significant amounts of forest (mainly Pinus), a result that was also found by Tarasov et al. (2000), and probably linked to favourable orographic precipitation and proximity to the Black Sea.

Comparison with LGM land cover from vegetation modelling studies driven by climate model simulations indicate a much wider presence of forest than that shown by the pollen data (Kaplan et al., 2016). Data-model agreement appears to be closest over eastern-central Europe where pollen indicates the presence of open Boreal forest, and over south-west Europe with the presence of cool mixed temperate forest, including broadleaf deciduous and thermophilious elements (Prentice et al., 2011; Allen et al., 2010; Cao et al., 2019; Velasquez et al., 2021). Nevertheless, agreement still appears to be weak over western-central Europe and Southern and Eastern Europe through to the Middle East, where pollen data continues to indicate widespread steppe. One proposed explanation for this data-model discrepancy has been the role of fire (including man-made fire) in maintaining forest openness, a factor influencing forest cover that is not included in most vegetation models (Kaplan et al., 2016). In the Carpathian basin Magyari et al. (2014a) noted that charcoal increased as forest cover declined, suggesting that wildfires played a role in decreasing forest cover during the LGM. Other studies have noted low levels of charcoal and therefore fires during the LGM, although these tend to be from steppe areas with low biomass and fuel availability (Connor et al., 2013; Kaltenrieder et al., 2009). Recent LGM vegetation simulations that include fire indicate much lower values of forest cover than those without fire over western central Europe, while forest remains in central eastern Europe (see figure 6 in Velasquez et al., 2021). This appears closer to the data, but the values are perhaps too low compared with our MAT reconstructions here (Figure 5).

4.2 Climate: Temperature

The climate of the LGM is generally considered to have been cooler and drier than today, but data-model comparisons continue to highlight important discrepancies, not only in the degree of cooling and drying but also in their seasonal and spatial distribution. Data-model comparisons over Europe have mainly used quantitative pollen-based climate reconstructions, especially the Palaeo-model Intercomparison Project (PMIP/CMIP) (Bartlein et al., 2011; Harrison et al., 2015; Kageyama et al., 2006). These pollen reconstructions use many of the same compilations of LGM pollen data used in the biome reconstructions mentioned earlier (Elenga et al., 2000), and therefore suffer from the same problems of dating control, unclear provenance and a potentially limited taxa assemblages.

https://doi.org/10.5194/cp-2022-59
Preprint. Discussion started: 31 August 2022


Climate of the Past Discussions
Open Access
EGU

We identified 10 LGM pollen records where we could directly compare our MAT-based pollen-climate reconstruction with previous pollen-climate reconstructions based on Inverse Modelling (INV) (Wu et al., 2007), and the Neural Networks method which is a version of MAT (MAT-NN) (Peyron et al., 1998a). This comparison showed that our MAT reconstructions were very similar to the INV method, but not as cold or dry as the MAT-NN method. This has two main implications. The first is that our reconstructions indicate greater agreement with the results of climate model simulations since climate models indicate temperatures closer to the INV reconstructions (Latombe et al., 2018) than the MAT-NN reconstructions (Jost et al., 2005; Kageyama et al., 2006). The difference between our MAT and the MAT-NN reconstructions is likely the result of the modern calibration datasets used, since the MAT-NN reconstruction by Peyron et al. (1998a) was based on a considerably smaller number of samples taken mainly from the cold dry steppes of Kazakstan and Mongolia. The second implication is that the MAT method may not be significantly impacted by the effects of lower CO2 (Cowling and Sykes, 1999; Prentice and Harrison, 2009; Williams et al., 2000) or indeed insolation changes during the LGM, since the MAT results are similar to those based on the INV method which specifically takes account of these non-climatic factors (Wu et al., 2007). This would also suggest that MAT could also work well for pollen-based climate reconstructions on longer glacial-interglacial timescales where insolation and CO2 vary significantly from their modern values.

Comparison with LGM climate reconstructions based on other (non-pollen) proxies provides another way of evaluating our pollen-based reconstruction. We reconstruct both summer and winter temperatures and show that cooling in winter was greater than in summer at most sites, associated with an increase in continentality (increased temperature difference between summer and winter). A similar seasonal pattern of temperature change has also been shown in other studies that reconstruct both summer and winter LGM temperatures, including Prud'homme et al. (2016) using d18O analysis of earthworm calcite granules at Nussloch near the French-German border, Bañuls-Cardona et al. (2014) using faunal remains of small mammals at 4 locations in western Spain, and Ferguson et al. (2011) who examined seasonal temperature change using d18O and Mg/Ca analysis of limpet shells at Gibraltar in southern Spain. The increase in continentality at Nussloch (Prud'homme et al., 2016) was reconstructed at between 11.6 to 15.6 ºC, comparable at the lower end with nearby pollen sites [site #28] 10.4 ± 5.8 ºC and [site #29] 7.9 ± 5.7 ºC. The faunal sites in western Spain studied by Bañuls-Cardona et al. (2014) gave much reduced increases in continentality, but nevertheless similar to nearby pollen sites. For instance at Valdavara 5.1 ºC [site #3] 5.2± 3.1 ºC , El Miron 1.2 ºC [site #19] 5.1 ± 6.2 ºC, El Portalon 0.9C [site #16] 2.8 ± 1.8 ºC and Cueva de Maltrvieso 6.1C [site #2] 4.8 ± 3.4 ºC. Further south at Gibraltar the limpet-based study of Ferguson et al. (2011) also shows a relatively small increase of 2 ºC. The nearest pollen site [site #5] however shows a larger increase of 4.7 ± 2.3 ºC, although differences could be expected given the different temporal resolution of annual laminae on mollusk shells compared to pollen assemblages that reflecting much slower changes in trees and other long-lived flora.

Summer temperatures were warm enough during the LGM over the Alpine areas that Swiss lakes were largely ice free in summer, while glacier ELA's around the time of the LGM suggest summers were -6.5 to -7.7 ºC cooler compared to the LIA (Heiri et al., 2014). This cooling was similar to that found at Nussloch some 200km north of the Swiss border by Prud'homme et al. (2016), who reconstructed anomalies of -6 to -8 ± 4 ºC from d18O

https://doi.org/10.5194/cp-2022-59
Preprint. Discussion started: 31 August 2022

analysis of earthworm calcite granules (representing warm season May-September temperatures). Slightly less cooling was found close by at the nearby site of Achenheim where analysis of Mollusc assemblages gave summer (August) cooling estimates of -3.5 to -6.5 ºC based on MAT (Rousseau, 1991), and -5.5 to -9.5 ºC based on the Mutual Climatic Range method (Moine et al., 2002). These reconstructions appear somewhat cooler than nearby pollen sites [site #28] -1.4 ± 3.6 ºC and [site #29] -2.7 ± 5.1 ºC, although comparable with the pollen site [site #32] 7.3 ± 5.0 ºC 200 km further east. Similar differences also occur at the site of Les Echets on the western edge of the Alps where a Diatom based reconstruction of summer (July) temperatures (Ampel et al., 2010) indicated a greater cooling (-10.5 to -11.5 ºC) than our pollen reconstruction [site #27] (-4 ± 2.7 ºC). However, the authors caution that the results were based on poor analogues and rare taxa, as well as a small training set of only 90 lakes in Switzerland.

South of the Alps, other proxies show the opposite relationship with the pollen reconstructions. For instance, at Lago dela Costa in the Po valley, a summer (July) temperature chironomid reconstruction by Samartin et al. (2016) is around 1-2 ºC less cool than the pollen reconstruction (JJA) for the same site [site #34] -11.4 ± 2.7C, although both reconstructions fall within their respective uncertainty ranges (Figure 8). In the Pindus Mountains in Greece, Hughes et al (Hughes et al., 2006) estimated LGM summer temperature anomalies of - 7 ºC based on glacier modelling, which is comparable with that reconstructed at the nearest pollen site [site #51] -7.7 ± 2.8 ºC. In Spain the analysis of small mammal remains by Bañuls-Cardona et al. (2014) shows similarly less cooling in summer or even warmer than present positive anomalies compared to the nearest pollen sites, such as Valdavara 1.4 ºC [site #3] -2.3 ± 2.8 ºC , El Miron -2.3 ºC [site #19] -5.7 ± 5.4 C, El Portalon 0.8 ºC [site #16] -2.6 ± 1.1 ºC and Cueva de Maltrvieso -1.1C [site #2] 10.4± 2.8 ºC. Further south at Gibraltar, the limpet-based study of Ferguson et al. (2012) suggests an anomaly of around -7 ºC, which is a greater cooling than the pollen reconstruction from this location [site #5] -1.3 ± 2.2 ºC, although comparable with other pollen sites slightly further east.

Winter temperature reconstructions from non-pollen proxies show a similar pattern in relation to pollen reconstructions as for summer temperatures. North of the Alps at Achenheim, Prud'homme et al. (2016) use d18O on earthworm remains to reconstruct particularly cold winter anomalies of -17.6 to -23.6 ºC compared to nearby pollen sites [site #28] -11.8 ± 8.0 ºC and [site #29] -10.6 ± 6.3 ºC. South of the Alps in Spain, the analysis by Bañuls-Cardona et al (2014) based on the remains of small mammals shows less cooling in winter compared to the nearest pollen sites, in particular Valdavara -3.7 ºC [site #3] -7.5 ± 3.4 ºC , El Miron -3.5 ºC [site #19] -10.8 ± 7.0 ºC, El Portalon -0.1 ºC [site #16] -5.4 ± 2.5 ºC and Cueva de Maltrvieso -7.2C [site #2] 15.2 ± 4.0 ºC. And again, in southern Spain at Gibralter, analysis of limpet shells by Ferguson et al (2011) suggests winter cooling of around -9 ºC while the pollen reconstruction suggests [site #5] -6.0 ± 2.5 ºC, although sites further east indicate cooler conditions.

A number of additional proxies have also been used to reconstruct LGM mean annual temperature. Heyman et al. (2013) applied glacier mass balance modelling at sites located in the smaller mountain regions north of the Alps. These are generally slightly cooler than our pollen-based reconstructions at sites close to the Vosge Mountains -12.7 ± 2.0 ºC and Black Forest -11.4± 2.3 ºC [site #29] -8.2 ± 3.3 ºC, Bavarian Forest -10.7± 2.2 [site #32] -9.2 ± 1.2 ºC and Giant Mountains -8.5 ± 1.8 [site #46] -7.3 ± 0.3 ºC. These values obtained by Heyman et al. (2013) are

https://doi.org/10.5194/cp-2022-59
Preprint. Discussion started: 31 August 2022

warmer than Pud'homme et al. (2016) who estimated annual mean temperature anomalies of -15.1 to 19.1 ºC based on d18O of earthworm calcite at the Nussloch site just north of the Vosge and Black Forest. The annual temperatures reconstructed by Heyman et al. (2013) are also around 2C warmer than Allen et al. (2008) who applied a similar, although simpler method to over 29 different mountainous regions across Europe that had been glaciated during the LGM. Since glacier mass balance is a function of both snowfall and temperature, these estimated temperatures vary according to estimated changes in precipitation. For instance, mean annual temperature estimates by Allen et al. (2008) are much cooler than reconstructed by pollen, with an average anomaly of -13.2 ºC for the 29 sites assuming a 40% reduction in precipitation, but this is reduced to -11.8 ºC assuming the same precipitation as modern. This compares with -7.2 ºC for our 63 pollen sites. The glacier mass balance modelling by Allen et al. (2008) assumes a seasonal distribution of precipitation that is similar to the present day, and does not consider increases in winter precipitation or mean annual precipitation above present day levels. Both of these are suggested by the pollen data in some regions, and both could explain glacier extent found during the LGM based on less extreme temperature anomalies more comparable with the pollen data.

To the east of the Alps in the Panonian basin, mean annual temperature anomaly estimates have been made from noble gas measurements on groundwater ranging from -2 to -4 ºC (Stute and Deak, 1990) up to -9 ºC (Varsányi et al., 2011). These are similar to estimates ranging from -2 to -9 ºC from oxygen isotope ratios from mammoth tooth enamel (Kovács et al., 2012) and are comparable with nearby pollen sites [site #50] -8.2 ± 3.3 ºC and [site #52] -4.5 ± 2.3 ºC. On a broader scale, Sanchi et al (2014) estimated LGM cooling in the Danube and Dneiper basins based on Lipid biomarkers in a core from the Black Sea and came up with similar mean annual temperature anomalies between -6 to -10 ºC, which again are comparable with pollen sites from the region that range from [site #48] -10.5 ± 4.1 ºC to [site #57] -4.3 ± 5.8 ºC.

Further south and west, García-Amorena et al. (2007) reported mean annual temperature anomalies of -2.0 to -11.3 ºC at LGM sites along the Portuguese coast, based on an indicator species method using plant macrofossils. This is similar to the closest marine pollen sites off the coast, which recorded values of [site #1] -10.5 ± 4.6 ºC and [site #3] -5.3± 2.9 ºC. Meanwhile, in the far east of the study area, Zaarur et al. (2016) estimated a mean annual temperature anomaly of around -3 ºC based on clumped isotope analysis of Melanopsis shells from LGM sediments in the Sea of Galilee. This limited cooling appears similar to the nearest pollen site [site #63] where we reconstruct a cooling of -2.2 ± 4.6 ºC.

Reconstructions of LGM sea surface temperatures (SST's) provide yet another source of comparison with our terrestrial pollen-based reconstructions, although many of the physical processes controlling surface sea temperatures such as upwelling, surface mixing, surface currents, stratification and thermal inertia through the seasonal cycle, represent quite different processes to those controlling surface temperatures over land, particularly at the sub-regional scale. Nevertheless, the Atlantic coastal waters of Iberia and the waters throughout the Mediterranean Sea include many SST sites that lie in relative proximity to our terrestrial pollen-sites, allowing us to make a comparison at the largest scale. Within this area the MARGO database (MARGO Members, 2009) includes 13 Alkenone, 2 Mg/Ca and 41 Foraminifera based SST records of mean annual temperature, with the Foraminifera records also providing an additional 41 winter (JFM) and summer (JAS) SST estimates. We compare

https://doi.org/10.5194/cp-2022-59
Preprint. Discussion started: 31 August 2022

Climate of the Past Discussions
Open Access
EGU

795 the SST records with the 36 closest terrestrial pollen records which fall within a box of -11 to 35 degrees longitude
796 and 32 to 43 degrees latitude containing all of the SST records. A simple site average indicates a mean annual
797 SST anomaly of -5.5 ± 1.0 ºC which is relatively close to the value of -7.2 ± 3.4 ºC obtained from the terrestrial
798 pollen sites [sites #1-4, 5, 7-24, 25, 26, 30, 35-38, 41, 47, 51, 53, 56-59]. Interestingly the inter-site variance
799 (standard deviation of the reconstructed temperatures across all sites) is almost identical for the two datasets, 2.57
800 ºC for the SST sites and 2.63 ºC for the pollen sites, despite representing very different environments, proxies and
801 uncertainties. However, when we look at the seasonal temperature anomalies, we find very different results. Site
802 averaged winter SST anomalies are -3.7 ± 1.1 ºC compared to -9.3 ± 4.2 ºC for winter temperatures from terrestrial
803 pollen sites, while in summer the values are reversed, -7.0 ± 0.8 ºC compared to -5.38 ± 3.3 ºC respectively. This
804 suggests that SST's experienced greater cooling in summer compared to winter, which is the opposite to that
805 generally found in terrestrial seasonal temperature reconstructions throughout the region, although this is
806 consistent with model simulations (Mikolajewicz, 2011).
807
808 **4.3 Climate: Precipitation**
809
810 Few proxies apart from pollen provide quantitative reconstructions of precipitation during the LGM. Glacier mass
811 balance modelling includes assumptions about precipitation in order to derive temperatures (Allen et al., 2008a),
812 but neither is independent of the other. Hughes et al (2006) estimate from glacier modelling that mean annual
813 precipitation during the LGM at sites in the Pindus mountains in Greece was around 2300 ± 200, which they
814 consider to be similar to the present day (>2000mm). A small change in precipitation compared to modern values
815 is also indicated by the nearest pollen site, which is around 47km to the south [site #51], and indicates a mean
816 annual precipitation anomaly of -152 ± 294mm, representing just 15% of the modern value. A larger reduction in
817 mean annual precipitation of -45% (maximum) is reconstructed by García-Amorena et al. (2007) based on plant
818 macrofossil remains from sites on the Portuguese coast. In comparison, the closest pollen sites record values
819 which are a little lower, ranging from [site #1] -22% to [site #3] -34%. Further north in south-west Germany,
820 Prud'homme et al. (2018) reconstructed mean annual precipitation from the delta 13C of earthworm calcite
821 granules at Fussloch. They estimate a field site average of 333 (159-574) mm/yr at the LGM, which represents an
822 anomaly of -503 mm/yr (-60%) relative to the modern precipitation of 836 mm/yr. This is comparable with the
823 closest pollen site [site #29] with an anomaly of -540 mm/yr.
824
825 As with glaciers, lake levels reflect changes in moisture balance that includes the effects of both temperature (via
826 evapotranspiration) and precipitation, rather than just precipitation. They also represent semi-quantitative data at
827 best, with changes often described relative to the modern or other baseline. There are few lake level records
828 available north of the Alps, but to the south, many records indicate high lake levels in areas such as Spain (Lacey
829 et al., 2016; Moreno et al., 2012; Vegas et al., 2010), Italy (Belis et al., 1999; Giraudi, 2017), Greece and Turkey
830 (Harrison et al., 1996; Reimer et al., 2009) and the Middle East (Kolodny et al., 2005; Lev et al., 2019). These
831 lake records are also supported by evidence of higher river levels in Morocco (El Amrani et al., 2008). The cause
832 of the higher lake levels has been the subject of some debate, since many pollen records (and especially early
833 biome reconstructions) show steppe vegetation that would suggest aridity that appears incompatible with higher
834 lake levels. Prentice et al. (1992) proposed that the co-existence of steppe vegetation and high lake levels could

https://doi.org/10.5194/cp-2022-59
Preprint. Discussion started: 31 August 2022


Climate of the Past Discussions
Open Access
EGU

be possible if precipitation increased outside of the summer growing season, while summers themselves were drier and cooler with decreased evaporation. However, the results of our analysis tend to indicate the opposite in regions with higher lake levels, with increased summer rainfall and decreased winter rainfall. In addition, the increase in summer precipitation was enough to compensate for the decrease in winter rainfall, leading to an overall increase in mean annual precipitation at many pollen sites in Spain and Greece for instance. This together with depressed temperatures and consequently decreased evaporation could explain the higher lake levels, whilst also limiting the growth of trees as a result of cooler temperatures and prolonged aridity outside of the summer season. Davis & Stevenson (2007) also note a differential hydrological response between summer and winter rainfall in the Mediterranean during the Holocene that may also provide an explanation. In this case sporadic summer storms may result in high rates of runoff that may fill run-off fed lakes, but low rates of soil moisture recharge that fails to benefit vegetation in the same way winter rainfall does.

Overall, we reconstruct only a small reduction in precipitation during the LGM of around 91mm (13%) averaged over all sites, which is less than the ~200mm reduction based on the sites in the pollen-climate compilation used by PMIP (Bartlein et al., 2011). Since our precipitation reconstruction on average matches that of the INV reconstruction by Wu et al (REF), we can attribute much of the difference to the greater aridity shown in the MAT-NN reconstruction by Peyron et al and Jost et al (2005) (see figure 7). As with temperature, this is probably a reflection of the modern training set used in the MAT-NN reconstruction which is much smaller than our training set and is largely taken from the arid steppes of Kazakhstan and Mongolia. However, it is also important to recognize the significant spatial variability in precipitation, which means that a simple average of different sets of sites from different regions may not accurately reflect the change in LGM precipitation at the European scale. Nevertheless, one of the most consistent signals in our dataset is for an increase in summer precipitation over many areas of Southern Europe and the Mediterranean. This is also found in climate models, where it has been attributed to an increase in convection-driven precipitation, although the amount of precipitation generated by this mechanism varies significantly between models (Beghin et al., 2016). A more consistent response in models is for an increase in winter precipitation across Southern Europe and the Mediterranean related to a stronger and more southerly displaced jet stream, with winter precipitation also accounting for much of the change in mean annual precipitation (Beghin et al., 2016). Our reconstruction of winter precipitation however shows less support for this scenario with a more general decrease in winter precipitation apart from southern and eastern Iberia, and with summer precipitation generally more important in those sites that show an overall increase in mean annual precipitation. This may not necessarily contradict the models in terms of the strength and position of the winter jet stream, but may instead indicate that models over-estimate the amount of moisture being carried westward from the cold North Atlantic along the storm track, especially across the far northern Mediterranean. The increase in winter precipitation across southern and eastern Iberia is however entirely consistent with a strengthened and more southerly jet stream, which also brings increased winter precipitation to the region today as a result of blocking over northern Europe/Atlantic and a negative NAO (Vicente-Serrano et al., 2011).

Other areas that show an increase in winter precipitation include pollen sites around the eastern end of the Alps. This is consistent with a recent study by Spötl et al (2021) who argued, on the basis of cryogenic carbonates preserved in a cave in Austria, that heavy winter (and autumn) precipitation was a significant factor in driving

https://doi.org/10.5194/cp-2022-59
Preprint. Discussion started: 31 August 2022


Climate of the Past Discussions

LGM glaciation in the region. The seasonally specific nature of this precipitation is also supported by the same pollen sites, which do not show any increase in summer precipitation at this time.

5.0 Conclusions

We have reconstructed the climate and vegetation cover across Europe, North Africa and the Middle East at the time of the LGM based on 63 pollen records. These records were selected using strict quality control criteria, with particular attention paid to dating control, which led to the exclusion of many records that have been used in previous studies. This fully documented dataset represents the most chronologically precise and spatially resolved view of LGM climate and vegetation during the PMIP benchmarking time window at 21 ± 2 ka. Nevertheless, it is important to recognize that there are still significant spatial gaps in pollen sites especially north of the Alps, the Balkans, Turkey and the Middle East, and we continue to have only a partial understanding of the LGM over these areas.

Distribution maps were created using a standardized pollen taxonomy and sum to enable direct comparison between sites/records. Pollen biomes and quantitative MAT estimates of tree cover have also been reconstructed allowing us to determine the relative proportion of forest and woodland cover. These results show that although steppe and tundra was extensive at the time of the LGM, areas of open forest also occurred in many regions, particularly (but not exclusively) in Iberia, northern Italy and Central Europe. These forest or woodland stands are likely to have been located in environmentally favourable areas, with good soils, elevated rainfall and shelter from cold, desiccating winds. In those areas where woodland existed, Boreal taxa generally dominated north and east of the Alps, while temperate and thermophilious (mainly drought adapted) taxa were generally confined to areas south of the Alps and around the Mediterranean. The temperate deciduous forests that compose the climax community in many areas of Europe today were displaced to the south and reduced to a partnership role with Boreal elements. Overall our new reconstruction indicates greater agreement with model land cover simulations, but models still appear to over-estimate the amount of forest and woodland over areas such as France and the Benelux, Greece, Turkey and the Far East.

We reconstructed the LGM climate of Europe based on a MAT in combination with a large modern pollen calibration dataset covering the Eurasian region. In a direct comparison we found no significant difference between LGM temperatures and precipitation reconstructed from pollen using MAT, and that reconstructed by Inverse Modelling. We therefore do not find MAT performance at the time of the LGM to be significantly impaired by non-climatic plant growth factors, such as atmospheric CO2 concentration, that were significantly different compared to modern. Our results are also much closer to climate model simulations than previous studies using the Neural Network method (a variant on MAT), which suggested a climate that was much cooler and drier. The difference between our MAT reconstruction and the Neural Network reconstruction is probably attributable to the much smaller size and spatial bias of the modern calibration dataset that was used in this earlier analysis.

We also found little difference between our MAT reconstruction and a Chironomid-based summer temperature record using downcore sample by sample comparison, as well as records from a variety of other proxies based on

https://doi.org/10.5194/cp-2022-59
Preprint. Discussion started: 31 August 2022


Climate of the Past Discussions

915 a more general site by site comparison at a regional scale. However, it is notable that some studies using glacier
916 mass balance modelling methods indicate LGM temperatures that are much cooler than our pollen-based
917 reconstruction as well as reconstructions based on other proxies. The reasons behind this are not clear, but our
918 pollen-based results indicate higher than present precipitation in some areas that could explain low altitude LGM
919 ELA's without the need for such cold temperatures. We also find that although our pollen-based reconstruction
920 and those of SST's generally agree in terms of mean annual temperatures, SST's indicate greater cooling in
921 summer compared to winter, while terrestrial records indicate greater cooling in winter compared to summer.
922 These differences area also reproduced in climate models, and probably reflect the different processes driving
923 seasonal temperature change in the terrestrial and marine domain.
924
925 Reconstructions of precipitation show large spatial and seasonal variability, but generally indicate less overall
926 aridity than previously suggested from smaller scale studies which sampled less of the spatial domain. We find
927 that in some regions of Southern Europe precipitation may actually have been greater than present, especially in
928 summer, but also in winter in southern and eastern Iberia and around the southern slopes of the Alps. This may
929 have important implications in understanding the development of LGM glaciation, which may be less a function
930 of temperature than previously supposed. This could also help better explain the observed asynchronous nature
931 of glaciation even within relatively small regions such as Europe, as a result of more localized controls on ice
932 sheet development such as precipitation.
933
934 **Code/Data availability**
935
936 All of the data shown in the figures together with the fossil and modern pollen datasets will be made available on
937 pangaea.de once the review process has been completed and these datasets are therefore no longer subject to
938 change.
939
940 **Author contribution**
941
942 BASD designed the study, undertook the analysis and wrote the manuscript. MF and ER designed and prepared
943 the maps. JOK and AB reviewed the manuscript and provided additional input.
944
945 **Competing interests**
946
947 The authors declare that they have no conflict of interest.
948
949 **Acknowledgements**
950
951 This work was supported by a grant from the Fonds de Recherche du Québéc Société et Culture (2019-SE3-
952 254686) to AB. Data were obtained from the European Pollen Database (EPD), based within the Neotoma
953 Paleoecology Database (http://www.neotomadb.org). The work of data contributors, data stewards, and the

https://doi.org/10.5194/cp-2022-59
Preprint. Discussion started: 31 August 2022

Climate of the Past Discussions
Open Access
EGU

954 Neotoma and EPD community is gratefully acknowledged. We dedicate this paper in memory of Eric Grimm,
955 whose tireless work for the EPD and Neotoma helped make this study possible.
956

https://doi.org/10.5194/cp-2022-59
Preprint. Discussion started: 31 August 2022

Climate of the Past Discussions

957
958
959 **References**
960
961 ACER project members, Goñi, M. F. S., Desprat, S., Daniau, A. L., Bassinot, F. C., Polanco-Martínez, J. M.,
962 Harrison, S. P., Allen, J. R. M., Scott Anderson, R., Behling, H., Bonnefille, R., Burjachs, F., Carrión, J. S.,
963 Cheddadi, R., Clark, J. S., Combourieu-Nebout, N., Mustaphi, C. J. C., Debusk, G. H., Dupont, L. M., Finch, J.
964 M., Fletcher, W. J., Giardini, M., González, C., Gosling, W. D., Grigg, L. D., Grimm, E. C., Hayashi, R., Helmens,
965 K., Heusser, L. E., Hill, T., Hope, G., Huntley, B., Igarashi, Y., Irino, T., Jacobs, B., Jiménez-Moreno, G., Kawai,
966 S., Peter Kershaw, A., Kumon, F., Lawson, I. T., Ledru, M. P., Lézine, A. M., Mei Liew, P., Magri, D., Marchant,
967 R., Margari, V., Mayle, F. E., Merna Mckenzie, G., Moss, P., Müller, S., Müller, U. C., Naughton, F., Newnham,
968 R. M., Oba, T., Pérez-Obiol, R., Pini, R., Ravazzi, C., Roucoux, K. H., Rucina, S. M., Scott, L., Takahara, H.,
969 Tzedakis, P. C., Urrego, D. H., Van Geel, B., Guido Valencia, B., Vandergoes, M. J., Vincens, A., Whitlock, C.
970 L., Willard, D. A. and Yamamoto, M.: The ACER pollen and charcoal database: A global resource to document
971 vegetation and fire response to abrupt climate changes during the last glacial period, Earth Syst. Sci. Data, 9(2),
972 679–695, doi:10.5194/essd-9-679-2017, 2017.
973
974 Allen, J. R. M., Hickler, T., Singarayer, J. S., Sykes, M. T., Valdes, P. J. and Huntley, B.: Last glacial vegetation
975 of northern Eurasia, Quat. Sci. Rev., 29(19–20), 2604–2618, doi:10.1016/j.quascirev.2010.05.031, 2010.
976
977 Allen, R., Siegert, M. J. and Payne, A. J.: Reconstructing glacier-based climates of LGM Europe and Russia –
978 Part 2 : A dataset of LGM precipitation / temperature relations derived from degree-day modelling of palaeo
979 glaciers, , 249–263, 2008a.
980
981 Allen, R., Siegert, M. J. and Payne, A. J.: Reconstructing glacier-based climates of LGM Europe and Russia –
982 Part 3 : Comparison with previous climate reconstructions, , (1999), 265–280, 2008b.
983 Ampel, L., Bigler, C., Wohlfarth, B., Risberg, J., Lotter, A. F. and Veres, D.: Modest summer temperature
984 variability during DO cycles in western Europe, Quat. Sci. Rev., 29(11–12), 1322–1327,
985 doi:10.1016/j.quascirev.2010.03.002, 2010.
986
987 El Amrani, M., Macaire, J. J., Zarki, H., Bréhéret, J. G. and Fontugne, M.: Contrasted morphosedimentary activity
988 of the lower Kert River (northeastern Morocco) during the Late Pleistocene and the Holocene. Possible impact of
989 bioclimatic variations and human action, Comptes Rendus - Geosci., 340(8), 533–542,
990 doi:10.1016/j.crte.2008.05.004, 2008.
991
992 Anderson, P. M., Barnosky, C. W., Bartlein, P. J., Behling, P. J., Brubaker, L., Cushing, E. J., Dodson, J.,
993 Dworetsky, B., Guetter, P. J., Harrison, S. P., Huntley, B., Kutzbach, J. E., Markgraf, V., Marvel, R., McGlone,
994 M. S., Mix, A., Moar, N. T., Morley, J., Perrott, R. A., Peterson, G. M., Prell, W. L., Prentice, I. C., Ritchie, J. C.,
995 Roberts, N., Ruddiman, W. F., Salinger, M. J., Spaulding, W. G., Street-Perrott, F. A., Thompson, R. S., Wang,

https://doi.org/10.5194/cp-2022-59
Preprint. Discussion started: 31 August 2022

P. K., Webb, T., Winkler, M. G. and Wright, H. E.: Climatic changes of the last 18,000 years: Observations and model simulations, Science (80-.)., 241(4869), 1043–1052, doi:10.1126/science.241.4869.1043, 1988.

Arpe, K., Leroy, S. A. G. and Mikolajewicz, U.: A comparison of climate simulations for the last glacial maximum with three different versions of the ECHAM model and implications for summer-green tree refugia, Clim. Past, 91–114, doi:10.5194/cp-7-91-2011, 2011.

Arslanov, K. A., Dolukhanov, P. M. and Gei, N. A.: Climate, Black Sea levels and human settlements in Caucasus Littoral 50,000-9000 BP, Quat. Int., 167–168, 121–127, doi:10.1016/j.quaint.2007.02.013, 2007.

Bañuls-Cardona, S., López-García, J. M., Blain, H. A., Lozano-Fernández, I. and Cuenca-Bescós, G.: The end of the Last Glacial Maximum in the Iberian Peninsula characterized by the small-mammal assemblages, J. Iber. Geol., 40(1), 19–27, doi:10.5209/rev_JIGE.2014.v40.n1.44085, 2014.

Bartlein, P. J., Harrison, S. P., Brewer, S., Connor, S., Davis, B. A. S., Gajewski, K., Guiot, J., Harrison-Prentice, T. I., Henderson, A., Peyron, O., Prentice, I. C., Scholze, M., Seppä, H., Shuman, B., Sugita, S., Thompson, R. S., Viau, A. E., Williams, J. and Wu, H.: Pollen-based continental climate reconstructions at 6 and 21 ka: A global synthesis, Clim. Dyn., 37(3), 775–802, doi:10.1007/s00382-010-0904-1, 2011.

de Beaulieu, J.-L. and Reille, M.: Pollen analysis of a long upper Pleistocene continental sequence in a Velay maar (Massif Central, France), Palaeogeogr. Palaeoclimatol. Palaeoecol., 80(1), 35–48, 1990.

Beghin, P., Charbit, S., Kageyama, M., Combourieu-Nebout, N., Hatté, C., Dumas, C. and Peterschmitt, J. Y.: What drives LGM precipitation over the western Mediterranean? A study focused on the Iberian Peninsula and northern Morocco, Clim. Dyn., 46(7–8), 2611–2631, doi:10.1007/s00382-015-2720-0, 2016.

Belis, C. A., Lami, A., Guilizzoni, P., Ariztegui, D. and Geiger, W.: The late Pleistocene ostracod record of the crater lake sediments from Lago di Albano (Central Italy): Changes in trophic status, water level and climate, J. Paleolimnol., 21(2), 151–169, doi:10.1023/A:1008095805748, 1999.

Berto, C., López-García, J. M. and Luzi, E.: Changes in the Late Pleistocene small-mammal distribution in the Italian Peninsula, Quat. Sci. Rev., 225, doi:10.1016/j.quascirev.2019.106019, 2019.

Binney, H., Edwards, M., Macias-Fauria, M., Lozhkin, A., Anderson, P., Kaplan, J. O., Andreev, A., Bezrukova, E., Blyakharchuk, T., Jankovska, V., Khazina, I., Krivonogov, S., Kremenetski, K., Nield, J., Novenko, E., Ryabogina, N., Solovieva, N., Willis, K. and Zernitskaya, V.: Vegetation of Eurasia from the last glacial maximum to present: Key biogeographic patterns, Quat. Sci. Rev., 157, 80–97, doi:10.1016/j.quascirev.2016.11.022, 2017.

Birks, H. J. B. and Willis, K. J.: Alpines, trees, and refugia in Europe, Plant Ecol. Divers., 1(2), 147–160, doi:10.1080/17550870802349146, 2008.

https://doi.org/10.5194/cp-2022-59
Preprint. Discussion started: 31 August 2022

Bonatti, E.: Pollen sequence in the lake sediments. In: lanula: an account of the history and development of the Lago di Monterosi, Latium, Italy, in Trans. Am. phil. Soc., vol. 60, edited by G. E. Hutchinson, pp. 26–31., 1970.

Brewer, S., Guiot, J., Sánchez-Goñi, M. F. and Klotz, S.: The climate in Europe during the Eemian: a multi-method approach using pollen data, Quat. Sci. Rev., 27(25–26), 2303–2315, doi:10.1016/j.quascirev.2008.08.029, 2008.

Brewer, S., Giesecke, T., Davis, B. A. S., Finsinger, W., Wolters, S., Binney, H., de Beaulieu, J. L., Fyfe, R., Gil-Romera, G., Kühl, N., Kuneš, P., Leydet, M. and Bradshaw, R. H.: Mapping Lateglacial and Holocene European pollen data: The maps, J. Maps, 13(2), 921–928, doi:10.1080/17445647.2016.1197613, 2017.

Camuera, J., Jiménez-Moreno, G., Ramos-Román, M. J., García-Alix, A., Toney, J. L., Anderson, R. S., Jiménez-Espejo, F., Bright, J., Webster, C., Yanes, Y. and Carrión, J. S.: Vegetation and climate changes during the last two glacial-interglacial cycles in the western Mediterranean: A new long pollen record from Padul (southern Iberian Peninsula), Quat. Sci. Rev., 205, 86–105, doi:10.1016/j.quascirev.2018.12.013, 2019.

Cao, X., Tian, F., Dallmeyer, A. and Herzschuh, U.: Northern Hemisphere biome changes (>30°N) since 40 cal ka BP and their driving factors inferred from model-data comparisons, Quat. Sci. Rev., 220, 291–309, doi:10.1016/j.quascirev.2019.07.034, 2019.

Carrión, J. S.: Late quaternary pollen sequence from Carihuela Cave, southern Spain, Rev. Palaeobot. Palynol., 71(1–4), doi:10.1016/0034-6667(92)90157-C, 1992.

Carrión, J. S.: Patterns and processes of Late Quaternary environmental change in a montane region of southwestern Europe, Quat. Sci. Rev., 21, 2047–2066, 2002.

Carrión, J. S., Finlayson, C., Fernández, S., Finlayson, G., Allué, E., López-Sáez, J. A., López-García, P., Gil-Romera, G., Bailey, G. and González-Sampériz, P.: A coastal reservoir of biodiversity for Upper Pleistocene human populations: palaeoecological investigations in Gorham's Cave (Gibraltar) in the context of the Iberian Peninsula, Quat. Sci. Rev., 27(23–24), 2118–2135, doi:10.1016/j.quascirev.2008.08.016, 2008.

Cheddadi, R., Yu, G., Guiot, J., Harrison, S. P. and Colin Prentice, I.: The climate of Europe 6000 years ago, Clim. Dyn., 13(1), 1–9, 1996.

Chevalier, M., Davis, B. A. S., Heiri, O., Seppä, H., Chase, B. M., Gajewski, K., Lacourse, T., Telford, R. J., Finsinger, W., Guiot, J., Kühl, N., Maezumi, S. Y., Tipton, J. R., Carter, V. A., Brussel, T., Phelps, L. N., Dawson, A., Zanon, M., Vallé, F., Nolan, C., Mauri, A., de Vernal, A., Izumi, K., Holmström, L., Marsicek, J., Goring, S., Sommer, P. S., Chaput, M. and Kupriyanov, D.: Pollen-based climate reconstruction techniques for late Quaternary studies, Earth-Science Rev., 210, doi:10.1016/j.earscirev.2020.103384, 2020.

https://doi.org/10.5194/cp-2022-59
Preprint. Discussion started: 31 August 2022

1076
1077 Cleator, S. F., Harrison, S. P., Nichols, N. K., Colin Prentice, I. and Roulstone, I.: A new multivariable benchmark
1078 for Last Glacial Maximum climate simulations, Clim. Past, 16(2), 699–712, doi:10.5194/cp-16-699-2020, 2020.
1079
1080 Collins, P. M., Davis, B. A. S. and Kaplan, J. O.: The mid-Holocene vegetation of the Mediterranean region and
1081 southern Europe, and comparison with the present day, J. Biogeogr., 39(10), doi:10.1111/j.1365-
1082 2699.2012.02738.x, 2012.
1083
1084 Combourieu Nebout, N., Peyron, O., Dormoy, I., Desprat, S., Beaudouin, C., Kotthoff, U. and Marret, F.: Rapid
1085 climatic variability in the west Mediterranean during the last 25 000 years from high resolution pollen data, Clim.
1086 Past, 5(3), 503–521, doi:10.5194/cp-5-503-2009, 2009.
1087
1088 Connor, S. E., Ross, S. A., Sobotkova, A., Herries, A. I. R., Mooney, S. D., Longford, C. and Iliev, I.:
1089 Environmental conditions in the SE Balkans since the Last Glacial Maximum and their influence on the spread of
1090 agriculture into Europe, Quat. Sci. Rev., 68, 200–215, doi:10.1016/j.quascirev.2013.02.011, 2013.
1091
1092 Cowling, S. A. and Sykes, M. T.: Physiological significance of low atmospheric CO2 for plant-climate
1093 interactions, Quat. Res., 52(2), 237–242, doi:10.1006/qres.1999.2065, 1999.
1094
1095 Damblon, F.: L'enregistrement palynologique de la sequence pléistocène et holocène de la grotte Walou, in La
1096 grotte Walou à Trooz (Belgique), edited by C. Draily, S. Pirson, and M. Toussaint, pp. 84–129, Service public de
1097 Wallonie (Etudes et Documents, Archéologie, 21)., 2011.
1098
1099 Daniau, A.-L., Desprat, S., Aleman, J. C., Bremond, L., Davis, B., Fletcher, W., Marlon, J. R., Marquer, L.,
1100 Montade, V., Morales-Molino, C., Naughton, F., Rius, D. and Urrego, D. H.: Terrestrial plant microfossils in
1101 palaeoenvironmental studies, pollen, microcharcoal and phytolith. Towards a comprehensive understanding of
1102 vegetation, fire and climate changes over the past one million years, Rev. Micropaleontol., 63,
1103 doi:10.1016/j.revmic.2019.02.001, 2019.
1104
1105 Davis, B. A. S. and Stevenson, A. C.: The 8.2 ka event and Early-Mid Holocene forests, fires and flooding in the
1106 Central Ebro Desert, NE Spain, Quat. Sci. Rev., 26(13–14), doi:10.1016/j.quascirev.2007.04.007, 2007.
1107
1108 Davis, B. A. S., Brewer, S., Stevenson, A. C., Guiot, J., Allen, J., Almqvist-Jacobson, H., Ammann, B., Andreev,
1109 A. A., Argant, J., Atanassova, J., Balwierz, Z., Barnosky, C. D., Bartley, D. D., De Beaulieu, J. L., Beckett, S. C.,
1110 Behre, K. E., Bennett, K. D., Berglund, B. E. B., Beug, H.-J., Bezusko, L., Binka, K., Birks, H. H., Birks, H. J.
1111 B., Björck, S., Bliakhartchouk, T., Bogdel, I., Bonatti, E., Bottema, S., Bozilova, E. D. B., Bradshaw, R., Brown,
1112 A. P., Brugiapaglia, E., Carrion, J., Chernavskaya, M., Clerc, J., Clet, M., Coûteaux, M., Craig, A. J., Cserny, T.,
1113 Cwynar, L. C., Dambach, K., De Valk, E. J., Digerfeldt, G., Diot, M. F., Eastwood, W., Elina, G., Filimonova,
1114 L., Filipovitch, L., Gaillard-Lemdhal, M. J., Gauthier, A., Göransson, H., Guenet, P., Gunova, V., Hall, V. A. H.,
1115 Harmata, K., Hicks, S., Huckerby, E., Huntley, B., Huttunen, A., Hyvärinen, H., Ilves, E., Jacobson, G. L., Jahns,

https://doi.org/10.5194/cp-2022-59
Preprint. Discussion started: 31 August 2022

1116 S., Jankovská, V., Jóhansen, J., Kabailiene, M., Kelly, M. G., Khomutova, V. I., Königsson, L. K., Kremenetski,
1117 C., Kremenetskii, K. V., Krisai, I., Krisai, R., Kvavadze, E., Lamb, H., Lazarova, M. A., Litt, T., Lotter, A. F.,
1118 Lowe, J. J., Magyari, E., Makohonienko, M., Mamakowa, K., Mangerud, J., Mariscal, B., Markgraf, V.,
1119 McKeever, Mitchell, F. J. G., Munuera, M., Nicol-Pichard, S., Noryskiewicz, B., Odgaard, B. V., Panova, N. K.,
1120 Pantaleon-Cano, J., Paus, A. A., Pavel, T., Peglar, S. M., Penalba, M. C., Pennington, W., Perez-Obiol, R., et al.:
1121 The temperature of Europe during the Holocene reconstructed from pollen data, Quat. Sci. Rev., 22(15–17),
1122 doi:10.1016/S0277-3791(03)00173-2, 2003.
1123
1124 Davis, B. A. S., Chevalier, M., Sommer, P., Carter, V. A., Finsinger, W., Mauri, A., Phelps, L. N., Zanon, M.,
1125 Abegglen, R., Åkesson, C. M., Alba-Sánchez, F., Scott Anderson, R., Antipina, T. G., Atanassova, J. R., Beer,
1126 R., Belyanina, N. I., Blyakharchuk, T. A., Borisova, O. K., Bozilova, E., Bukreeva, G., Jane Bunting, M., Clò, E.,
1127 Colombaroli, D., Combourieu-Nebout, N., Desprat, S., Di Rita, F., Djamali, M., Edwards, K. J., Fall, P. L.,
1128 Feurdean, A., Fletcher, W., Florenzano, A., Furlanetto, G., Gaceur, E., Galimov, A. T., Gałka, M., García-
1129 Moreiras, I., Giesecke, T., Grindean, R., Guido, M. A., Gvozdeva, I. G., Herzschuh, U., Hjelle, K. L., Ivanov, S.,
1130 Jahns, S., Jankovska, V., Jiménez-Moreno, G., Karpińska-Kołaczek, M., Kitaba, I., Kołaczek, P., Lapteva, E. G.,
1131 Latałowa, M., Lebreton, V., Leroy, S., Leydet, M., Lopatina, D. A., López-Sáez, J. A., Lotter, A. F., Magri, D.,
1132 Marinova, E., Matthias, I., Mavridou, A., Mercuri, A. M., Mesa-Fernández, J. M., Mikishin, Y. A., Milecka, K.,
1133 Montanari, C., Morales-Molino, C., Mrotzek, A., Sobrino, C. M., Naidina, O. D., Nakagawa, T., Nielsen, A. B.,
1134 Novenko, E. Y., Panajiotidis, S., Panova, N. K., Papadopoulou, M., Pardoe, H. S., Pędziszewska, A., Petrenko,
1135 T. I., Ramos-Román, M. J., Ravazzi, C., Rösch, M., Ryabogina, N., Ruiz, S. S., Sakari Salonen, J., Sapelko, T.
1136 V., Schofield, J. E., Seppä, H., Shumilovskikh, L., Stivrins, N., Stojakowits, P., Svitavska, H. S., Święta-
1137 Musznicka, J., Tantau, I., Tinner, W., Tobolski, K., Tonkov, S., Tsakiridou, M., et al.: The Eurasian Modern
1138 Pollen Database (EMPD), version 2, Earth Syst. Sci. Data, 12(4), 2423–2445, doi:10.5194/essd-12-2423-2020,
1139 2020.
1140
1141 Douda, J., Doudová, J., Drašnarová, A., Kuneš, P., Hadincová, V., Krak, K., Zákravský, P. and Mandák, B.:
1142 Migration patterns of subgenus Alnus in Europe since the last glacial maximum: A systematic review, PLoS One,
1143 9(2), doi:10.1371/journal.pone.0088709, 2014.
1144
1145 Duprat-Oualid, F., Rius, D., Bégeot, C., Magny, M., Millet, L., Wulf, S. and Appelt, O.: Vegetation response to
1146 abrupt climate changes in Western Europe from 45 to 14.7k cal a BP: the Bergsee lacustrine record (Black Forest,
1147 Germany), J. Quat. Sci., 32(7), 1008–1021, doi:10.1002/jqs.2972, 2017.
1148
1149 Dupre Ollivier, M.: Palinología y paleoambiente- nuevos datos españoles referencias, Universidad de Valencia.,
1150 1988.
1151
1152 Ehlers, J., Gibbard, P. L. and Hughes, P. D.: Quaternary Glaciations - Extent and Chronology A Closer Look,
1153 edited by J. Ehlers, P. L. Gibbard, and P. D. Hughes, Elsevier., 2011.
1154

https://doi.org/10.5194/cp-2022-59
Preprint. Discussion started: 31 August 2022

1155 Elenga, H., Peyron, O., Bonnefille, R., Jolly, D., Cheddadi, R., Guiot, J., Andrieu, V., Bottema, S., Buchet, G.,
1156 De Beaulieu, J. L., Hamilton, A. C., Maley, J., Marchant, R., Perez-Obiol, R., Reille, M., Riollet, G., Scott, L.,
1157 Straka, H., Taylor, D., Van Campo, E., Vincens, A., Laarif, F. and Jonson, H.: Pollen-based biome reconstruction
1158 for southern Europe and Africa 18,000 yr BP, J. Biogeogr., 27(3), 621–634, doi:10.1046/j.1365-
1159 2699.2000.00430.x, 2000.
1160
1161 Ferguson, J. E., Henderson, G. M., Fa, D. A., Finlayson, J. C. and Charnley, N. R.: Increased seasonality in the
1162 Western Mediterranean during the last glacial from limpet shell geochemistry, Earth Planet. Sci. Lett., 308(3–4),
1163 325–333, doi:10.1016/j.epsl.2011.05.054, 2011.
1164
1165 Feurdean, A., Perşoiu, A., Tanţău, I., Stevens, T., Magyari, E. K., Onac, B. P., Marković, S., Andrič, M., Connor,
1166 S., Fărcaş, S., Gałka, M., Gaudeny, T., Hoek, W., Kolaczek, P., Kuneš, P., Lamentowicz, M., Marinova, E.,
1167 Michczyńska, D. J., Perşoiu, I., Płóciennik, M., Słowiński, M., Stancikaite, M., Sumegi, P., Svensson, A., Tămaş,
1168 T., Timar, A., Tonkov, S., Toth, M., Veski, S., Willis, K. J. and Zernitskaya, V.: Climate variability and associated
1169 vegetation response throughout Central and Eastern Europe (CEE) between 60 and 8ka, Quat. Sci. Rev., 106,
1170 206–224, doi:10.1016/j.quascirev.2014.06.003, 2014.
1171
1172 Fick, S. E. and Hijmans, R. J.: WorldClim 2: new 1-km spatial resolution climate surfaces for global land areas,
1173 Int. J. Climatol., 37(12), 4302–4315, doi:10.1002/joc.5086, 2017.
1174
1175 Fletcher, W. J., Goni, M. F. S., Peyron, O. and Dormoy, I.: Abrupt climate changes of the last deglaciation detected
1176 in a Western Mediterranean forest record, Clim. Past, 6(2), 245–264, doi:10.5194/cp-6-245-2010, 2010.
1177
1178 Gaillard, M. J., Sugita, S., Mazier, F., Trondman, A. K., Broström, A., Hickler, T., Kaplan, J. O., Kjellström, E.,
1179 Kokfelt, U., Kuneš, P., Lemmen, C., Miller, P., Olofsson, J., Poska, A., Rundgren, M., Smith, B., Strandberg, G.,
1180 Fyfe, R., Nielsen, A. B., Alenius, T., Balakauskas, L., Barnekow, L., Birks, H. J. B., Bjune, A., Björkman, L.,
1181 Giesecke, T., Hjelle, K., Kalnina, L., Kangur, M., Van Der Knaap, W. O., Koff, T., Lageras, P., Latałowa, M.,
1182 Leydet, M., Lechterbeck, J., Lindbladh, M., Odgaard, B., Peglar, S., Segerström, U., Von Stedingk, H. and Seppä,
1183 H.: Holocene land-cover reconstructions for studies on land cover-climate feedbacks, Clim. Past, 6(4), 483–499,
1184 doi:10.5194/cp-6-483-2010, 2010.
1185
1186 García-Amorena, I., Gómez Manzaneque, F., Rubiales, J. M., Granja, H. M., Soares de Carvalho, G. and Morla,
1187 C.: The Late Quaternary coastal forests of western Iberia: A study of their macroremains, Palaeogeogr.
1188 Palaeoclimatol. Palaeoecol., 254(3–4), 448–461, doi:10.1016/j.palaeo.2007.07.003, 2007.
1189
1190 Genov, I.: The Black Sea level from the Last Glacial Maximum to the present time, Geol. Balc., 45(1–3), 3–19,
1191 2016.
1192
1193 Giesecke, T.: Did thermophilous trees spread into central Europe during the Late Glacial?, New Phytol., 212(1),
1194 15–18, doi:10.1111/nph.14149, 2016.

https://doi.org/10.5194/cp-2022-59
Preprint. Discussion started: 31 August 2022

1195
1196 Giesecke, T., Davis, B., Brewer, S., Finsinger, W., Wolters, S., Blaauw, M., de Beaulieu, J.-L., Binney, H., Fyfe,
1197 R. M., Gaillard, M.-J., Gil-Romera, G., van der Knaap, W. O., Kuneš, P., Kühl, N., van Leeuwen, J. F. N., Leydet,
1198 M., Lotter, A. F., Ortu, E., Semmler, M. and Bradshaw, R. H. W.: Towards mapping the late Quaternary vegetation
1199 change of Europe, Veg. Hist. Archaeobot., 23(1), doi:10.1007/s00334-012-0390-y, 2014.
1200
1201 Giraudi, C.: Lake levels and climate for the last 30,000 years in the fucino area (Abruzzo-Central Italy) - A review,
1202 Palaeogeogr. Palaeoclimatol. Palaeoecol., 70(1–3), 249–260, doi:10.1016/0031-0182(89)90094-1, 1989.
1203
1204 Giraudi, C.: Climate evolution and forcing during the last 40 ka from the oscillations in Apennine glaciers and
1205 high mountain lakes, Italy, J. Quat. Sci., 32(8), 1085–1098, doi:10.1002/jqs.2985, 2017.
1206 Guido, M. A., Molinari, C., Moneta, V., Branch, N., Black, S., Simmonds, M., Stastney, P. and Montanari, C.:
1207 Climate and vegetation dynamics of the Northern Apennines (Italy) during the Late Pleistocene and Holocene,
1208 Quat. Sci. Rev., 231, doi:10.1016/j.quascirev.2020.106206, 2020.
1209 Hansen, M. C., Potapov, P. V., Moore, R., Hancher, M., Turubanova, S. A., Tyukavina, A., Thau, D., Stehman,
1210 S. V., Goetz, S. J., Loveland, T. R., Kommareddy, A., Egorov, A., Chini, L., Justice, C. O. and Townshend, J. R.
1211 G.: High-resolution global maps of 21st-century forest cover change, Science (80-.)., 342(6160), 850–853,
1212 doi:10.1126/science.1244693, 2013.
1213
1214 Harrison, S. P., Yu, G. E. and Tarasov, P. E.: Late Quaternary Lake-Level Record from Northern Eurasia, Quat.
1215 Res., 45(2), 138–159, doi:10.1006/qres.1996.0016, 1996.
1216
1217 Harrison, S. P., Bartlein, P. J., Brewer, S., Prentice, I. C., Boyd, M., Hessler, I., Holmgren, K., Izumi, K. and
1218 Willis, K.: Climate model benchmarking with glacial and mid-Holocene climates, Clim. Dyn., 43(3–4), 671–688,
1219 doi:10.1007/s00382-013-1922-6, 2014.
1220
1221 Harrison, S. P., Bartlein, P. J., Izumi, K., Li, G., Annan, J., Hargreaves, J., Braconnot, P. and Kageyama, M.:
1222 Evaluation of CMIP5 palaeo-simulations to improve climate projections, Nat. Clim. Chang., 5(8), 735–743,
1223 doi:10.1038/nclimate2649, 2015.
1224
1225 Heiri, O., Koinig, K. A., Spötl, C., Barrett, S., Brauer, A., Drescher-Schneider, R., Gaar, D., Ivy-Ochs, S.,
1226 Kerschner, H., Luetscher, M., Moran, A., Nicolussi, K., Preusser, F., Schmidt, R., Schoeneich, P., Schwörer, C.,
1227 Sprafke, T., Terhorst, B. and Tinner, W.: Palaeoclimate records 60-8 ka in the Austrian and Swiss Alps and their
1228 forelands, Quat. Sci. Rev., 106, 186–205, doi:10.1016/j.quascirev.2014.05.021, 2014.
1229
1230 Heyman, B. M., Heyman, J., Fickert, T., Harbor, J. M. and Forest, B.: Paleo-climate of the central European
1231 uplands during the last glacial maximum based on glacier mass-balance modeling Bavarian Forest Republic, Quat.
1232 Res., 79(1), 49–54, doi:10.1016/j.yqres.2012.09.005, 2013.
1233

https://doi.org/10.5194/cp-2022-59
Preprint. Discussion started: 31 August 2022

1234 Hughes, A. L. C., Gyllencreutz, R., Lohne, Ø. S., Mangerud, J. and Svendsen, J. I.: The last Eurasian ice sheets -
1235 a chronological database and time-slice reconstruction, DATED-1, Boreas, 45(1), 1–45, doi:10.1111/bor.12142,
1236 2016.
1237
1238 Hughes, P. D. and Gibbard, P. L.: A stratigraphical basis for the Last Glacial Maximum (LGM), Quat. Int.,
1239 383(June 2014), 174–185, doi:10.1016/j.quaint.2014.06.006, 2015.
1240
1241 Hughes, P. D., Woodward, J. C. and Gibbard, P. L.: Late Pleistocene glaciers and climate in the Mediterranean,
1242 Glob. Planet. Change, 50(1–2), 83–98, doi:10.1016/j.gloplacha.2005.07.005, 2006.
1243 Huntley, B.: Dissimilarity mapping between fossil and contemporary pollen spectra in Europe for the past 13,000
1244 years, Quat. Res., 33(3), 360–376, doi:10.1016/0033-5894(90)90062-P, 1990.
1245
1246 Huntley, B. and Allen, J. R. M.: Glacial environments III. Palaeovegetation patterns in late glacial Europe, in
1247 Neanderthals and modern humans in the European landscape during the last glaciation, edited by T. H. Van Andel
1248 and H. C. Davies, pp. 79–102, McDonald Institute for Archaeological Research, Cambridge., 2003.
1249
1250 Huntley, B. and Birks, H. J. B.: An Atlas of Past and Present Pollen Maps for Europe: 0–13,000 B.P. years ago,
1251 Cambridge University Press, Cambridge., 1983.
1252
1253 Jalut, G., Andrieu, V., Delibrias, G., Fontaugne, M. and Pages, P.: Palaeoenvironment of the valley of Ossau
1254 (Western French Pyrenees) during the last 27 000 year, Pollen et Spores, 30(3–4), 357–393, 1988.
1255
1256 Jalut, G., Marti, J. M., Fontugne, M., Delibrias, G., Vilaplana, J. M. and Julia, R.: Glacial to interglacial vegetation
1257 changes in the northern and southern Pyrénées: Deglaciation, vegetation cover and chronology, Quat. Sci. Rev.,
1258 11(4), 449–480, doi:10.1016/0277-3791(92)90027-6, 1992.
1259
1260 Jankovska, V.: Vegetation cover in West Carpathians during the Last Glacial period - analogy of present day
1261 siberian forest-tundra nad taiga, Palynol. Stratigr. geoecology, (SEPTEMBER 2008), 282–289, 2008.
1262
1263 Janská, V., Jiménez-Alfaro, B., Chytrý, M., Divíšek, J., Anenkhonov, O., Korolyuk, A., Lashchinskyi, N. and
1264 Culek, M.: Palaeodistribution modelling of European vegetation types at the Last Glacial Maximum using modern
1265 analogues from Siberia: Prospects and limitations, Quat. Sci. Rev., 159, 103–115,
1266 doi:10.1016/j.quascirev.2017.01.011, 2017.
1267
1268 Jost, A., Lunt, D., Abe-Ouchi, A., Abe-Ouchi, A., Peyron, O., Valdes, P. J. and Ramstein, G.: High-resolution
1269 simulations of the last glacial maximum climate over Europe: A solution to discrepancies with continental
1270 palaeoclimatic reconstructions?, Clim. Dyn., 24(6), 577–590, doi:10.1007/s00382-005-0009-4, 2005.
1271
1272 Juggins, S.: Quantitative reconstructions in palaeolimnology : new paradigm or sick science ?, Quat. Sci. Rev.,
1273 64, 20–32, doi:10.1016/j.quascirev.2012.12.014, 2013.

https://doi.org/10.5194/cp-2022-59
Preprint. Discussion started: 31 August 2022

1274
1275 Juggins, S.: Rioja: Analysis of Quaternary Science Data, [online] Available from: https://cran.r-
1276 project.org/package=rioja, 2020.
1277
1278 Juggins, S. and Birks, H. J. B.: Quantitative Environmental Reconstructions from Biological Data, in
1279 Developments in Paleoenvironmental Research 5, edited by H. J. B. Birks, pp. 431–494, Springer
1280 ScienceCBusiness Media B.V., 2012.
1281
1282 Juřičková, L., Horáčková, J. and Ložek, V.: Direct evidence of central European forest refugia during the last
1283 glacial period based on mollusc fossils, Quat. Res. (United States), 82(1), 222–228,
1284 doi:10.1016/j.yqres.2014.01.015, 2014.
1285
1286 Kageyama, M., Laîné, A., Abe-Ouchi, A., Braconnot, P., Cortijo, E., Crucifix, M., de Vernal, A., Guiot, J., Hewitt,
1287 C. D., Kitoh, A., Kucera, M., Marti, O., Ohgaito, R., Otto-Bliesner, B., Peltier, W. R., Rosell-Melé, A., Vettoretti,
1288 G., Weber, S. L. and Yu, Y.: Last Glacial Maximum temperatures over the North Atlantic, Europe and western
1289 Siberia: a comparison between PMIP models, MARGO sea-surface temperatures and pollen-based
1290 reconstructions, Quat. Sci. Rev., 25(17–18), 2082–2102, doi:10.1016/j.quascirev.2006.02.010, 2006.
1291
1292 Kaltenrieder, P., Belis, C. A., Hofstetter, S., Ammann, B., Ravazzi, C. and Tinner, W.: Environmental and climatic
1293 conditions at a potential Glacial refugial site of tree species near the Southern Alpine glaciers. New insights from
1294 multiproxy sedimentary studies at Lago della Costa (Euganean Hills, Northeastern Italy), Quat. Sci. Rev., 28(25–
1295 26), 2647–2662, doi:10.1016/j.quascirev.2009.05.025, 2009.
1296
1297 Kaplan, J. O., Pfeiffer, M., Kolen, J. C. A. and Davis, B. A. S.: Large scale anthropogenic reduction of forest
1298 cover in last glacial maximum Europe, PLoS One, 11(11), doi:10.1371/journal.pone.0166726, 2016.
1299
1300 Kehrwald, N. M., McCoy, W. D., Thibeault, J., Burns, S. J. and Oches, E. A.: Paleoclimatic implications of the
1301 spatial patterns of modern and LGM European land-snail shell δ18O, Quat. Res., 74(1), 166–176,
1302 doi:10.1016/j.yqres.2010.03.001, 2010.
1303
1304 Kelly, A., Charman, D. J. and Newnham, R. M.: A last glacial maximum pollen record from bodmin moor
1305 showing a possible cryptic Northern refugium in Southwest England, J. Quat. Sci., 25(3), 296–308,
1306 doi:10.1002/jqs.1309, 2010.
1307
1308 Kolodny, Y., Stein, M. and Machlus, M.: Sea-rain-lake relation in the Last Glacial East Mediterranean revealed
1309 by δ18O-δ13C in Lake Lisan aragonites, Geochim. Cosmochim. Acta, 69(16), 4045–4060,
1310 doi:10.1016/j.gca.2004.11.022, 2005.
1311

https://doi.org/10.5194/cp-2022-59
Preprint. Discussion started: 31 August 2022

1312 Kovács, J., Moravcová, M., Újvári, G. and Pintér, A. G.: Reconstructing the paleoenvironment of East Central
1313 Europe in the Late Pleistocene using the oxygen and carbon isotopic signal of tooth in large mammal remains,
1314 Quat. Int., 276–277, 145–154, doi:10.1016/j.quaint.2012.04.009, 2012.
1315
1316 Krebs, P., Pezzatti, G. B., Beffa, G., Tinner, W. and Conedera, M.: Revising the sweet chestnut (Castanea sativa
1317 Mill.) refugia history of the last glacial period with extended pollen and macrofossil evidence, Quat. Sci. Rev.,
1318 206, 111–128, doi:10.1016/j.quascirev.2019.01.002, 2019.
1319
1320 Kuneš, P., Pelánková, B., Chytrý, M., Jankovská, V., Pokorný, P. and Petr, L.: Interpretation of the last-glacial
1321 vegetation of eastern-central Europe using modern analogues from southern Siberia, J. Biogeogr., 35(12), 2223–
1322 2236, doi:10.1111/j.1365-2699.2008.01974.x, 2008.
1323
1324 Küster, H.: Postglaziale Vegetationsgeschichte Südbayerns. Geobotanische Studien zur Prähistorischen
1325 Landschaftskunde, Akademie Verlag, Berlin., 1995.
1326
1327 Lacey, J. H., Leng, M. J., Höbig, N., Reed, J. M., Valero-Garcés, B. and Reicherter, K.: Western Mediterranean
1328 climate and environment since Marine Isotope Stage 3: a 50,000-year record from Lake Banyoles, Spain, J.
1329 Paleolimnol., 55(2), 113–128, doi:10.1007/s10933-015-9868-9, 2016.
1330
1331 Latombe, G., Burke, A., Vrac, M., Levavasseur, G. and Dumas, C.: Comparison of spatial downscaling methods
1332 of general circulation model results to study climate variability during the Last Glacial Maximum, , 2563–2579,
1333 2018.
1334
1335 Leroy, S. A. G. and Arpe, K.: Glacial refugia for summer-green trees in Europe and south-west Asia as proposed
1336 by ECHAM3 time-slice atmospheric model simulations, J. Biogeogr., 34(12), 2115–2128, doi:10.1111/j.1365-
1337 2699.2007.01754.x, 2007.
1338
1339 Lev, L., Stein, M., Ito, E., Fruchter, N., Ben-Avraham, Z. and Almogi-Labin, A.: Sedimentary, geochemical and
1340 hydrological history of Lake Kinneret during the past 28,000 years, Quat. Sci. Rev., 209, 114–128,
1341 doi:10.1016/j.quascirev.2019.02.015, 2019.
1342
1343 Lister, A. M. and Stuart, A. J.: The impact of climate change on large mammal distribution and extinction:
1344 Evidence from the last glacial/interglacial transition, Comptes Rendus - Geosci., 340(9–10), 615–620,
1345 doi:10.1016/j.crte.2008.04.001, 2008.
1346
1347 López-García, J. M. and Blain, H. A.: Quaternary small vertebrates: State of the art and new insights, Quat. Sci.
1348 Rev., 233, doi:10.1016/j.quascirev.2020.106242, 2020.
1349

https://doi.org/10.5194/cp-2022-59
Preprint. Discussion started: 31 August 2022

1350 Ludwig, P., Pinto, J. G., Raible, C. C. and Shao, Y.: Impacts of surface boundary conditions on regional climate
1351 model simulations of European climate during the Last Glacial Maximum, Geophys. Res. Lett., 44(10), 5086–
1352 5095, doi:10.1002/2017GL073622, 2017.
1353
1354
1355 Luetscher, M., Boch, R., Sodemann, H., Spötl, C., Cheng, H., Edwards, R. L., Frisia, S., Hof, F. and Müller, W.:
1356 North Atlantic storm track changes during the Last Glacial Maximum recorded by Alpine speleothems, Nat.
1357 Commun., 6, 27–32, doi:10.1038/ncomms7344, 2015.
1358
1359 Magri, D.: Persistence of tree taxa in Europe and Quaternary climate changes, Quat. Int., 219(1–2), 145–151,
1360 doi:10.1016/j.quaint.2009.10.032, 2010.
1361
1362 Magri, D. and Parra, I.: Late Quaternary western Mediterranean pollen records and African winds, Earth Planet.
1363 Sci. Lett., 200(3–4), 401–408, doi:10.1016/S0012-821X(02)00619-2, 2002.
1364
1365 Magri, D. and Sadori, L.: Late Pleistocene and Holocene pollen stratigraphy at Lago di Vico, central Italy, Veg.
1366 Hist. Archaeobot., 8(4), 247–260, doi:10.1007/BF01291777, 1999.
1367
1368 Magyari, E., Jakab, G., Rudner, E. and Sümegi, P.: Palynological and plant macrofossil data on Late Pleistocene
1369 short-term climatic oscillations in NE-Hungary, Acta Palaeobot. Suppl., 2(January), 491–502, 1999.
1370
1371 Magyari, E. K., Kuneš, P., Jakab, G., Sümegi, P., Pelánková, B., Schäbitz, F., Braun, M. and Chytrý, M.: Late
1372 Pleniglacial vegetation in eastern-central Europe: Are there modern analogues in Siberia?, Quat. Sci. Rev., 95,
1373 60–79, doi:10.1016/j.quascirev.2014.04.020, 2014a.
1374
1375 Magyari, E. K., Veres, D., Wennrich, V., Wagner, B., Braun, M., Jakab, G., Karátson, D., Pál, Z., Ferenczy, G.,
1376 St-Onge, G., Rethemeyer, J., Francois, J. P., von Reumont, F. and Schäbitz, F.: Vegetation and environmental
1377 responses to climate forcing during the Last Glacial Maximum and deglaciation in the East Carpathians:
1378 Attenuated response to maximum cooling and increased biomass burning, Quat. Sci. Rev., 106, 278–298,
1379 doi:10.1016/j.quascirev.2014.09.015, 2014b.
1380
1381 Magyari, E. K., Pál, I., Vincze, I., Veres, D., Jakab, G., Braun, M., Szalai, Z., Szabó, Z. and Korponai, J.: Warm
1382 Younger Dryas summers and early late glacial spread of temperate deciduous trees in the Pannonian Basin during
1383 the last glacial termination (20-9 kyr cal BP), Quat. Sci. Rev., 225, doi:10.1016/j.quascirev.2019.105980, 2019.
1384
1385 Margari, V., Gibbard, P. L., Bryant, C. L. and Tzedakis, P. C.: Character of vegetational and environmental
1386 changes in southern Europe during the last glacial period; evidence from Lesvos Island, Greece, Quat. Sci. Rev.,
1387 28(13–14), 1317–1339, doi:10.1016/j.quascirev.2009.01.008, 2009.
1388

https://doi.org/10.5194/cp-2022-59
Preprint. Discussion started: 31 August 2022

1389 Marsicek, J., Shuman, B. N., Bartlein, P. J., Shafer, S. L. and Brewer, S.: Reconciling divergent trends and
1390 millennial variations in Holocene temperatures, Nature, 554(7690), 92–96, doi:10.1038/nature25464, 2018.
1391
1392 Mauch Lenardić, J., Oros Sršen, A. and Radović, S.: Quaternary fauna of the Eastern Adriatic (Croatia) with the
1393 special review on the Late Pleistocene sites, Quat. Int., 494, 130–151, doi:10.1016/j.quaint.2017.11.028, 2018.
1394
1395 Mauri, A., Davis, B. A. S., Collins, P. M. and Kaplan, J. O.: The influence of atmospheric circulation on the mid-
1396 Holocene climate of Europe: A data-model comparison, Clim. Past, 10(5), 1925–1938, doi:10.5194/cp-10-1925-
1397 2014, 2014.
1398
1399 Mauri, A., Davis, B. A. S., Collins, P. M. and Kaplan, J. O.: The climate of Europe during the Holocene: A gridded
1400 pollen-based reconstruction and its multi-proxy evaluation, Quat. Sci. Rev., 112,
1401 doi:10.1016/j.quascirev.2015.01.013, 2015.
1402
1403 MARGE Project Members.: Constraints on the magnitude and patterns of ocean cooling at the Last Glacial
1404 Maximum, , (January), 1–6, doi:10.1038/ngeo411, 2009.
1405
1406 Mikolajewicz, U.: Modeling mediterranean ocean climate of the last glacial maximum, Clim. Past, 7(1), 161–180,
1407 doi:10.5194/cp-7-161-2011, 2011.
1408
1409 Miola, A., Bondesan, A., Corain, L., Favaretto, S., Mozzi, P., Piovan, S. and Sostizzo, I.: Wetlands in the Venetian
1410 Po Plain (northeastern Italy) during the Last Glacial Maximum: Interplay between vegetation, hydrology and
1411 sedimentary environment, Rev. Palaeobot. Palynol., 141(1–2), 53–81, doi:10.1016/j.revpalbo.2006.03.016, 2006.
1412
1413 Mix, A. C., Bard, E. and Schneider, R.: Environmental processes of the ice age: Land, oceans, glaciers (EPILOG),
1414 Quat. Sci. Rev., 20(4), 627–657, doi:10.1016/S0277-3791(00)00145-1, 2001.
1415 Moine, O., Rousseau, D. D., Jolly, D. and Vianey-Liaud, M.: Paleoclimatic reconstruction using mutual climatic
1416 range on terrestrial mollusks, Quat. Res., 57(1), 162–172, doi:10.1006/qres.2001.2286, 2002.
1417
1418 Monegato, G., Ravazzi, C., Donegana, M., Pini, R., Calderoni, G. and Wick, L.: Evidence of a two-fold glacial
1419 advance during the last glacial maximum in the Tagliamento end moraine system (eastern Alps), Quat. Res., 68(2),
1420 284–302, doi:10.1016/j.yqres.2007.07.002, 2007.
1421
1422 Monegato, G., Ravazzi, C., Culiberg, M., Pini, R., Bavec, M., Calderoni, G., Jež, J. and Perego, R.: Sedimentary
1423 evolution and persistence of open forests between the south-eastern Alpine fringe and the Northern Dinarides
1424 during the Last Glacial Maximum, Palaeogeogr. Palaeoclimatol. Palaeoecol., 436, 23–40,
1425 doi:10.1016/j.palaeo.2015.06.025, 2015.
1426

https://doi.org/10.5194/cp-2022-59
Preprint. Discussion started: 31 August 2022

1427 Moreno, A., González-Sampériz, P., Morellón, M., Valero-Garcés, B. L. and Fletcher, W. J.: Northern Iberian
1428 abrupt climate change dynamics during the last glacial cycle: A view from lacustrine sediments, Quat. Sci. Rev.,
1429 36, 139–153, doi:10.1016/j.quascirev.2010.06.031, 2012.
1430
1431 Williams, J.W., Grimm, E.G., Blois, J., Charles, D.F., Davis, E., Goring, S.J., Graham, R., Smith, A.J., Anderson,
1432 M., Arroyo-Cabrales, J., Ashworth, A.C., Betancourt, J.L., Bills, B.W., Booth, R.K., Buckland, P., Curry, B.,
1433 Giesecke, T., Hausmann, S., Jackson, S.T., Latorre, C., Nichols, J., Purdum, T., Roth, R.E., Stryker, M., Takahara,
1434 H. :The Neotoma Paleoecology Database: A multi-proxy, international community-curated data resource. Quat.
1435 Res. 89, 156-177, doi:10.1017/qua.2017.105, 2018.
1436
1437 Nolan, C., Overpeck, J. T., Allen, J. R. M., Anderson, P. M., Betancourt, J. L., Binney, H. A., Brewer, S., Bush,
1438 M. B., Chase, B. M., Cheddadi, R., Djamali, M., Dodson, J., Edwards, M. E., Gosling, W. D., Haberle, S.,
1439 Hotchkiss, S. C., Huntley, B., Ivory, S. J., Kershaw, A. P., Kim, S. H., Latorre, C., Leydet, M., Lézine, A. M.,
1440 Liu, K. B., Liu, Y., Lozhkin, A. V., McGlone, M. S., Marchant, R. A., Momohara, A., Moreno, P. I., Müller, S.,
1441 Otto-Bliesner, B. L., Shen, C., Stevenson, J., Takahara, H., Tarasov, P. E., Tipton, J., Vincens, A., Weng, C., Xu,
1442 Q., Zheng, Z. and Jackson, S. T.: Past and future global transformation of terrestrial ecosystems under climate
1443 change, Science (80-.)., 361(6405), 920–923, doi:10.1126/science.aan5360, 2018.
1444
1445 Normand, S., Treier, U. A. and Odgaard, B. V.: Tree refugia and slow forest development in response to post -
1446 LGM warming in North - Eastern European Russia, , 2(4), 2–5, 2011.
1447
1448 Paganelli, A.: Evolution of vegetation and climate in the Veneto-Po Plain during the Late-Glacial and Early
1449 Holocene using pollen-strat-igraphical data, Alp. Mediterr. Quat., 9(2), 581–589, 1996.
1450
1451 Peyron, O., Guiot, J., Cheddadi, R., Tarasov, P., Reille, M., De Beaulieu, J. L., Bottema, S. and Andrieu, V.:
1452 Climatic Reconstruction in Europe for 18,000 YR B.P. from Pollen Data, Quat. Res., 49(2), 183–196,
1453 doi:10.1006/qres.1997.1961, 1998a.
1454
1455 Peyron, O., Cheddadi, R., Tarasov, P. and Reille, M.: Climatic Reconstruction in Europe for 18 , 000 YR B . P .
1456 from Pollen Data, , 196(49), 183–196, 1998b.
1457
1458 Pons, A. and Reille, M.: The Holocene- and upper Pleistocene pollen record from Padul (Granada, Spain): A new
1459 study, Palaeogeogr. Palaeoclimatol. Palaeoecol., 66(3–4), doi:10.1016/0031-0182(88)90202-7, 1988.
1460
1461 Potì, A., Kehl, M., Broich, M., Carrión Marco, Y., Hutterer, R., Jentke, T., Linstädter, J., López-Sáez, J. A.,
1462 Mikdad, A., Morales, J., Pérez-Díaz, S., Portillo, M., Schmid, C., Vidal-Matutano, P. and Weniger, G. C.: Human
1463 occupation and environmental change in the western Maghreb during the Last Glacial Maximum (LGM) and the
1464 Late Glacial. New evidence from the Iberomaurusian site Ifri El Baroud (northeast Morocco), Quat. Sci. Rev.,
1465 220, 87–110, doi:10.1016/j.quascirev.2019.07.013, 2019.
1466

https://doi.org/10.5194/cp-2022-59
Preprint. Discussion started: 31 August 2022

1467 Prentice, I. C. and Harrison, S. P.: Ecosystem effects of CO2 concentration: Evidence from past climates, Clim.
1468 Past, 5(3), 297–307, doi:10.5194/cp-5-297-2009, 2009.
1469
1470 Prentice, I. C., Guiot, J. and Harrison, S. P.: Mediterranean vegetation, lake levels and palaeoclimate at the Last
1471 Glacial Maximum, Nature, 360(6405), 658–660, doi:10.1038/360658a0, 1992.
1472
1473 Prentice, I. C., Guiot, J., Huntley, B., Jolly, D. and Cheddadi, R.: Reconstructing biomes from palaeoecological
1474 data: A general method and its application to European pollen data at 0 and 6 ka, Clim. Dyn., 12(3), 185–194,
1475 doi:10.1007/BF00211617, 1996.
1476
1477 Prentice, I. C., Harrison, S. P. and Bartlein, P. J.: Global vegetation and terrestrial carbon cycle changes after the
1478 last ice age, New Phytol., 189(4), 988–998, doi:10.1111/j.1469-8137.2010.03620.x, 2011.
1479
1480 Prud'homme, C., Lécuyer, C., Antoine, P., Moine, O., Hatté, C., Fourel, F., Martineau, F. and Rousseau, D. D.:
1481 Palaeotemperature reconstruction during the Last Glacial from δ18O of earthworm calcite granules from Nussloch
1482 loess sequence, Germany, Earth Planet. Sci. Lett., 442, 13–20, doi:10.1016/j.epsl.2016.02.045, 2016.
1483
1484 Prud'homme, C., Lécuyer, C., Antoine, P., Hatté, C., Moine, O., Fourel, F., Amiot, R., Martineau, F. and
1485 Rousseau, D. D.: δ13C signal of earthworm calcite granules: A new proxy for palaeoprecipitation reconstructions
1486 during the Last Glacial in western Europe, Quat. Sci. Rev., 179, 158–166, doi:10.1016/j.quascirev.2017.11.017,
1487 2018.
1488
1489 Puzachenko, A. Y., Markova, A. K. and Pawłowska, K.: Evolution of Central European regional mammal
1490 assemblages between the late Middle Pleistocene and the Holocene (MIS7–MIS1), Quat. Int., (November),
1491 doi:10.1016/j.quaint.2021.11.009, 2021.
1492
1493 Ramstein, G., Kageyama, M., Guiot, J. and Wu, H.: How cold was Europe at the Last Glacial Maximum ? A
1494 synthesis of the progress achieved since the first PMIP model-data comparison, , 331–339, 2007.
1495
1496 Reille, M. and Andrieu, V.: The late Pleistocene and Holocene in the Lourdes Basin, Western Pyrénées, France:
1497 new pollen analytical and chronological data, Veg. Hist. Archaeobot., 4(1), 1–21, doi:10.1007/BF00198611,
1498 1995.
1499
1500 Reille, M. and de Beaulieu, J. L.: History of the Würm and Holocene vegetation in western velay (Massif Central,
1501 France): A comparison of pollen analysis from three corings at Lac du Bouchet, Rev. Palaeobot. Palynol., 54(3–
1502 4), 233–248, doi:10.1016/0034-6667(88)90016-4, 1988.
1503
1504 Reimer, A., Landmann, G. and Kempe, S.: Lake Van, Eastern Anatolia, hydrochemistry and history, Aquat.
1505 Geochemistry, 15(1–2), 195–222, doi:10.1007/s10498-008-9049-9, 2009.
1506

https://doi.org/10.5194/cp-2022-59
Preprint. Discussion started: 31 August 2022

1507 Rousseau, D. D.: Climatic transfer function from quaternary molluscs in European loess deposits, Quat. Res.,
1508 36(2), 195–209, doi:10.1016/0033-5894(91)90025-Z, 1991.
1509
1510 Royer, A., Montuire, S., Legendre, S., Discamps, E., Jeannet, M. and Lécuyer, C.: Investigating the influence of
1511 climate changes on rodent communities at a regional-scale (MIS 1-3, Southwestern France), PLoS One, 11(1), 1–
1512 25, doi:10.1371/journal.pone.0145600, 2016.
1513
1514 Ruiz-Zapata, M. B., Vegas, J., Garcia-Cortes, A., Gil Garcia, M. J., Torres, T., Ortiz, J. E. and Perez-Gonzalez,
1515 A.: Vegetation evolution during the Last Maximum Glacial Period in FU-1 sequence (Fuentillejo Lacustrin Maar,
1516 Campo de Calatrava, Ciudad Real), Polen, 18, 37–49, 2008.
1517
1518 Samartin, S., Heiri, O., Kaltenrieder, P., Kühl, N. and Tinner, W.: Reconstruction of full glacial environments and
1519 summer temperatures from Lago della Costa, a refugial site in Northern Italy, Quat. Sci. Rev., 143, 107–119,
1520 doi:10.1016/j.quascirev.2016.04.005, 2016.
1521
1522 Sanchi, L., Ménot, G. and Bard, E.: Insights into continental temperatures in the northwestern Black Sea area
1523 during the Last Glacial period using branched tetraether lipids, Quat. Sci. Rev., 84, 98–108,
1524 doi:10.1016/j.quascirev.2013.11.013, 2014.
1525
1526 Satkūnas, J. and Grigienė, A.: Eemian-Weichselian palaeoenvironmental record from the Mickūnai glacial
1527 depression (Eastern Lithuania), Geologija, 54(2), 35–51, doi:10.6001/geologija.v54i2.2482, 2012.
1528 Schäfer, I. K., Bliedtner, M., Wolf, D., Faust, D. and Zech, R.: Evidence for humid conditions during the last
1529 glacial from leaf wax patterns in the loess-paleosol sequence El Paraíso, Central Spain, Quat. Int., 407, 64–73,
1530 doi:10.1016/j.quaint.2016.01.061, 2016.
1531
1532 Scourse, J. D.: Late Pleistocene stratigraphy and palaeobotany of the Isles of Scilly, Philos. Trans. - R. Soc.
1533 London, B, 334(1271), 405–448, doi:10.1098/rstb.1991.0125, 1991.
1534
1535 Spötl, C., Koltai, G., Jarosch, A. H. and Cheng, H.: Increased autumn and winter precipitation during the Last
1536 Glacial Maximum in the European Alps, Nat. Commun., 12(1), doi:10.1038/s41467-021-22090-7, 2021.
1537
1538 Stewart, J. R. and Lister, A. M.: Cryptic northern refugia and the origins of the modern biota, Trends Ecol. Evol.,
1539 16(11), 608–613, doi:10.1016/S0169-5347(01)02338-2, 2001.
1540
1541 Stivrins, N., Soininen, J., Amon, L., Fontana, S. L., Gryguc, G., Heikkilä, M., Heiri, O., Kisielienė, D., Reitalu,
1542 T., Stančikaitė, M., Veski, S. and Seppä, H.: Biotic turnover rates during the Pleistocene-Holocene transition,
1543 Quat. Sci. Rev., 151, 100–110, doi:10.1016/j.quascirev.2016.09.008, 2016.
1544
1545 Strahl, J.: Zur Pollenstratigraphie des Weichselspätglazials von Berlin-Brandenburg [On the palynostratigraphy
1546 of the Late Weichselian in Berlin-Brandenburg], Brand. Geowissenschaftliche Beiträge, 12, 87–112, 2005.

https://doi.org/10.5194/cp-2022-59
Preprint. Discussion started: 31 August 2022

Stute, M. and Deak, J.: Environmental isotope study (14C, 13C, 18O, D, noble gases) on deep groundwater circulation systems in Hungary with reference to paleoclimate, Radiocarbon, 31(3), 902–918, doi:10.1017/s0033822200012522, 1990.

Svenning, J., Normand, S. and Kageyama, M.: Glacial refugia of temperate trees in Europe : insights from species distribution modelling, , (Svenning 2003), 1117–1127, doi:10.1111/j.1365-2745.2008.01422.x, 2008.

Tarasov, P. E., Webb, T., Andreev, A. A., Afanas'eva, N. B., Berezina, N. A., Bezusko, L. G., Blyakharchuk, T. A., Bolikhovskaya, N. S., Cheddadi, R., Chernavskaya, M. M., Chernova, G. M., Dorofeyuk, N. I., Dirksen, V. G., Elina, G. A., Filimonova, L. V., Glebov, F. Z., Guiot, J., Gunova, V. S., Harrison, S. P., Jolly, D., Khomutova, V. I., Kvavadze, E. V., Osipova, I. M., Panova, N. K., Prentice, I. C., Saarse, L., Sevastyanov, D. V., Volkova, V. S. and Zernitskaya, V. P.: Present-day and mid-Holocene biomes reconstructed from pollen and plant macrofossil data from the former Soviet Union and Mongolia, J. Biogeogr., 25(6), 1029–1053, doi:10.1046/j.1365-2699.1998.00236.x, 1998.

Tarasov, P. E., Volkova, V. S., Webb, T., Guiot, J., Andreev, A. A., Bezusko, L. G., Bezusko, T. V., Bykova, G. V., Dorofeyuk, N. I., Kvavadze, E. V., Osipova, I. M., Panova, N. K. and Sevastyanov, D. V.: Last glacial maximum biomes reconstructed from pollen and plant macrofossil data from northern Eurasia, J. Biogeogr., 27(3), 609–620, doi:10.1046/j.1365-2699.2000.00429.x, 2000.

Telford, R. J. and Birks, H. J. B.: Evaluation of transfer functions in spatially structured environments, Quat. Sci. Rev., 28(13–14), 1309–1316, doi:10.1016/j.quascirev.2008.12.020, 2009.

Valero-Garcés, B. L., González-Sampériz, P., Navas, A., Machin, J., Delgado-Huertas, A., Pena-Monné, J. L., Sancho-Marcén, C., Stevenson, T. and Davis, B.: Paleohydrological fluctuations and steppe vegetation during the last glacial maximum in the central Ebro valley (NE Spain), Quat. Int., 122(1 SPEC. ISS.), doi:10.1016/j.quaint.2004.01.030, 2004.

Valsecchi, V., Sanchez Goñi, M. F. and Londeix, L.: Vegetation dynamics in the Northeastern Mediterranean region during the past 23 000 yr: Insights from a new pollen record from the Sea of Marmara, Clim. Past, 8(5), 1941–1956, doi:10.5194/cp-8-1941-2012, 2012.

Vandenberghe, J., French, H. M., Gorbunov, A., Marchenko, S., Velichko, A. A., Jin, H., Cui, Z., Zhang, T. and Wan, X.: The Last Permafrost Maximum (LPM) map of the Northern Hemisphere: Permafrost extent and mean annual air temperatures, 25-17ka BP, Boreas, 43(3), 652–666, doi:10.1111/bor.12070, 2014.

Varsányi, I., Palcsu, L. and Kovács, L. Ó.: Groundwater flow system as an archive of palaeotemperature: Noble gas, radiocarbon, stable isotope and geochemical study in the Pannonian Basin, Hungary, Appl. Geochemistry, 26(1), 91–104, doi:10.1016/j.apgeochem.2010.11.006, 2011.

https://doi.org/10.5194/cp-2022-59
Preprint. Discussion started: 31 August 2022

1587
1588 Vegas-Vilarrúbia, T., González-Sampériz, P., Morellón, M., Gil-Romera, G., Pérez-Sanz, A. and Valero-Garcés,
1589 B.: Diatom and vegetation responses to late glacial and early holocene climate changes at lake estanya (southern
1590 pyrenees, NE spain), Palaeogeogr. Palaeoclimatol. Palaeoecol., 392, 335–349, doi:10.1016/j.palaeo.2013.09.011,
1591 2013.
1592
1593 Vegas, J., Ruiz-Zapata, B., Ortiz, J. E., Galán, L., Torres, T., García-Cortés, Á., Gil-García, M. J., Pérez-González,
1594 A. and Gallardo-Millán, J. L.: Identification of arid phases during the last 50 cal. ka BP from the Fuentillejo maar-
1595 lacustrine record (Campo de Calatrava Volcanic Field, Spain), J. Quat. Sci., 25(7), 1051–1062,
1596 doi:10.1002/jqs.1262, 2010.
1597
1598 Velasquez, P., Kaplan, J. O., Messmer, M., Ludwig, P. and Raible, C. C.: The role of land cover in the climate of
1599 glacial Europe, Clim. Past, 17(3), 1161–1180, doi:10.5194/cp-17-1161-2021, 2021.
1600
1601 Vicente-Serrano, S. M., Trigo, R. M., López-Moreno, J. I., Liberato, M. L. R., Lorenzo-Lacruz, J., Beguería, S.,
1602 Morán-Tejeda, E. and El Kenawy, A.: Extreme winter precipitation in the Iberian Peninsula in 2010: Anomalies,
1603 driving mechanisms and future projections, Clim. Res., 46(1), 51–65, doi:10.3354/cr00977, 2011.
1604
1605 Williams, J. W. and Jackson, S. T.: Palynological and AVHRR observations of modern vegetational gradients in
1606 eastern North America, , 4, 485–497, 2003.
1607
1608 Williams, J. W., Webb, T., Shurman, B. N. and Bartlein, P. J.: Do Low CO 2 Concentrations Affect Pollen-Based
1609 Reconstructions of LGM Climates? A Response to “Physiological Significance of Low Atmospheric CO 2 for
1610 Plant–Climate Interactions” by Cowling and Sykes, Quat. Res., 53(3), 402–404, doi:10.1006/qres.2000.2131,
1611 2000.
1612
1613 Willis, K. J. and Van Andel, T. H.: Trees or no trees? The environments of central and eastern Europe during the
1614 Last Glaciation, Quat. Sci. Rev., 23(23–24), 2369–2387, doi:10.1016/j.quascirev.2004.06.002, 2004.
1615
1616 Wu, H., Guiot, J., Brewer, S. and Guo, Z.: Climatic changes in Eurasia and Africa at the last glacial maximum
1617 and mid-Holocene: Reconstruction from pollen data using inverse vegetation modelling, Clim. Dyn., 29(2–3),
1618 211–229, doi:10.1007/s00382-007-0231-3, 2007.
1619
1620 Yu, G. and Harrison, S. P.: Lake status records from Europe: data base documentation, NOAA Paleoclimatology
1621 Publications Series, Boulder, Colorado., 1995.
1622
1623 Zaarur, S., Affek, H. P. and Stein, M.: Last glacial-Holocene temperatures and hydrology of the Sea of Galilee
1624 and Hula Valley from clumped isotopes in Melanopsis shells, Geochim. Cosmochim. Acta, 179, 142–155,
1625 doi:10.1016/j.gca.2015.12.034, 2016.
1626

https://doi.org/10.5194/cp-2022-59
Preprint. Discussion started: 31 August 2022

1627 Zanon, M., Davis, B. A. S., Marquer, L., Brewer, S. and Kaplan, J. O.: European forest cover during the past
1628 12,000 years: A palynological reconstruction based on modern analogs and remote sensing, Front. Plant Sci., 9,
1629 doi:10.3389/fpls.2018.00253, 2018.
1630
1631 Zech, M., Buggle, B., Leiber, K., Marković, S., Glaser, B., Hambach, U., Huwe, B., Stevens, T., Sümegi, P.,
1632 Wiesenberg, G. and Zöller, L.: Reconstructing Quaternary vegetation history in the Carpathian Basin, SE-Europe,
1633 using n-alkane biomarkers as molecular fossils: Problems and possible solutions, potential and limitations, Quat.
1634 Sci. J., 58(2), 148–155, doi:10.3285/eg.58.2.03, 2010.
1635
1636

https://doi.org/10.5194/cp-2022-59
Preprint. Discussion started: 31 August 2022

Climate of the Past Discussions
Open Access
EGU

Tables

Site	Site Name	Country/Ocean	Latitude	Longitude	Elevation	Site Type	Data Type	Samples	Source	Reference
1	MD95-2039 (M)	Atlantic	40.578333	-10.348333	-3381	Marine	Raw Count	21	EPD (E#1472)	Roucoux et al. 2005
2	SU81-18 (M)	Atlantic	37.77	-9.82	-3135	Marine	Raw Count	10	ACER	Turon et al. 2003
3	MD99-2331 (M)	Atlantic	41.15	-9.68	-2110	Marine	Raw Count	41	ACER	Naughton et al. 2006
4	Carn Morval	United Kingdom	49.926111	-6.313889	5	Lake	Digitised	1	Publication	Scourse 1991
5	Gorham Cave	Spain	36.132826	-5.347358	0	Cave	Digitised	1	Publication	Carrion et al. 2008
6	Dozmary Pool	United Kingdom	50.5347222	-4.5358333	265	Lake	Raw Count	32	Author	Kelly et al. 2010
7	Bajondillo	Spain	36.619722	-4.496389	20	Cave	Raw Count	1	EPD (E#1570)	Cortes-Sanchez et al 2011
8	Laguna del maar de Fuentillejo	Spain	38.937996	-4.0539	637	Lake	Digitised	1	Publication	Ruiz-Zapata et al. 2009
9	Padul-1	Spain	37.016338	-3.608503	785	Peat Bog	Digitised	13	Publication	Pons & Reille 1988
10	Padul-2	Spain	37.010833	-3.603889	726	Peat Bog	Digitised	1	Publication	Camuera et al. 2019
11	Cova di Carihuela	Spain	37.4489	-3.4297	1020	Cave	Digitised	1	Publication	Carrion 1992
12	Ifri El Baroud	Morocco	34.75	-3.3	539	Cave	Digitised	1	Publication	Poti et al. 2019
13	MD95-2043 (M)	Mediterranean	36.14	-2.621	-1841	Marine	Raw Count	7	ACER	Fletcher et al. 2008
14	San Rafael	Spain	36.773611	-2.601389	0	Peat Bog	Raw Count	2	EPD (E#574)	Pantaléon-Cano 1997
15	Siles	Spain	38.24	-2.3	1320	Lake	Digitised	1	Publication	Carrion 2002
16	Torrecilla de Valmadrid	Spain	41.4469444	-0.895	570	Colluvium	Digitised	1	Publication	Valero-Garces et al. 2004
17	Navarrés-1	Spain	39.1	-0.683333	225	Peat Bog	Raw Count	1	EPD (E#469)	Carrión & Dupré-Olivier 1996
18	Navarrés-2	Spain	39.1	-0.683333	225	Peat Bog	Raw Count	1	EPD (E#470)	Carrión & Dupré-Olivier 1996
19	Tourbiere de l'Estarres	France	43.0933	-0.3792	356	Lake	Digitised	1	Publication	Jalut et al. 1988
20	Cova de les Malladetes	Spain	39.058	-0.321	20	Cave	Digitised	1	Publication	Dupré Ollivier 1988
21	Lourdes	France	43.033333	-0.075	430	Lake	Digitised	15	Publication	Reille & Andrieu 1995
22	Lake Estanya	Spain	42.0333333	0.53333333	670	Lake	Digitised	1	Publication	Vegas-Villarubia et al. 2013
23	Freychinede	France	42.7833	1.4333	1350	Lake	Digitised	1	Publication	Jalut et al. 1992
24	Banyoles	Spain	42.133333	2.75	173	Lake	Raw Count	13	EPD (E#931)	Pérez-Obiol & Julia 1994
25	Lac du Bouchet B5	France	44.916667	3.783333	1200	Lake	Digitised	14	Publication	Reille & de Beaulieu 1988
26	MD99-2348 (103) (M)	Mediterranean	42.692778	3.841667	-296	Marine	Raw Count	41	EPD (E#1474)	Beaudouin et al. 2007
27	Les Echets G	France	45.9	4.93	267	Peat Bog	Digitised	136	ACER	de Beaulieu & Reille 1984
28	La Grotte Walou	Belgium	50.585278	5.536389	252	Cave	Digitised	1	Publication	Damblon 2011
29	Bergsee	Germany	47.5722222	7.93638889	382	Lake	Digitised	1	Publication	Duprat-Oualid et al. 2017
30	Garaat El-Ouez	Algeria	36.818333	8.33333	45	Peat Bog	Raw Count	6	EPD (E#1501)	Benslama et al 2010
31	Pian del Lago	Italy	44.321561	9.485682	833	Lake	Digitised	1	Publication	Guido et al. 2020
32	Pilsensee	Germany	48.0267	11.1883	534	Lake	Digitised	1	Publication	Küster 1995
33	Orgiano	Italy	45.29	11.43	19	Peat Bog	Digitised	1	Publication	Paganelli 1996
34	Lago della Costa	Italy	45.2702778	11.7430556	7	Lake	Digitised	8	Publication	Kaltenrieder et al. 2009
35	Lagaccione	Italy	42.566667	11.85	355	Lake	Raw Count	7	ACER	Magri 1999
36	Lago Vico	Italy	42.3166667	12.1666667	510	Lake	Digitised	15	Publication	Magri & Sadori 1999
37	Stracciacappa	Italy	42.13	12.32	220	Lake	Raw Count	2	ACER	Giardini 2007
38	Lago di Monterosi	Italy	42.2166667	12.4333333	237	Lake	Raw Count	1	Publication	Bonatti 1970
39	Venice	Italy	45.629523	12.654086	0	Peat Bog	Digitised	1	Publication	Miola et al. 2006
40	Azzano Decimo	Italy	45.8833	12.7165	10	Alluvial Fan	Raw Count	6	ACER	Pini et al. 2009
41	Valle di Castiglione	Italy	41.89	12.75	44	Lake	Raw Count	2	ACER	Follieri et al. 1989
42	Travesio	Italy	46.2	12.87	220	Lake	Digitised	1	Publication	Monegato et al. 2007
43	Orvenco	Italy	46.252088	13.169771	380	Alluvial Fan	Digitised	1	Publication	Monegato et al. 2007
44	Rio Doidis	Italy	46.12	13.19	152	Lake	Digitised	1	Publication	Monegato et al. 2007
45	Billerio	Italy	46.22	13.21	300	Lake	Digitised	1	Publication	Monegato et al. 2007
46	Kersdorf-Briesen	Germany	52.333704	14.269142	44	Lake	Digitised	1	Publication	Strahl 2005
47	Lago Grande di Monticchio	Italy	40.944444	15.6	1326	Lake	Raw Count	6	EPD (E#932)	Watts et al. 1996
48	Nagymohos	Hungary	48.326944	20.436389	297	Peat Bog	Raw Count	14	Publication	Magyari et al 1999
49	Safarka	Slovakia	48.8819444	20.575	600	Peat Bog	Digitised	1	Publication	Jankovska 2008
50	Feher Lake	Hungary	46.45	20.65	86	Lake	Raw Count	10	Publication	Magyari et al. 2014
51	Ioannina	Greece	39.75	20.85	470	Peat Bog	Raw Count	20	ACER	Tzedakis et al. 2004
52	Kokad	Hungary	47.4027778	21.9286111	112	Peat Bog	Raw Count	2	Publication	Magyari et al. 2019
53	Lake Xinias	Greece	39.05	22.27	500	Lake	Raw Count	5	EPD (E#976)	Bottema 1979
54	Mickunai	Lithuania	54.722114	25.532218	143	Lake	Digitised	1	Publication	Satkunas & Grigiene 2012
55	Lake Sfanta Anna	Romania	46.1263889	25.8880556	946	Lake	Digitised	1	Publication	Magyari et al. 2014
56	Megali Limni	Greece	39.1	26.3	323	Lake	Digitised	1	Publication	Margari et al. 2009
57	Straldzha	Bulgaria	42.630278	26.77	138	Peat Bog	Raw Count	3	Publication	Connor et l. 2013
58	MD01-2430 (M)	Turkey	40.796833	27.725166	-580	Marine	Digitised	1	Publication	Valsecchi et al. 2012
59	Lake Iznik	Turkey	40.433889	29.533056	88	Lake	Raw Count	7	EPD (E#714)	Miebach et al 2016
60	M72/5 628-1 (M)	Black Sea	42.1035	36.62383	-418	Marine	Raw Count	6	Pangaea (833387)	Shumilovskikh et al. 2014
61	Dziguta	Georgia	42.99	41.07	35	Peat Bog	Digitised	1	Publication	Arslanov et al. 2007
62	Lake Van LG	Turkey	38.667	42.669	1649	Lake	Raw Count	10	Pangaea (853779)	Pickarski et al. 2015
63	Lake Zeribar	Iran	35.533333	46.116667	1286	Lake	Raw Count	17	EPD (E#714)	van Zeist & Bottema 1977

Table 1. List of selected sites

https://doi.org/10.5194/cp-2022-59
Preprint. Discussion started: 31 August 2022

Climate of the Past Discussions
Open Access
EGU

Site	Site Name	COHMAP Quality	< 17k 18k 19k 20k 21k 22k 23k 24k 25k >	Upper 14C	Upper Cal. BP	Lower 14C	Lower Cal. BP
1	MD95-2039 (M)	3C		14830±80	18166±269	19950±210	23883±374
2	SU81-18 (M)	2C		17510±270	20952±404	21250±280	25420±441
3	MD99-2331 (M)	2C		16170±130	19325±303	19770±170	23682±336
4	Carn Morval	4C			18600±3700	21500±890/800	25867±1127
5	Gorham Cave	4D				18440±160	22055±341
6	Dozmary Pool	2C		14568±129	17569±523	18325±216	21769±602
7	Bajondillo	1C			18701±2154		
8	Laguna del maar de Fuentillejo	5D		16540±90	19847±308		
9	Padul-1	3D		18300±300	21821±412	19100±160	22922±308
10	Padul-2	1D				17450±539	21082±539
11	Cova di Carihuela	2C		15700±220	18958±280	21430±130	25659±226
12	Ifri El Baroud	2D		17296±87	20761±293		
13	MD95-2043 (M)	2C		15440±90	18533±294	18260±120	21951±335
14	San Rafael	3D		9980±60	11464±133	16860±120	20083±292
15	Siles	2D		17030±80	20345±351		
16	Torrecilla de Valmadrid	2D		17100±85	20456±366		
17	Navarrés-1	4D		18360±195	22001±353	20700±295	24664±411
18	Navarrés-2	5D		5150±50	5881±85	16000±	19144±
19	Tourbiere de l'Estarres	1C		17150±250	20522±470	18970±160	22847±317
20	Cova de les Malladetes	5D		16300±1500	19686±1723		
21	Lourdes	4D		18510±130	22112±130	20025±175	23952±355
22	Lake Estanya	5D			9498±50		19184±251
23	Freychinede	3C		14800±800	17912±856	21300±760	25615±1030
24	Banyoles	4C			19878±100		27862±3000
25	Lac du Bouchet B5	2C		15350±350	18513±435	19200±300	23006±384
26	MD99-2348 (103) (M)	1D		17660±60	21065±310	19350±90	23111±271
27	Les Echets G	1C		17530±270	20970±407	18030±250	21704±473
28	La Grotte Walou	1D					21200±700
29	Bergsee	2D				17780±90	21244±306
30	Garaat El-Ouez	2C		16010±320	19200±801		
31	Pian del Lago	2D					21260±320
32	Pilsensee	6D		15860±250	19073±290		
33	Orgiano	2D		17760±160	21221±373	19290±520	23141±621
34	Lago della Costa	2C		15400±150	18484±330	19285±160	23052±302
35	Lagaccione	2C		16080±450	19369±527	20615±940	24746±1201
36	Lago Vico	3C		14385±140	17541±272	20500±230	24430±376
37	Stracciacappa	4C		12060±130	14093±281	19745±820	22675±955
38	Lago di Monterosi	2D		17040±350	20398±544		
39	Venice	5D				18640±100	22277±336
40	Azzano Decimo	2D		18000±300	21637±529	21025±245	25179±449
41	Valle di Castiglione	3C		14220±145	17443±270	20300±700	24266±842
42	Travesio	5D				18780±200	22483±406
43	Orvenco	2D		17760±160	21221±373	19290±520	23141±621
44	Rio Doidis	5D				18860±190	22390±373
45	Billerio	3D				18165±200	21872±382
46	Kersdorf-Briesen	1D				17622±94	21183±356
47	Lago Grande di Monticchio	2C			20204±		24014±
48	Nagymohos	2C		14246±144	17361±425	18159±247	21735±622
49	Safarka	3D				18287±1512	21912±1781
50	Feher Lake	1D		17715±250	21190±463	19911±81	23841±313
51	Ioannina	3C		15330±140	18420±312	20760±230	24748±330
52	Kokad	5D		14326±63	17433±443	16280±90	19685±538
53	Lake Xinias	6C		11150±130	13049±160	21390±430	25671±648
54	Mickunai	1D			21000±2200		
55	Lake Sfanta Anna	1D		17626±96	20955±432		
56	Megali Limni	6D		19072±237	22906±340		
57	Straldzha	6C		14696±65	18022±364	23653±114	28580±390
58	MD01-2430 (M)	4C		12050±75	14904±324	18310±380	21746±968
59	Lake Iznik	7D		16910±100	19515±115		
60	M72/5 628-1 (M)	2C		16835±85	18490±	19495±90	21280±
61	Dziguta	4C		12990±160	15839±483	20560±880	24666±1126
62	Lake Van LG	2C			18590±62		23290±596
63	Lake Zeribar	4C		13650±160	16610±399	22000±500	26462±880

COHMAP chronological quality classification:

1C: Bracketing dates within 2000 14C (2360 Cal.) yr interval about the time being assessed

2C: Bracketing dates, one within 2000 14C (2360 Cal.) yr and the second within 4000 14C (4682 Cal.) yr of the time being assessed

3C: Bracketing dates within 4000 14C (4682 Cal.) yr interval about the time being assessed

4C: Bracketing dates, one being within 4000 14C (4682 Cal.) yr and the second being within 6000 14C (7490 Cal.) yr of the time being assessed

5C: Bracketing dates within 6000 14C (7490 Cal.) yr interval about the time being assessed

6C: Bracketing dates, one within 6000 14C (7490 Cal.) yr and the second within 8000 14C (9681 Cal.) yr of the time being assessed

7C: Poorly dated

1D: Date within 250 14C (206 Cal.) yr of the time being assessed

2D: Date within 500 14C (684 Cal.) yr of the time being assessed

3D: Date within 750 14C (975 Cal.) yr of the time being assessed

4D: Date within 1000 14C (1123 Cal.) yr of the time being assessed

5D: Date within 1500 14C (1881 Cal.) yr of the time being assessed

6D: Date within 2000 14C (2360 Cal.) yr of the time being assessed

7D: Poorly dated

Table 2. Chronological control

https://doi.org/10.5194/cp-2022-59
Preprint. Discussion started: 31 August 2022

Climate of the Past Discussions
Open Access
EGU

	RMSE	R2
TANN	2.28	0.9
TDJF	3.35	0.91
TJJA	2.21	0.81
PANN	224.94	0.69
PDJF	78.51	0.69
PJJA	52.49	0.75
Tree Cover	21.03	0.52

Table 3. MAT performance statistics based on the modern pollen sample training set. This includes Mean Annual Temperature and Precipitation (TANN and PANN), Mean Winter Temperature and Precipitation (TDJF and PDJF) and Mean Summer Temperature and Precipitation (TJJA and PJJA).

https://doi.org/10.5194/cp-2022-59
Preprint. Discussion started: 31 August 2022

Climate of the Past Discussions
Open Access
EGU

Figures

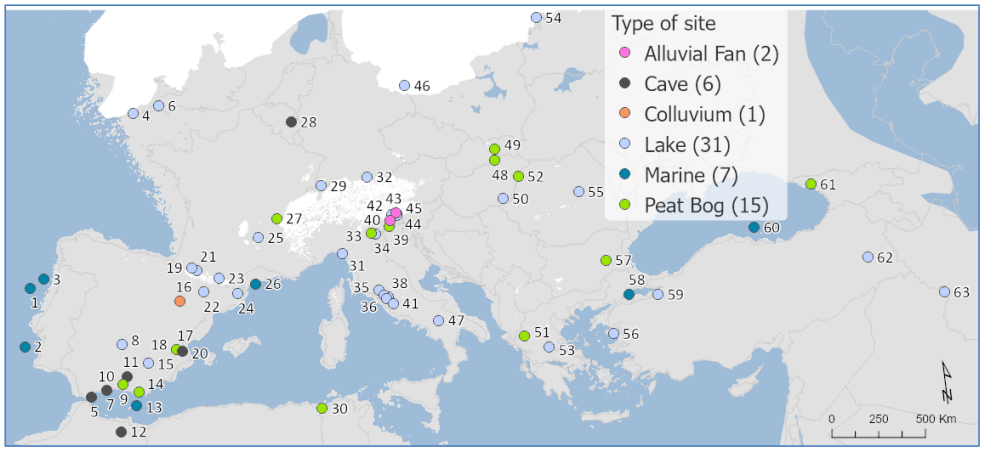

Figure 1. Site locations and archives (Site numbers are as shown in Table 1)

https://doi.org/10.5194/cp-2022-59
Preprint. Discussion started: 31 August 2022

Climate of the Past Discussions
Open Access
EGU

1685

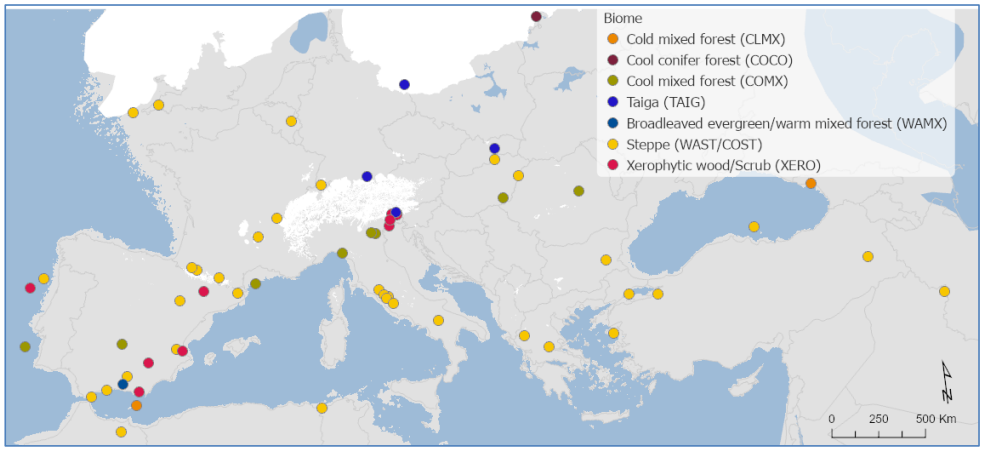

1686

1687

1688 Figure 2. Pollen biomes

1689

1690

https://doi.org/10.5194/cp-2022-59
Preprint. Discussion started: 31 August 2022

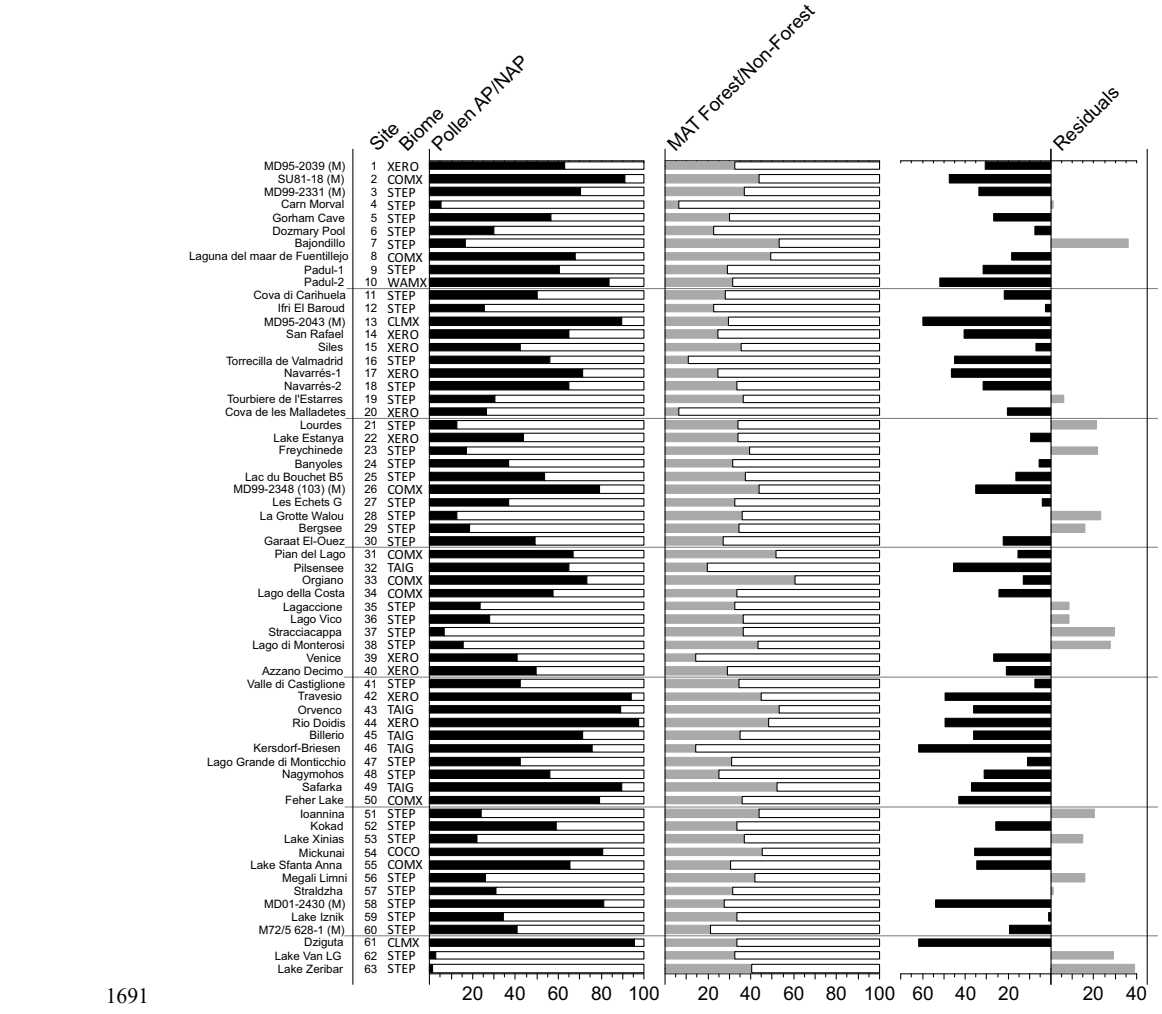

Figure 3. Pollen biomes (see figure 2 for key), Arboreal Pollen (AP) % forest cover, MAT % forest cover and residuals (AP % compared to MAT Forest %)

https://doi.org/10.5194/cp-2022-59
Preprint. Discussion started: 31 August 2022

Climate of the Past
Discussions
Open Access
EGU

1697

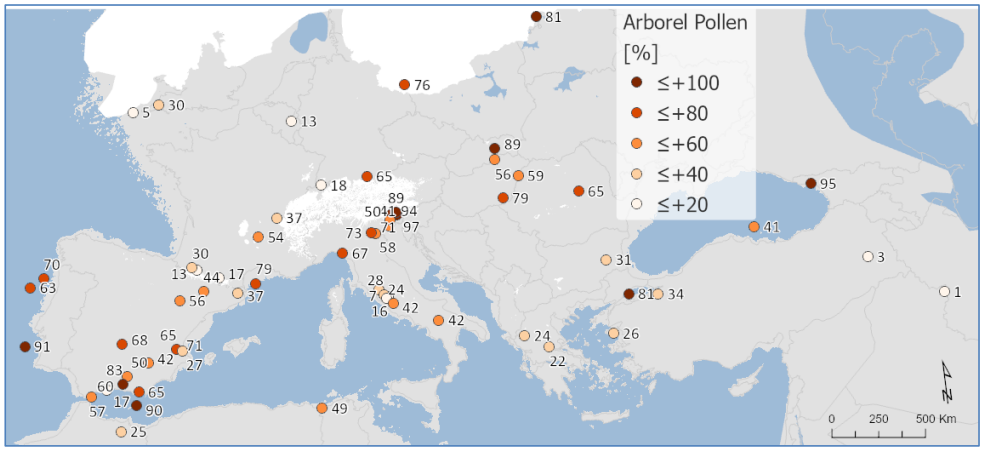

1698

1699

1700 Figure 4. Arboreal Pollen (AP) % forest cover

1701

1702

https://doi.org/10.5194/cp-2022-59
Preprint. Discussion started: 31 August 2022

Climate of the Past Discussions
Open Access
EGU

1703

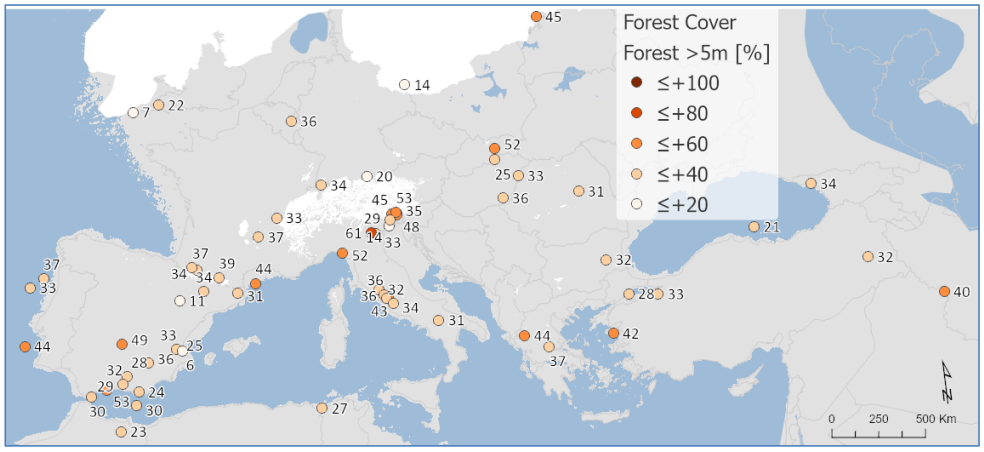

1704

1705

1706 Figure 5. Modern Analogue Technique (MAT) % forest cover

1707

1708

https://doi.org/10.5194/cp-2022-59
Preprint. Discussion started: 31 August 2022

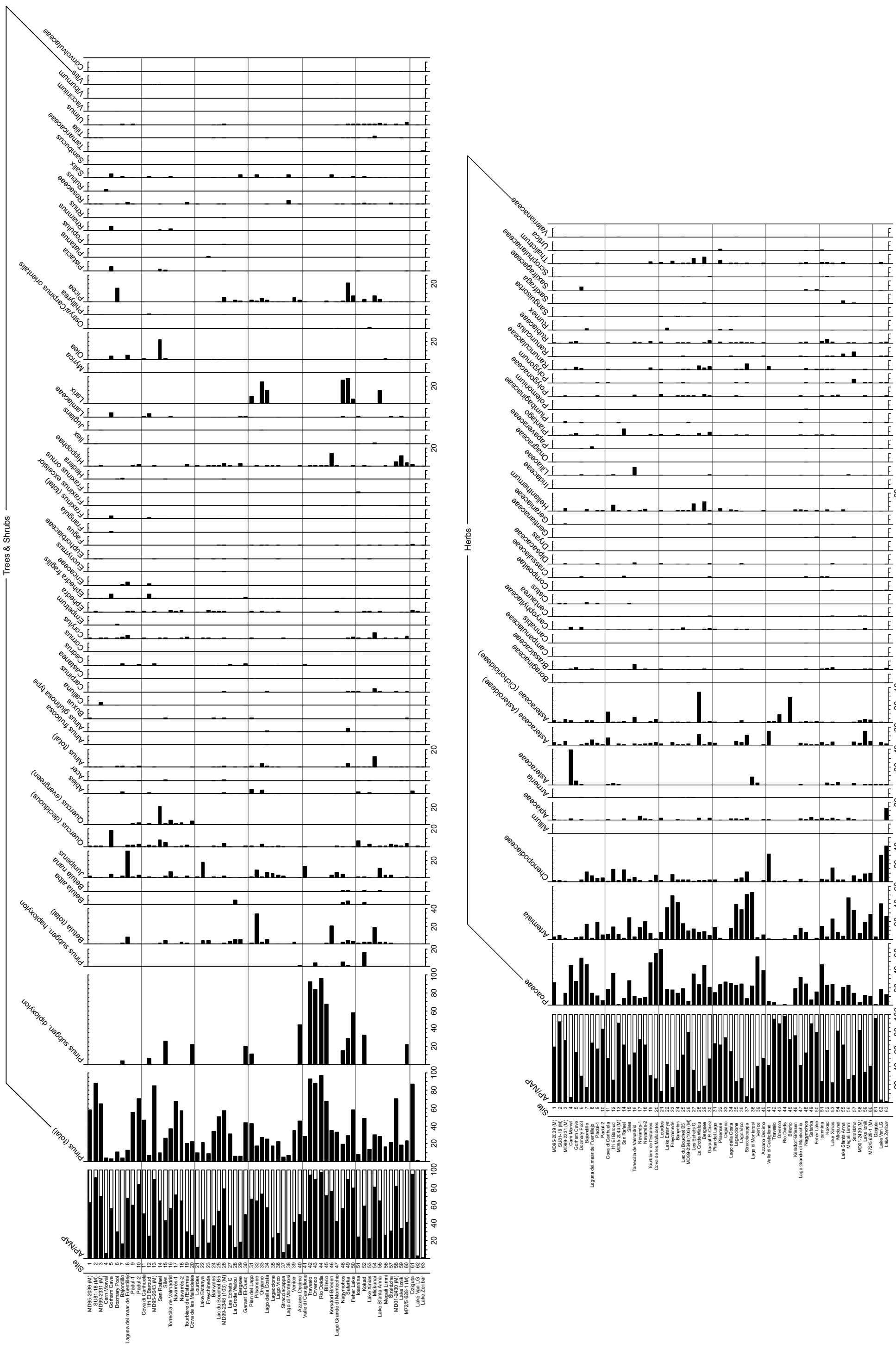

Figure 6. Pollen taxa percentages for all LGM sites/records

https://doi.org/10.5194/cp-2022-59
Preprint. Discussion started: 31 August 2022

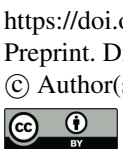

Climate of the Past Discussions
Open Access
EGU

1711

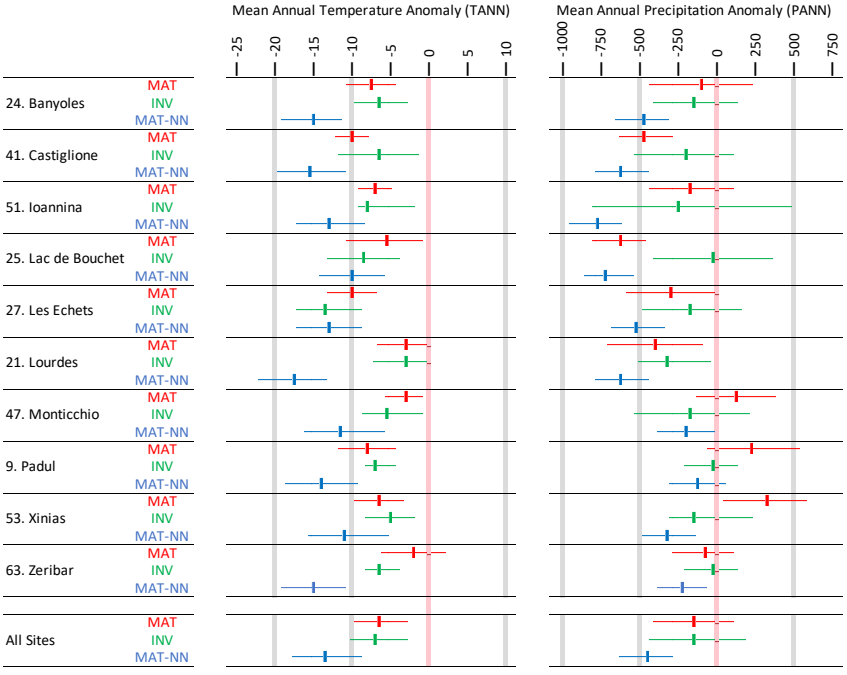

1712

1713

1714

1715 Figure 7. A site-by-site comparison between LGM pollen-climate reconstructions based on Modern Analogue
1716 Technique MAT (this study), neural-networks MAT-NN (Peyron et al., 1998), and Inverse Modelling INV (Wu
1717 et al., 2007). The results show that MAT and INV give similar climate reconstructions, but MAT-NN is
1718 significantly cooler/drier.

1719

https://doi.org/10.5194/cp-2022-59
Preprint. Discussion started: 31 August 2022

Climate of the Past Discussions
Open Access
EGU

1720
1721
1722

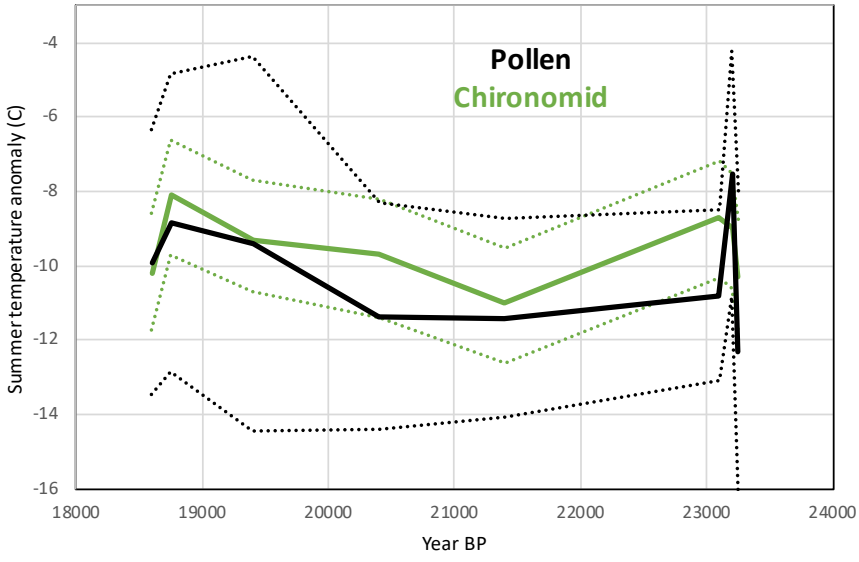

1723
1724
1725

1726 Figure 8. Comparison between LGM pollen-climate MAT and chironomid summer temperature reconstructions
1727 at Lago della Costa, Italy (chironomid reconstruction and pollen data from Samartin et al., 2016). Dash lines show
1728 uncertainties.

1729

https://doi.org/10.5194/cp-2022-59
Preprint. Discussion started: 31 August 2022

Climate of the Past Discussions
Open Access
EGU

1730

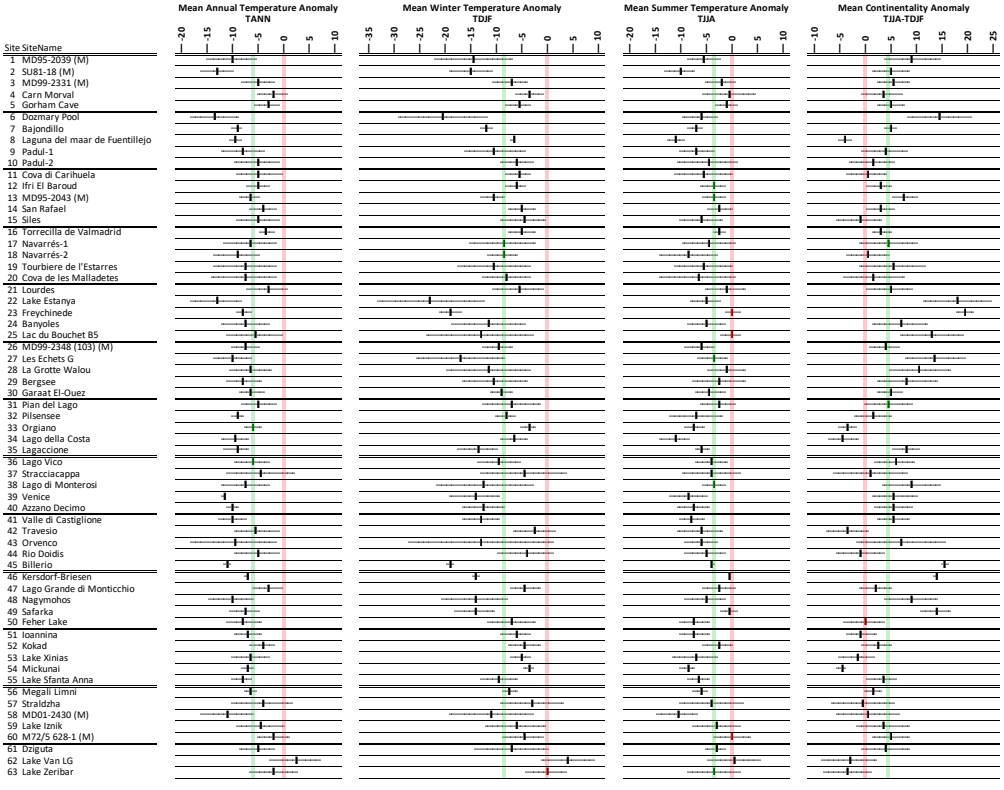

1731

1732

1733 Figure 9. Pollen-based MAT reconstructions for LGM annual, winter and summer temperature anomalies
1734 (uncertainties represent one standard deviation). Continentality represents the difference in temperature between
1735 summer and winter, with positive anomalies indicating an increase in the temperature difference between summer
1736 and winter. All values are expressed as anomalies compared with the present day. The green line indicates the
1737 mean for all the sites.

1738

1739

https://doi.org/10.5194/cp-2022-59
Preprint. Discussion started: 31 August 2022

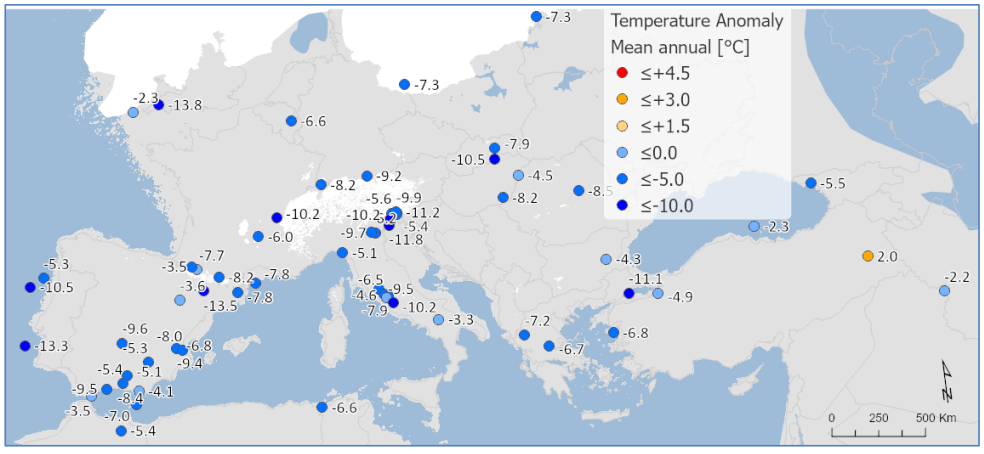

1740

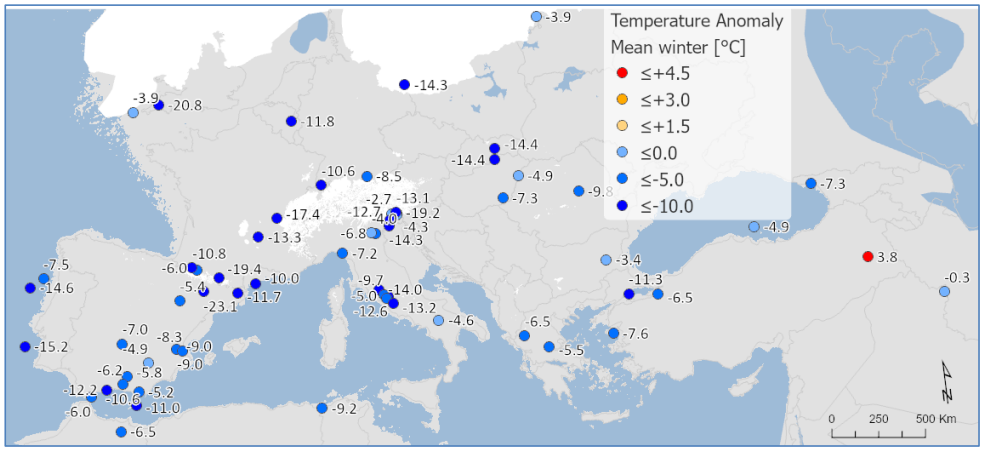

1741

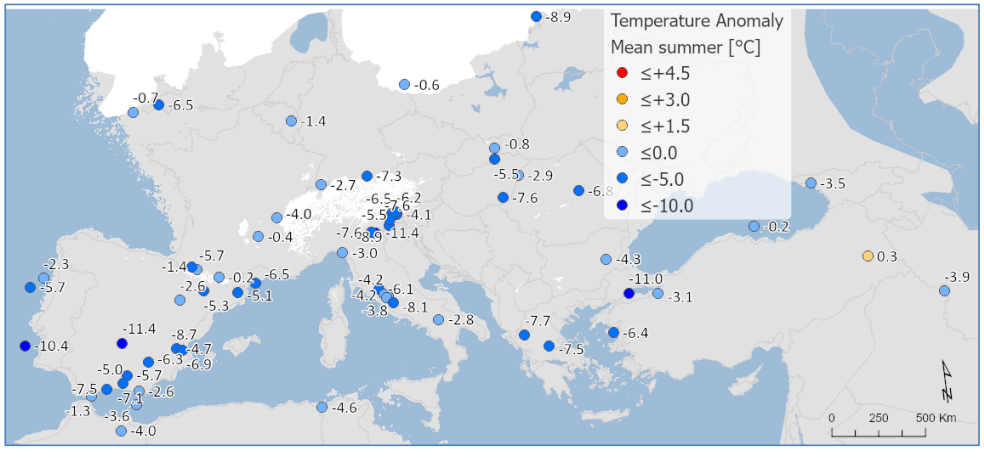

1742

https://doi.org/10.5194/cp-2022-59
Preprint. Discussion started: 31 August 2022

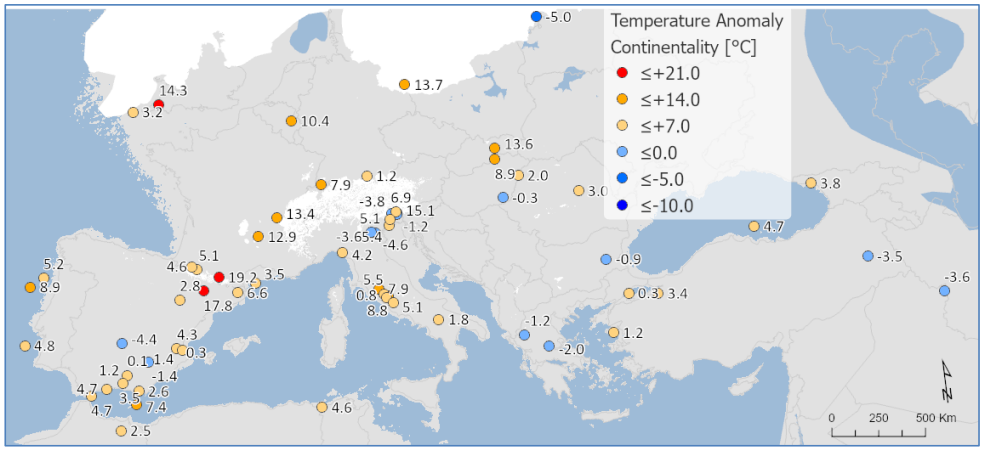

Figure 10. Maps of pollen-based MAT reconstructions for LGM annual, winter and summer temperature anomalies (as shown in figure 9). Continentality represents the difference in temperature between summer and winter, with positive anomalies indicating an increase in the temperature difference between summer and winter. All values are expressed as anomalies compared with the present day.

https://doi.org/10.5194/cp-2022-59
Preprint. Discussion started: 31 August 2022

Climate of the Past Discussions
Open Access
EGU

1750

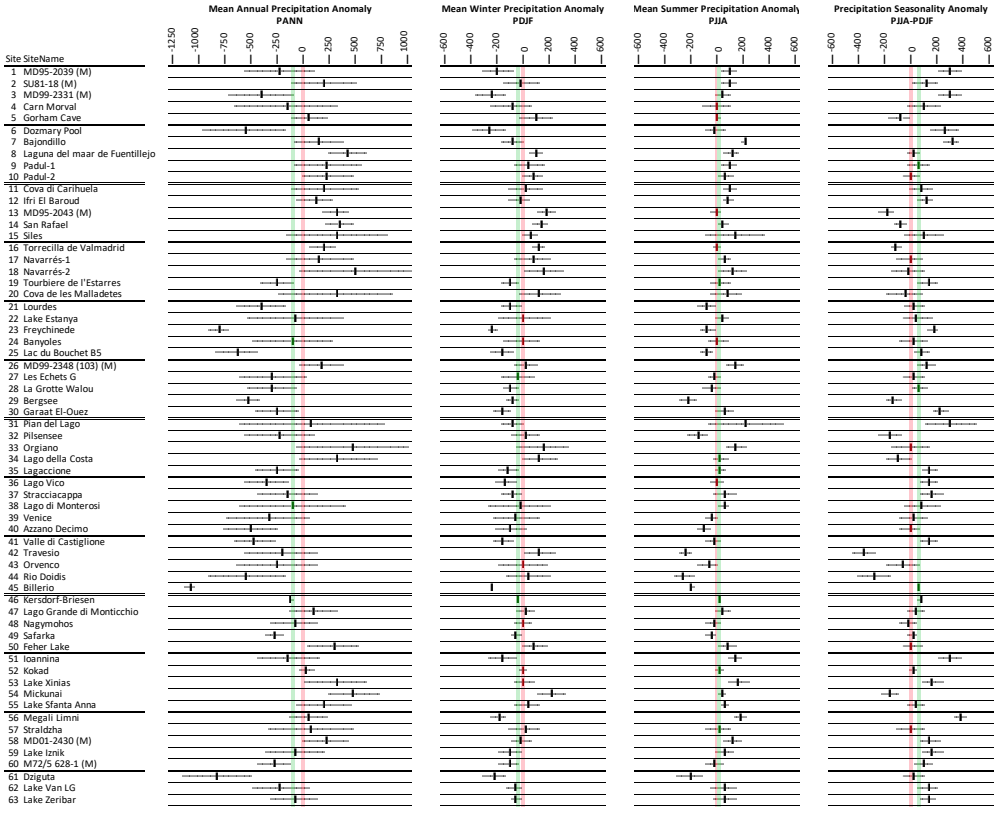

1751

1752

1753 Figure 11. Pollen-based MAT reconstructions for LGM annual, winter and summer precipitation anomalies
1754 (uncertainties represent one standard deviation). Seasonality represents the difference in precipitation between
1755 summer and winter, with positive anomalies indicating an increase in summer precipitation compared to winter.
1756 All values are expressed as anomalies compared with the present day. The green line indicates the mean for all
1757 the sites.

https://doi.org/10.5194/cp-2022-59
Preprint. Discussion started: 31 August 2022

Climate of the Past Discussions
Open Access
EGU

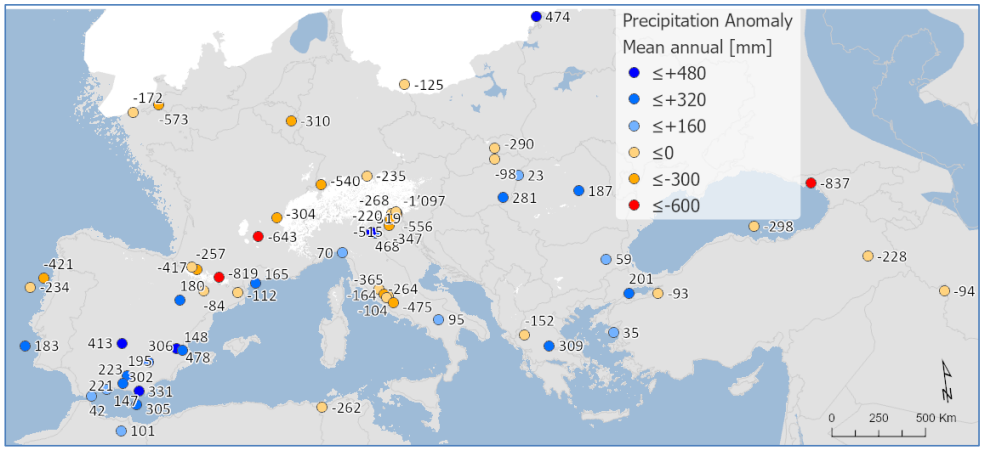

1758

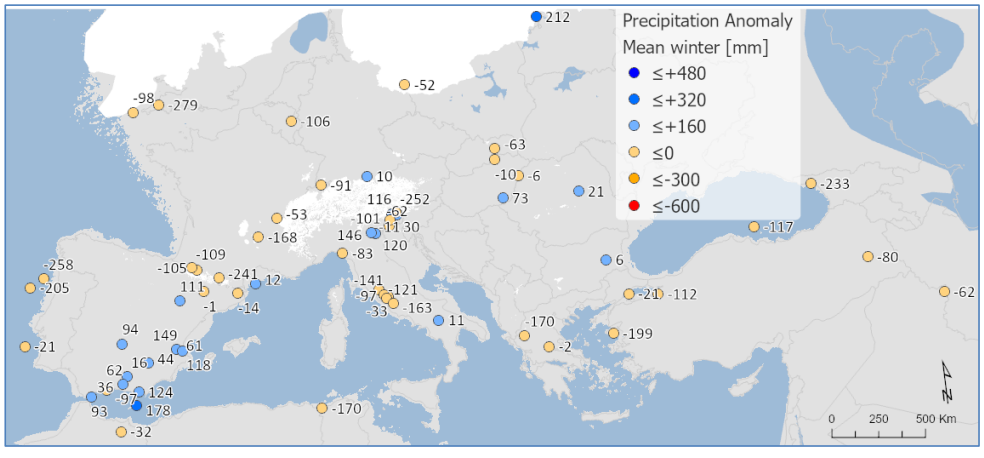

1759

https://doi.org/10.5194/cp-2022-59
Preprint. Discussion started: 31 August 2022

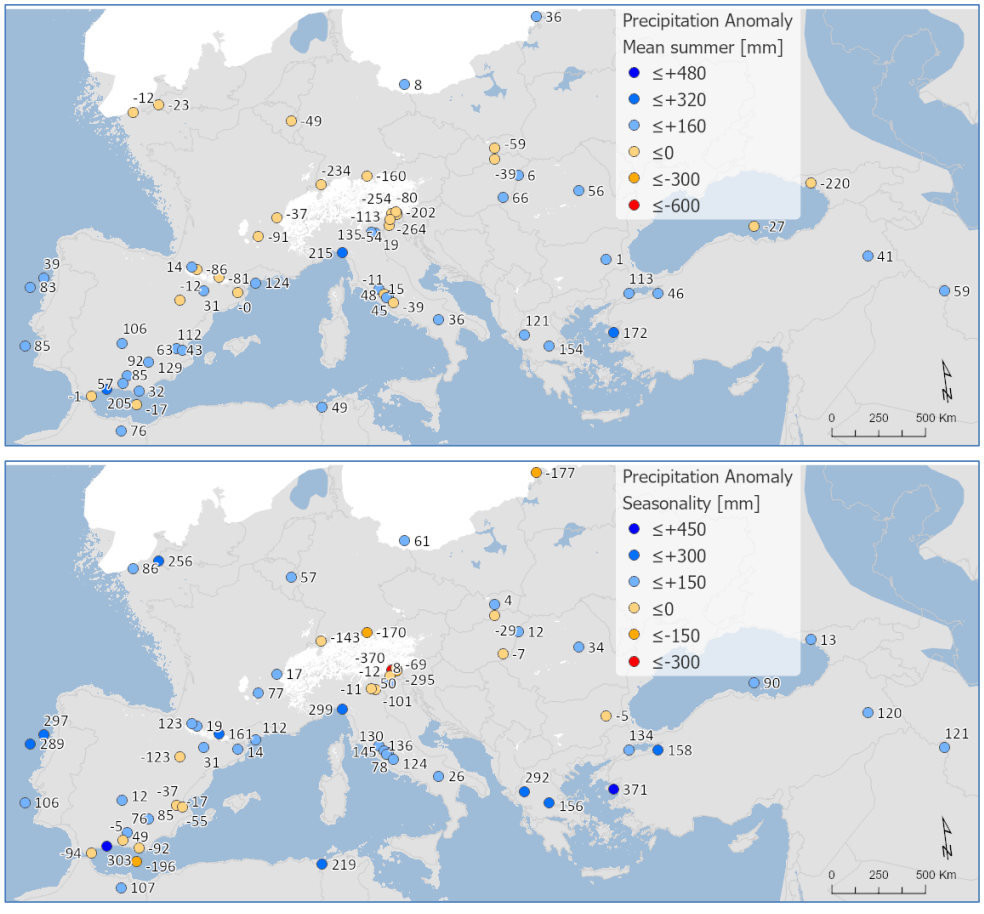

Figure 12. Maps of pollen-based MAT reconstructions for LGM annual, winter and summer precipitation anomalies (as shown in figure 11). Seasonality represents the difference in precipitation between summer and winter, with positive anomalies indicating an increase in summer precipitation compared to winter. All values are expressed as anomalies compared with the present day.

https://doi.org/10.5194/cp-2022-59
Preprint. Discussion started: 31 August 2022

Climate of the Past Discussions
Open Access
EGU

Appendix

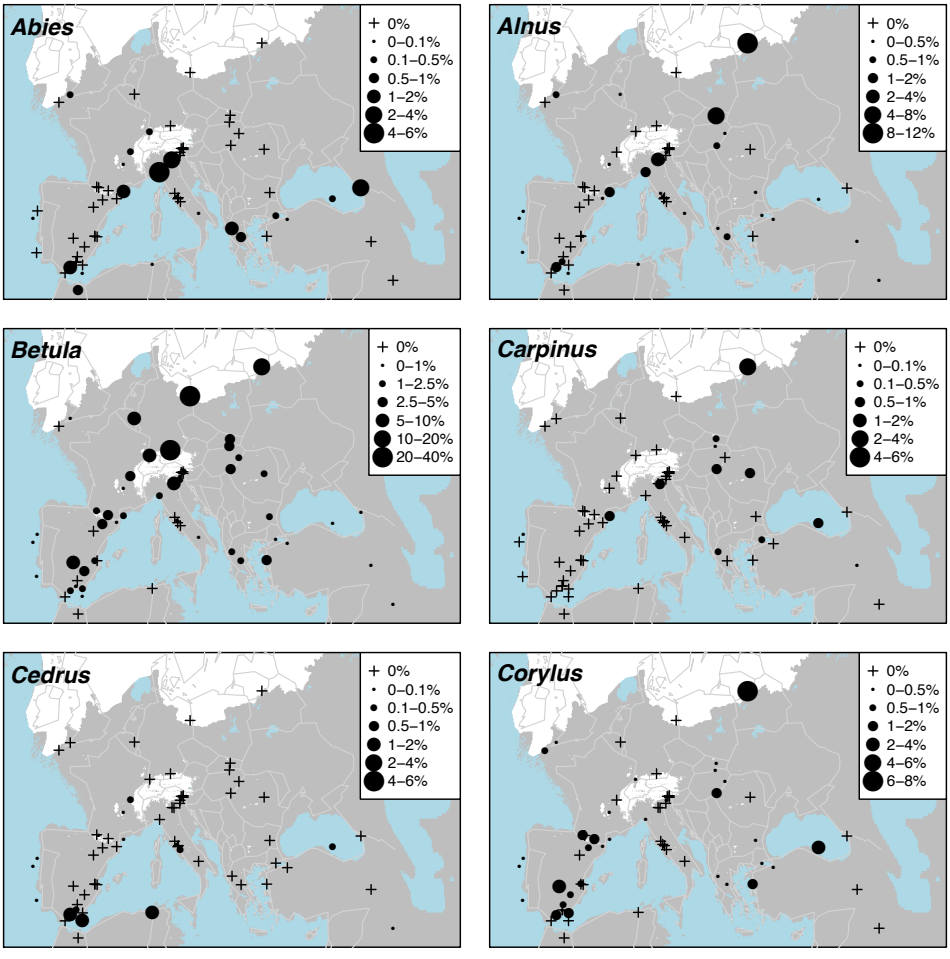

Figure A1a. Percentage maps of *Abies*, *Alnus*, *Betula*, *Carpinus*, *Cedrus* and *Corylus*

https://doi.org/10.5194/cp-2022-59
Preprint. Discussion started: 31 August 2022

Climate of the Past Discussions
Open Access
EGU

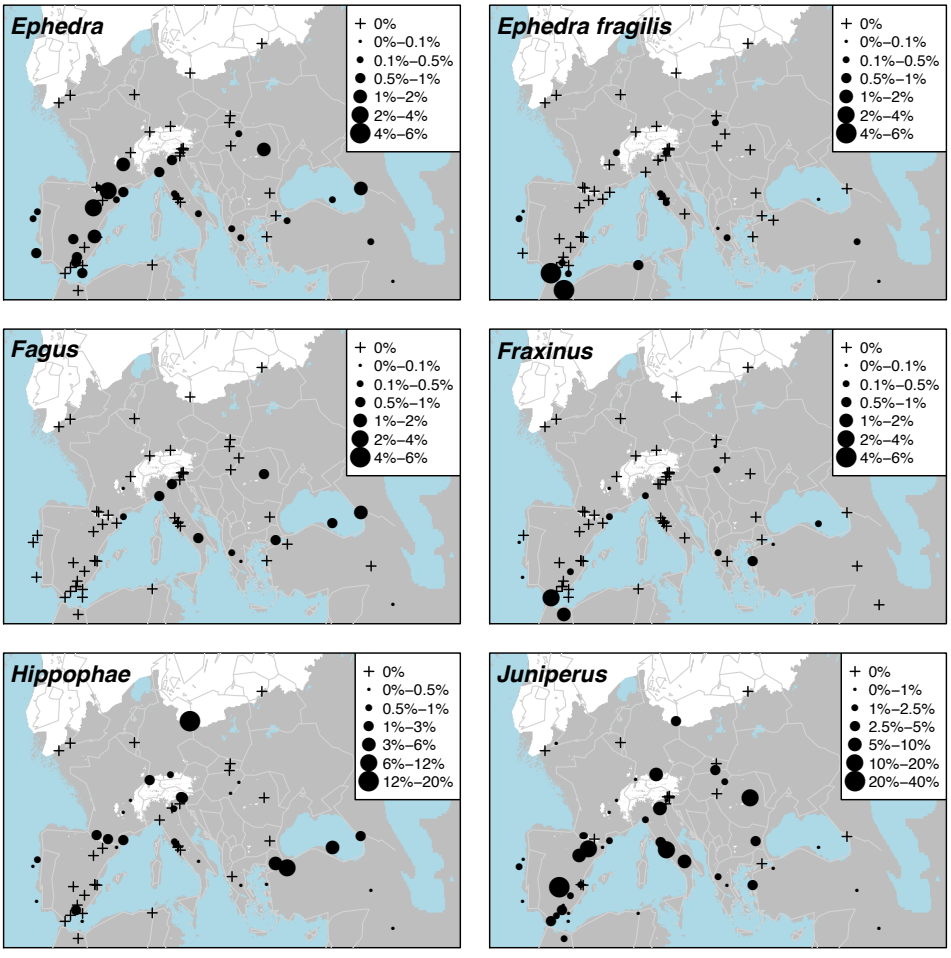

1776
1777
1778 Figure A1b. Percentage maps of *Ephedra*, *Ephedra fragilis*, *Fagus*, *Fraxinus*, *Hippophae* and *Juniperus*
1779

https://doi.org/10.5194/cp-2022-59
Preprint. Discussion started: 31 August 2022

Climate of the Past Discussions
Open Access
EGU

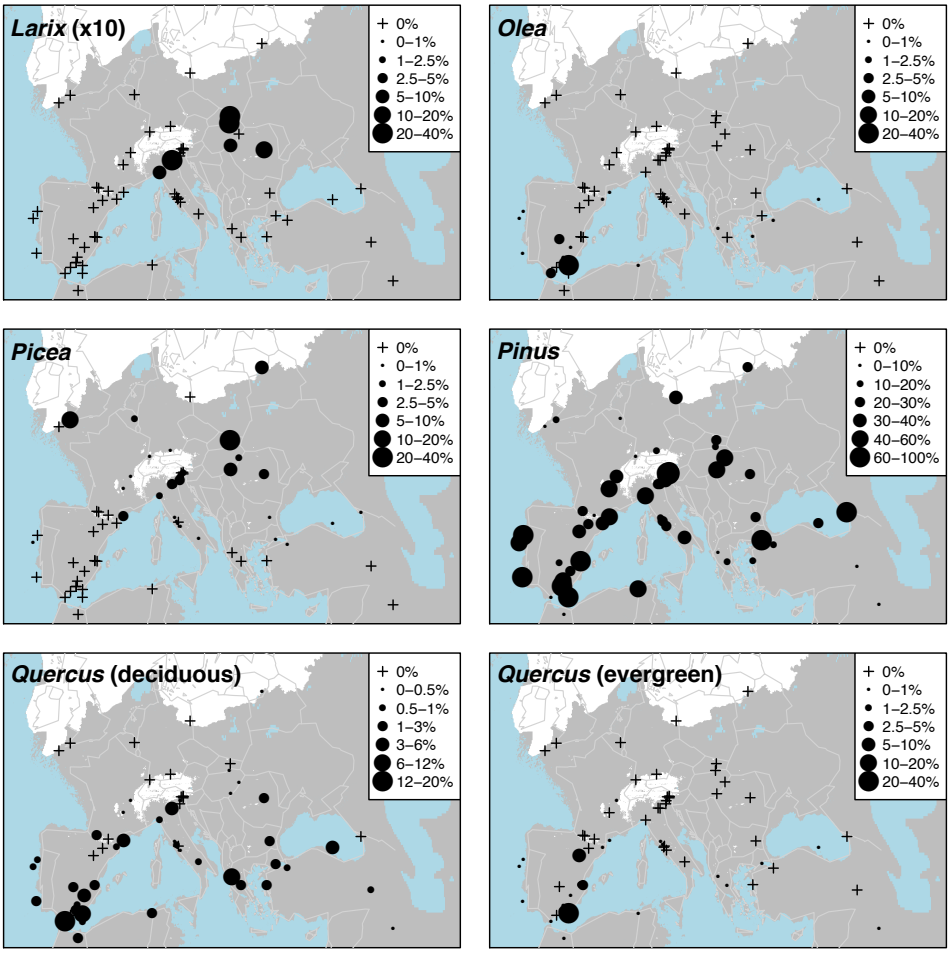

1780
1781
1782 Figure A1c. Percentage maps of *Larix* (x10 exaggeration), *Olea*, *Picea*, *Pinus*, *Quercus* (deciduous) and *Quercus*
1783 (evergreen)
1784

https://doi.org/10.5194/cp-2022-59
Preprint. Discussion started: 31 August 2022

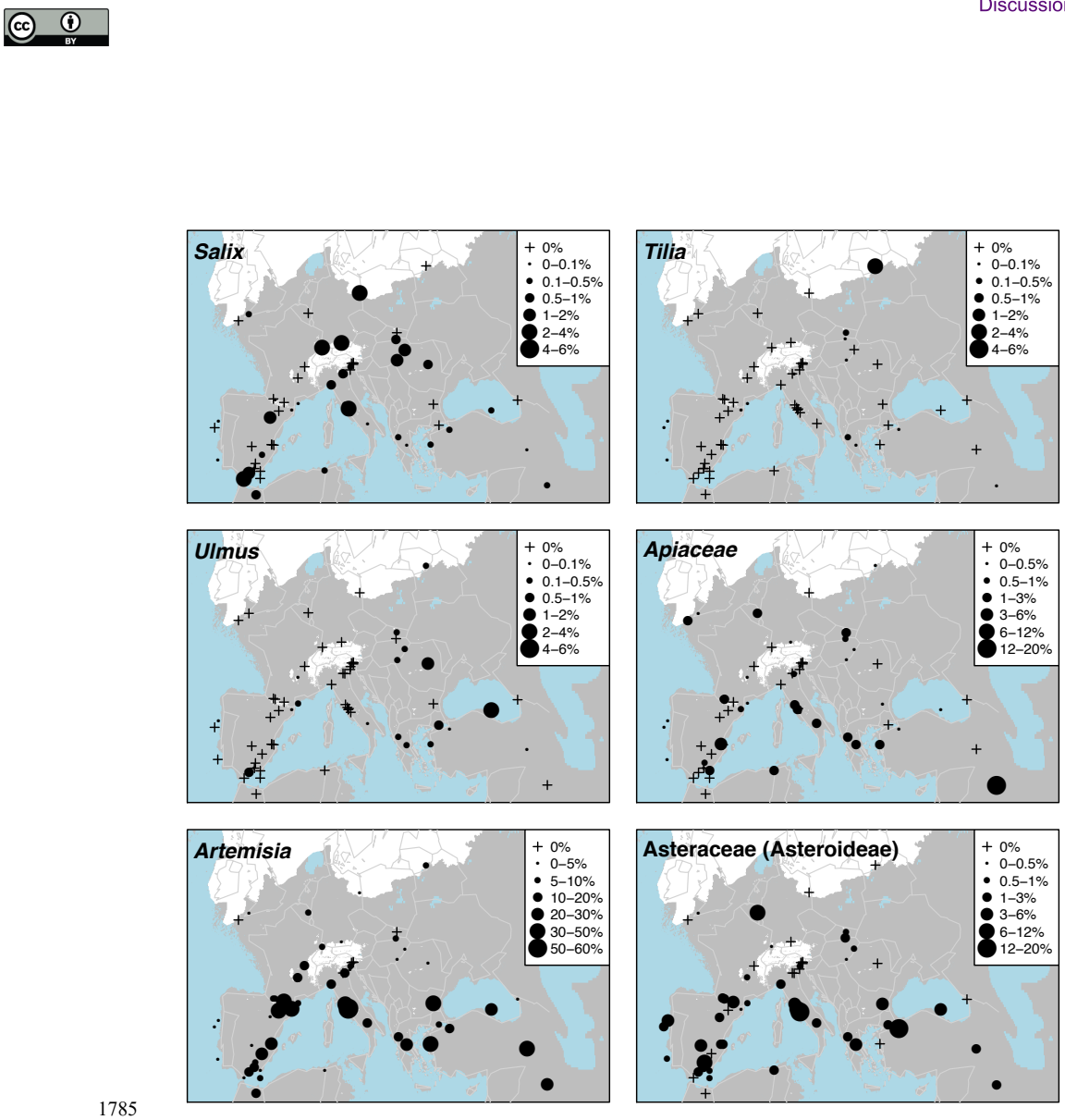

1785
1786
1787 Figure A1d. Percentage maps of *Salix*, *Tilia*, *Ulmus*, Apiaceae, *Artemisia* and Asteraceae (Asteroideae)

https://doi.org/10.5194/cp-2022-59
Preprint. Discussion started: 31 August 2022

Climate of the Past Discussions
Open Access
EGU

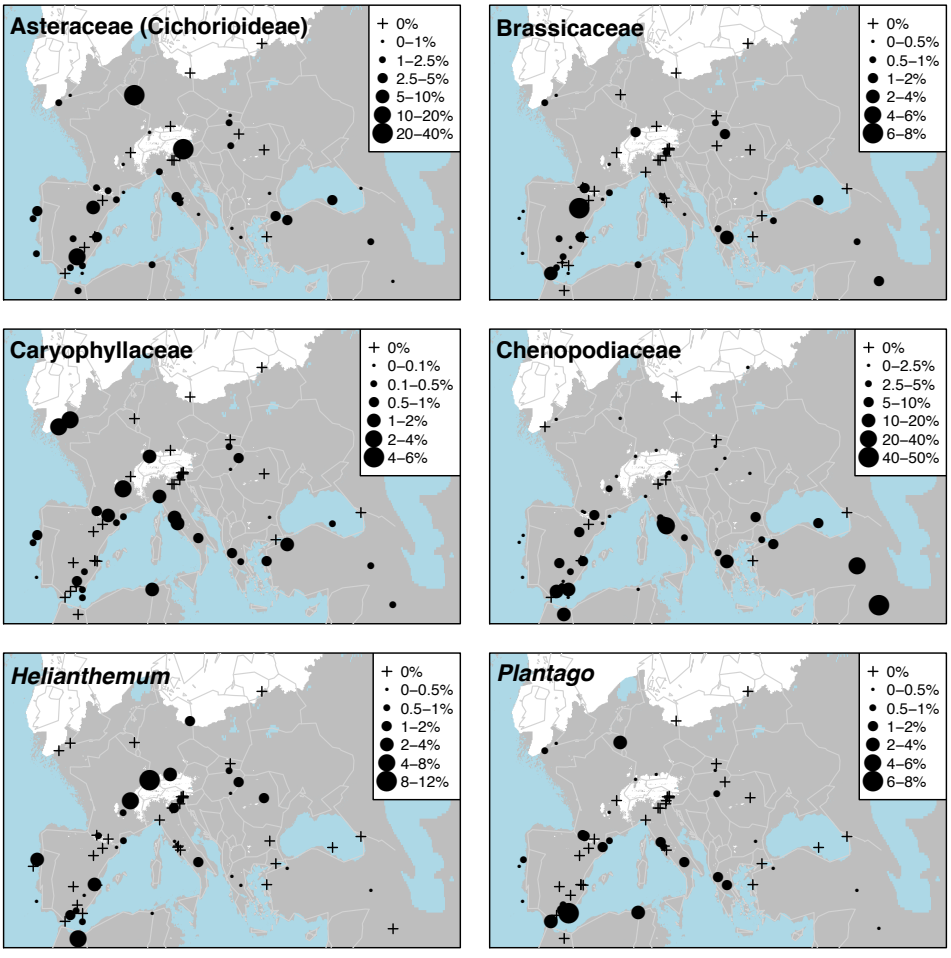

1788
1789
1790 Figure A1e. Percentage maps of Asteraceae (Cichorioideae), Brassicaceae, Caryophyllaceae, Chenopodiaceae,
1791 Helianthemum and *Plantago*
1792

https://doi.org/10.5194/cp-2022-59
Preprint. Discussion started: 31 August 2022

Climate of the Past Discussions

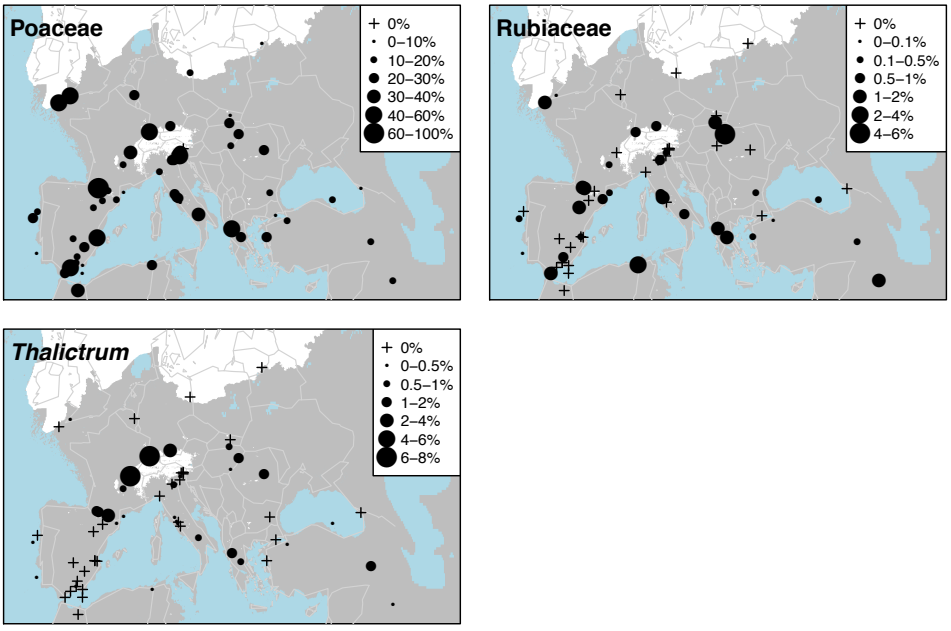

1793
1794
1795 Figure A1f. Percentage maps of Poaceae, Rubiaceae and *Thalictrum*
1796
1797
1798
1799
1800
1801
1802
1803